RATIONAL SYNTHESIS AND PROPERTIES OF NEW LONG-CHAIN LINEAR OLIGOMERIC GERMANIUM COMPOUNDS

By

KIMBERLY DIANE ROEWE

Bachelor of Science in Chemistry
Southwestern Oklahoma State University
Weatherford, Oklahoma
2009

Submitted to the Faculty of the
Graduate College of the
Oklahoma State University
in partial fulfillment of
the requirements for
the Degree of
DOCTOR OF PHILOSOPHY
May, 2014

RATIONAL SYNTHESIS AND PROPERTIES OF NEW LONG-CHAIN LINEAR OLIGOMERIC GERMANIUM COMPOUNDS

Dissertation Approved:

Dr. Charles S. Weinert

Dissertation Adviser

Dr. Allen Apblett

Dr. Richard Bunce

Dr. Nicholas Materer

Dr. Ulrich Melcher

Name: KIMBERLY DIANE ROEWE

Date of Degree: MAY, 2014

Title of Study: RATIONAL SYNTHESIS AND PROPERTIES OF NEW LONG-CHAIN LINEAR OLIGOMERIC GERMANIUM COMPOUNDS

Major Field: CHEMISTRY

Abstract:

Germanium compounds with single germanium-germanium bonds contain interesting optical and electronic properties such as absorption within the UV/visible range and conductivity, which can also be seen in other heavier Group 14 oligomers. In comparison to the tin and silicon analogues, the reported methods for synthesizing the germanium compounds are minimal. The longest linear oligogermane completely characterized, including its structure, is the perphenylated pentagermane, Ge_5Ph_{12}. Due to their inherent properties, it is of interest to synthesize longer, linear oligomeric germanium compounds. It is proposed that if a long enough chain of germanium atoms is obtained, properties characteristic of polygermane species may also be achieved. Protection/deprotection strategies, using a masked Ge – H bond, were initially attempted, however only a linear pentagermane could be obtain. All products were also liquid, preventing complete characterization using X-ray crystallography.

After synthetic efforts were shifted away from the protection/deprotection strategies, a successful strategy was achieved starting with a cyclic germanium species. The hexagermane $Pr^i_3Ge(GePh_2)_4GePr^i_3$ was synthesized in three steps from cyclic $(GePh_2)_4$ within reasonable overall yield. The hexagermane exhibits a λ_{max} of 310 nm in its UV/visible spectrum, which is more red-shifted than any other discrete oligogermanes synthesized with six or less consecutive germanium atoms, and the DPV contained 5 consecutive, irreversible oxidation waves, the first of which was observed at 1080 mV. The hexagermane is the first discrete organogermanium compound to exhibit fluorescence, with a broad emission at 370 nm when excited at 312 nm. Crystals of the hexagermane were dichroic. Though colorless under ambient light, the hexagermane crystals appeared blue under “right” plane polarized light and pale yellow under “left” polarized light.

Since 1986 when the first pentagermane was synthesized, progress has not been successful at synthesizing a longer oligogermane. A linear hexagermane has finally been synthesized and completely characterized indicating that discrete oligomeric germanium compounds have the ability to mirror properties of polymeric germanium species given enough consecutive germanium atoms.

TABLE OF CONTENTS

Chapter Page

LIST OF TABLES

Table Page

LIST OF SCHEMES

Scheme Page

Scheme Page

LIST OF FIGURES

Figure Page

Figure Page

CHAPTER I

INTRODUCTION

In 1886, Clemens Winkler published the report of a new element germanium, isolated from the mineral argyrodite.[1,2] The element contained many properties similar to the hypothesized element ekasilicon, which Dmitri Mendeleev predicted to exist 17 years earlier in 1869.[3] Ekasilicon was proposed to lie between silicon and tin on the periodic table. When argyrodite was originally found in 1885 in Himmelsfurst Fundgrube, Freiburg, Germany, it was thought to contain silver, sulfur and a small quantity of mercury. Winkler refuted the original claim of containing mercury, and reported on the corrected composition formula of Ag_8GeS_6. Today, germanium is primarily found in ores of sphalerite, (Zn,Fe)S, and can be recovered commercially from silver, lead and copper ores.

Germanium is a well-known semiconductor. Due to the interesting optical and electronic properties, it has been used in transistors, fiber optic systems, infrared optics, solar cells and nanowires.[4] Germanium compounds containing organic groups may also

be used as a semiconductor when doped with $FeCl_3$, SbF_5 or $NOBF_4$.[5] A few researchers are also attempting to use a few germanium compounds such as the germanium sesquioxides $((HOOCCH_2CH_2Ge)_2O_3)_n$ and $[O_{1.5}Ge(CH_2)_3NHSCNH_2]_n$ in anticancer protocols and as antibacterial agents.[5,6]

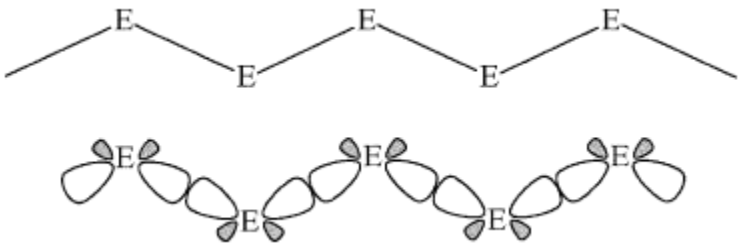

Figure 1.1. Orientation of the highest occupied molecular orbital, HOMO, in catenated group IV elements when present in consecutive *trans*-conformation, allowing for σ-delocalization.[7]

Catenated organometallic germanium compounds exhibit interesting optical and electronic properties. Though resembling saturated hydrocarbon systems, heavier group 14 compounds containing organic side groups possess electronic systems which behave more as poly-unsaturated conjugated hydrocarbons.[7] This phenomenon, known as σ-delocalization, occurs when heavy group 14 atoms along the backbone of the molecule are arranged in a sequential *trans*-coplanar confirmation (**Figure 1.1**).[8-10] By doing so, optimal overlap of the sp^3 hybridized molecular orbitals occurs and the electrons in the highest occupied molecular orbital, HOMO, are delocalized over the germanium backbone, as opposed to the traditional localization of electrons within a two center, two electron σ bond. It is of note that commonly a significant out-of-plane twist occurs after several consecutive heavy group 14 atoms align in a *trans*-coplanar geometry within a

chain. These regions of disordered geometry disrupt the σ-delocalization and limit the energy maximum of the σ-bonding HOMO.

In heavier group 14 molecules, the highest occupied molecular orbital to lowest occupied molecular orbital transition, or HOMO-LUMO transition, corresponds to the promotion of an electron from the σ bonding to the σ antibonding molecular orbital. This σ to σ* transition, typically in the ultraviolet region allowing for probing via ultraviolet-visible spectroscopy, can experience a bathochromic shift upon elongation of the backbone of the molecule. A bathochromic shift may also result by replacing electron withdrawing groups (or less electron donating groups) with more electron donating groups. The optical attributes of these compounds allow for the potential of using larger polymeric species as conductive and non-linear optic materials.[4,11] The smaller oligomers of catenated group 14, therefore serve as molecular models for the larger polymeric systems where the exact geometry and composition of the Ge_n chain is not known, which makes synthesizing these molecules a useful endeavor.

While carbon containing molecules are readily stable at room temperature, the heavier group 14 congeners require organic side groups to stabilize the Ge – Ge single bonds. Silicon, germanium, tin and lead compounds containing the general formula E_nH_{n+2} (E = Si, Ge, Sn, Pb), unlike their alkane analogues, are often highly reactive and are often pyrophoric. Even with organic side groups, germanium compounds are often difficult to purify due to their high sensitivity to air and moisture. Reactions and separations of compounds containing germanium, therefore, are not trivial and must be performed under an inert atmosphere of nitrogen or argon.

The first reported organogermanium compound, Et_4Ge, was synthesized by Winkler in 1887, just one year after the discovery of the element germanium.[12] It was not until 1925, 39 years after the discovery of the element germanium, that the first compound containing a germanium-germanium bond was synthesized, $Ph_3GeGePh_3$.[13] Since the report of the first Ge - Ge bond, relatively little research has been accomplished to synthesize longer, linear oligogermanes. The most thorough investigation surveying the synthesis, spectra, structure and reactivity of linear and cyclic catenates, containing between two and five linear germaniums in length, was completed by Dräger in the 1980s in a series of nineteen publications.[14-32] Though germanium is located between silicon and tin and exhibits some similar properties to its neighbors, the synthesis of compounds having germanium-germanium bonds has received significantly less attention than the silicon[9,33-42] and tin[43-58] congeners. It has been assumed that the reactivity leading to Ge – Ge bond formation would be similar to that of its neighbors; the reality was that many of the same bond forming reactions do not work for the germanium analogues.

Several differences and similarities may be found between organosilicon and organogermanium compounds. The germ anium halide bond is typically found to be more resistant to hydrolysis than silicon halide. When treated with an organolithium reagent, a trialkyl germanium hydride undergoes metallation to give the R_3GeLi species with an alkane byproduct, while the silicon counterpart would undergo metathesis producing a tetraalkyl silicon compound, R_3SiR', and lithium hydride.[59-61] It is also known that R_3GeCl will undergo a reduction with amalgamated zinc and HCl to give R_3GeH, but R_3SiCl does not.[62] While halides of both germanium and silicon may react

I. Wurtz-type coupling[12]

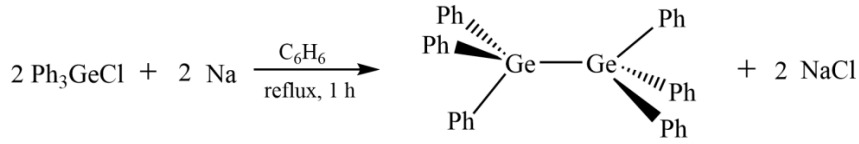

II. Mercuration/Demercuration of organogermanes[68,69]

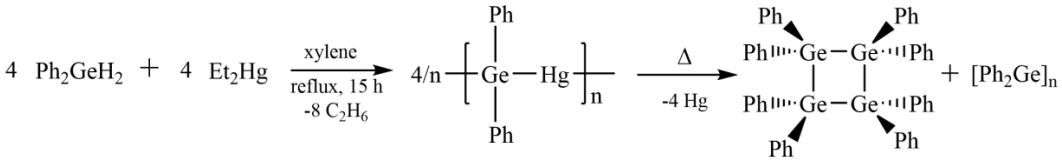

III. Nucleophilic substitution reactions involving triorganogermanium anions and organogermanium halides[74]

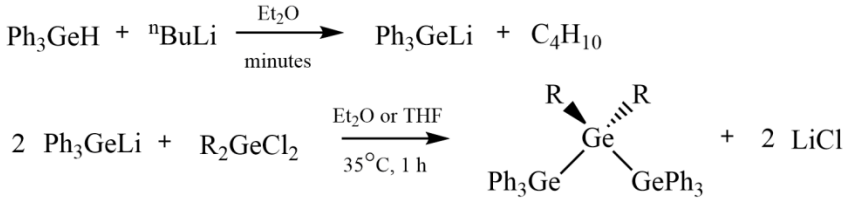

IV. The action of Grignard reagents on organogermanium halides[25,70,71]

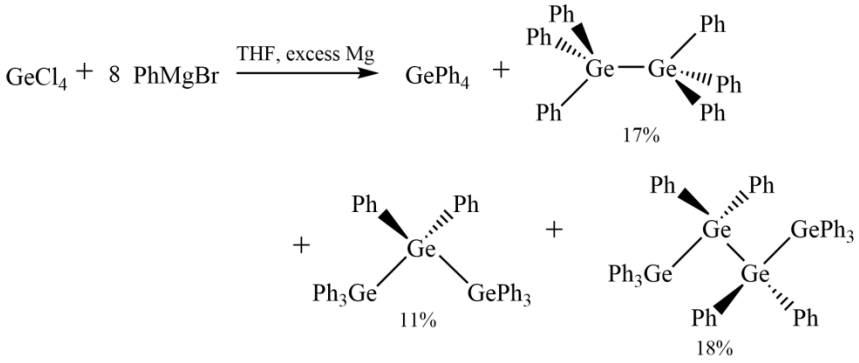

V. Samarium(II) iodide as a reducing agent[72,73]

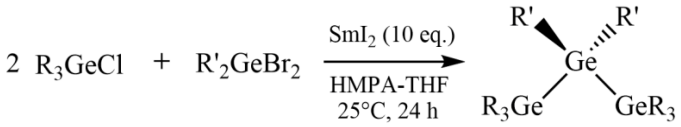

Scheme 1.1. Common reaction pathways for the formation of Ge – Ge bonds.

rapidly with water producing oxides and hydroxides, only the germanium oxides can be converted back to the halide using the corresponding acid.[63] Silicon oxides can only be converted to the corresponding halide using hydrofluoric acid to produce fluorosilanes. Germanium in the +2 oxidation state is accessible, with $GeCl_2$, $GeBr_2$ and GeI_2 all as isolable compounds; compounds with the formula SiX_2 (X = Cl, Br, I) have only been known as reactive intermediates being studied through trapping agents and emission bands.[3] Although some similar chemistry exists for both germanium and silicon, it is evident that the development of new synthetic methods is necessary for the preparation of germanium compounds.

Successful synthesis schemes for the formation of the Ge – Ge bond typically involve hazardous conditions, mixed products or low yields.[64] Before 2006, common reactions for the synthesis of Ge – Ge bonds included Wurtz-type coupling using alkali metals acting on organogermanium halides,[13,65-67] mercuration/demercuration of organogermanes,[68,69] the action of organolithium or Grignard reagents on organogermanium halides,[25,70,71] the use of samarium(II) iodide as a reducing agent,[72,73] and nucleophilic substitution reactions involving triorganogermanium anions and organogermanium halides[74] (**Scheme 1.1**).

The use of samarium (II) iodide as a reducing agent was a large synthetic improvement over previously used methods for the formation of di- and trigermanes, where yields were typically in excess of 60% as the only product. Previously used Wurtz-type polycondensation of heavier group 14 element dihalides with an alkali metal were often carried out under vigorous conditions and afforded low yields due to the heterogeneous nature of the reaction. Though a digermane may be formed using

reductive conditions,[75] organodigermanes are sensitive and may be cleaved by alkali metals to give the corresponding germyl anion under vigorous reaction conditions.[76] Samarium (II) iodide, having a much more mild reduction potential than its alkali metal counterparts (**Table 1.1**), was a viable option as a homogeneous, one-electron reductant.

Table 1.1. Reduction potentials of Sm^{2+} compared to alkali metals.[77]

Reaction	**Potential (V)**
$Sm^{3+} + e^- \leftrightarrow Sm^{2+}$	-1.55
$Li^+ + e^- \leftrightarrow Li$	-3.04
$Na^+ + e^- \leftrightarrow Na$	-2.71
$K^+ + e^- \leftrightarrow K$	-2.931

Table 1.2. Substrate and yield of various digermanes starting from R_3GeX (R = alkyl; X = halide) with 2 equivalents of SmI_2 in THF/HMPA.[72,73]

Substrate	**Time (h)**	**Yield (%)**	**Substrate**	**Time (h)**	**Yield (%)**
Et_3GeCl	24	69	*i*-Pr_3GeBr	15	45
Et_3GeBr	15	73	$Ph_2MeGeCl$	12	95
n-Bu_3GeCl	24	62	$Ph_2MeGeBr$	1	98
n-Bu_3GeBr	15	66	Et_3GeCl + Ph_3GeBr	1	96
i-Pr_3GeCl	24	39	*n*-Bu_3GeCl + Me_3GeBr	15	59

Samarium (II) iodide has been reported to be successful for the synthesis of di- and trigermanes.[72,73] As evident from **Table 1.2** and **Table 1.3**, moderate to excellent

yields were obtained in the synthesis of digermanes through the use of two equivalents of SmI_2 in tetrahydrofuran/hexamethylphosphoramide (THF/HMPA) solvent with a trialkylgermanium halide. Mochida *et al.* also reported changing reaction conditions in order to obtain polymeric mixtures.[72,73] Since 2005, no progress has been accomplished synthesizing longer linear discrete molecules while employing SmI_2 as a reducing agent.

Table 1.3. Synthesis of trigermanes using SmI_2 as a reductant.[73]

Product	**Conditions**	**Yield**	**Product**	**Conditions**	**Yield**
$Et_3GeGePh_2GeEt_3$	A	94	$Me_3GeGePh_2GeMe_3$	A	87
$Et_3GeGePh_2GeEt_3$	B	90	$Bu^n{}_3GeGePh_2GeBu^n{}_3$	B	87
$Et_3GeGePh_2GeEt_3$	C	89	$Pr^i{}_3GeGePh_2GePr^i{}_3$	A	30
$Et_3GeGePh_2GeEt_3$	D	83	$Et_3GeGeMePhGeEt_3$	A	70

Conditions: A, germanium reactants were combined in THF and then added to a THF/HMPA (12:1) solution of SmI_2 (0.6 mmol, 0.1 mol dm^{-3}) at room temperature and stirred for 1 hour. B, conc. = 3 mmol dm^{-3}. C, conc. = 15 mmol dm^{-3}. D, THF solutions of substrates were reacted for 1 hour.[73]

DIGERMANES

The history of germanium-germanium bond forming reactions has its origins in 1925 when Morgan and Drew prepared hexaphenyldigermane, $Ph_3GeGePh_3$[13]. This compound, as well as $Et_3GeGeEt_3$ reported in 1932,[78] and $Me_3GeGeMe_3$ reported in 1958,[79,80] were successfully synthesized using Wurtz-type coupling (**Table 1.4**). The three digermanes were synthesized by refluxing R_3GeBr (R = phenyl, ethyl, methyl) with either sodium or potassium metal in an aryl solvent.

Table 1.4. The synthesis of digermanes using Wurtz-type coupling.

Germanium Reactant	Reductant	Product	Yield (%)	Publish Date
Ph_3GeBr	Na	$Ph_3GeGePh_3$	24	1925[13]
Et_3GeBr	Na	$Et_3GeGeEt_3$	60	1932[78]
Me_3GeBr[a]	K	$Me_3GeGeMe_3$	74	1958[79,80]

[a] An alternative synthesis was reported in 1976.[80]

Besides Wurtz-type coupling, the action of Grignard reagents on a germanium tetrahalide is an alternative means of synthesizing digermanes. Depending on the stoichiometry and reaction conditions, multiple products may be achieved through the use of Grignard reagents.[13,25,70,81,82] The compound Ph_4Ge has been prepared synthetically by starting with $GeCl_4$ using many reaction conditions. When a large excess of PhMgBr was reacted with $GeBr_4$ in Et_2O, the monogermane Ph_4Ge was obtained.[13] Interestingly however, $Ph_3GeGePh_3$ was achieved in 69% yield by reacting $GeCl_4$ with 7.8 equivalents of PhMgBr and 20 mole percent excess of magnesium metal in tetrahydrofuran, THF. Hexaphenyldigermane, $Ph_3GeGePh_3$, was also obtained by the use of PhMgBr:$GeCl_4$ in a 14:4 molar ratio in 59% yield.[83] The pathway for the synthesis of both Ph_4Ge and $Ph_3GeGePh_3$ may be rationalized in a stepwise fashion as depicted in **Scheme 1.2**. When reacting PhMgBr with $GeCl_4$, the phenyl groups are added sequentially to the germanium, replacing a chlorine atom. Upon formation of Ph_3GeCl, a second equivalent of PhMgBr may react to form either Ph_4Ge or $Ph_3GeMgCl$. Addition of Ph_3GeCl to the germyl Grignard reagent $Ph_3GeMgCl$, completes the formation of the digermane. It is notable that the action of Grignard reagents on $GeCl_4$ may also undergo further reaction

to form the tri- and tetragermane in lower yields. The yields of the larger oligogermanes are reduced by use of Et_2O/toluene as solvent as opposed to THF.

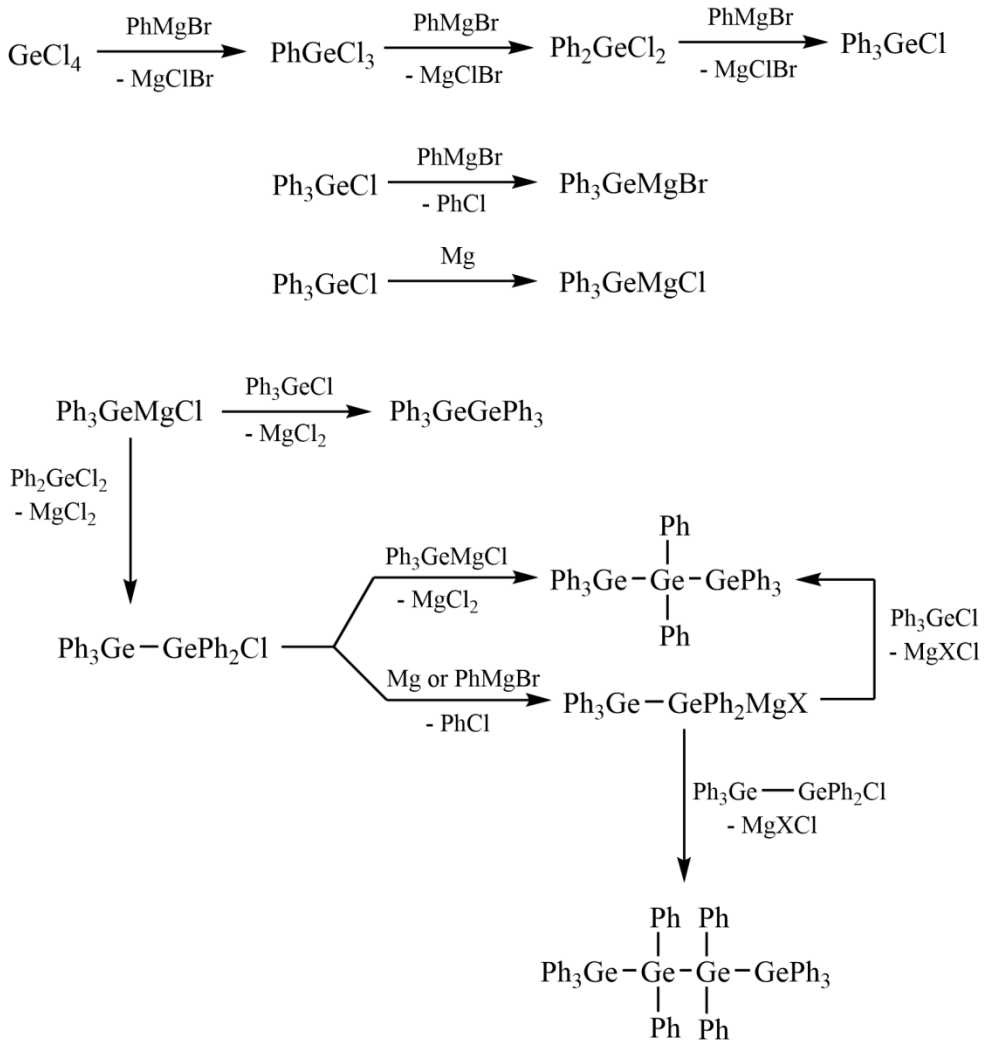

Scheme 1.2. Grignard reaction pathway for the synthesis of Ph_4Ge, $Ph_3GeGePh_3$, $Ph_3GeGePh_2GePh_3$, and $Ph_3GeGePh_2GePh_2GePh_3$.

Many solid peralkylated digermanes that have been synthesized, to date, have been structurally characterized (**Table 1.5**). The Ge – Ge bond distance in a digermane

typically range from 2.41 to 2.46 Å, with the average distance from **Table 1.5** being 2.435 Å ($Bu^t_3GeGeBu^t_3$ is not included in the average calculation). Elongation of the germanium-germanium bond is observed when the α or β carbon of the germanium bound alkyl group is of higher order, as would be expected due to the increased steric bulk. By comparison of the compounds $Ph_3GeGeBu^n_3$, $Ph_3GeGeBu^i3$, and $Ph_3GeGePr^i_3$, which have Ge – Ge bond distances of 2.421(8) Å, 2.4410(5) Å, and 2.4637(7) Å, respectively, a correlation is evident between the amount of steric bulk and the distance of the bulk from the germanium center. The germanium-germanium bond distance in these three compounds is elongated with the increasing bulk of the organic groups following the trend $Bu^n < Bu^i < Pr^i$.

Almost all of the digermanes listed in **Table 1.5** contain a phenyl group bound to, at minimum, one germanium atom. The average germanium – *ipso*-carbon distance between these compounds is 1.96(0) Å; $Ph_3GeGePr^i_3$ had the longest Ge – C distance in this series. The substituents on $Ph_3GeGePr^i_3$ and $Ph_3GeGePh_3$, which are the strongest electron donors as well as the sterically largest groups of the series, force the Ge–Ge bond length to increase. Averages for the angles ∠C – Ge – Ge and ∠C – Ge – C (C being the *ispo*-carbon located in the phenyl rings), are 110.7(5)° and 108.2(2)°, respectively, affording a slightly distorted tetrahedral geometry at the germanium atoms.

Table 1.5. Select bond distances (Å) and bond angles (degrees) for digermanes.

Compound	*d* Ge–Ge	d_{avg} Ge–C	$\angle_{avg}$ C–Ge–Ge	$\angle_{avg}$ C–Ge–C	ref
Ph_3Ge-$GePh_3$	2.437(2)	1.96(1)	110.8(3)	108.6(5)	[18]
Ph_3Ge-$GePh_3 \cdot 2\ C_6H_6$	2.446(1)	1.97(2)	110.9(3)	108.1(3)	[16]
Ph_3Ge-$GeBu^n{}_3$[a]	2.421(8)	1.953(4)	110.7(1)	108.0(2)	[84]
Ph_3Ge-$GeBu^i{}_3$[a]	2.4410(5)	1.958(7)	111.6(9)	107.0(8)	[85]
$Ph_3GeGeBu^tMe_2$	2.4255(3)	1.954(5)	110.82(8)	108.04(7)	[86]
Ph_3Ge-$GePr^i{}_3$	2.4637(7)	1.974(2)	110.51(6)	108.33(9)	[87]
Ph_3Ge-$GeEt_3$	2.4253(7)	1.957(2)	110.15(8)	108.77(8)	[84]
Ph_3Ge-$GeMe_3$	2.418(1)	1.950(3)	110.3(1)	108.7(1)	[88]
$Bu^t{}_3Ge$-$GeBu^t{}_3$[a]	2.710(1)	2.076(6)	112.1(2)	107.2(1)	[89]

All distance and angle values are listed for the *ipso*-carbon of the phenyl groups, or the alkyl group α-carbon for the first germanium listed. [a] Values are the average of two crystallographically independent molecules.

The first structurally characterized digermane reported by Dräger was hexaphenyldigermane, $Ph_3GeGePh_3$. This digermane can adopt three separate morphologies depending on the temperature and solvent used in the crystallization process. **Figure 1.2** shows an ORTEP diagram of $Ph_3GeGePh_3$, which was crystallized from benzene at 25 °C. Under these conditions, the compound adopts a rhombohedral morphology with two solvated benzene molecules, which are omitted from the structure shown in **Figure 1.2**.[16] The Ge – Ge bond distance is 2.447 Å, and the Ge – C bond distance is 1.964 Å. Both germanium atoms are in a slightly distorted tetrahedral environment, with the average C – Ge – C angle being 108.0° and the average C – Ge –

Ge angle being 110.8°. When crystallized from dichloromethane, CH_2Cl_2, at -15 °C the compound adopts a triclinic morphology[18], but when crystallized at 25 °C from the same solvent, a hexagonal form is obtained.[18]

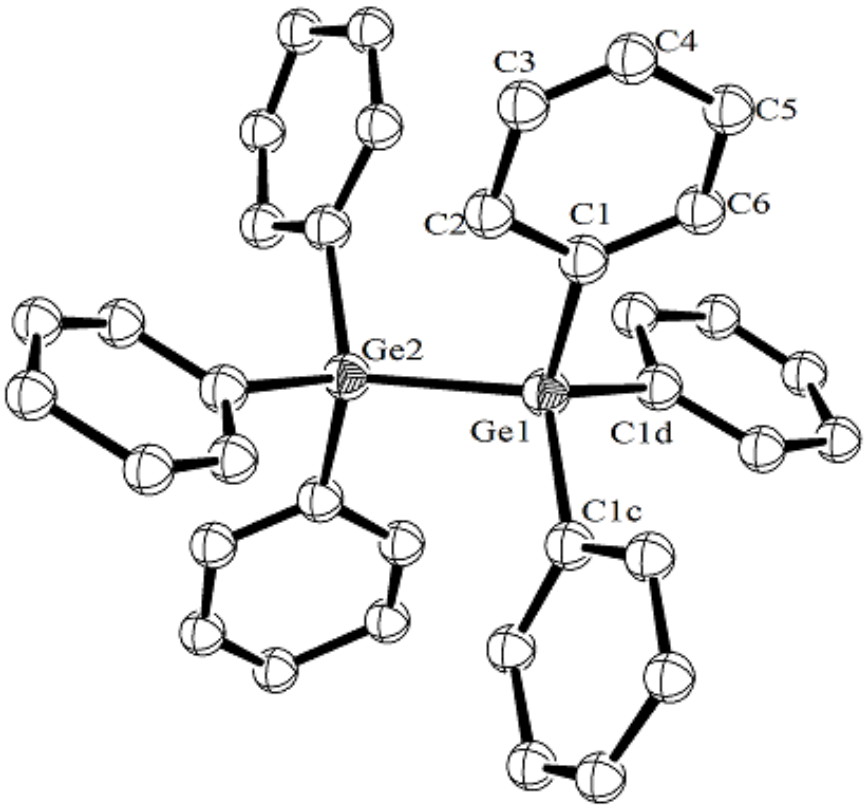

Figure 1.2. ORTEP diagram of $Ph_3GeGePh_3 \cdot 2\ C_6H_6$ with the benzene solvate omitted.[16]

While the most commonly utilized reactions to synthesize a digermane include Wurtz-type coupling, the action of Grignard reagents on a tetrahalogermane, and the samarium (II) iodide reduction as described earlier, many other less common reactions have been successful as well. Some useful reactions include the production of halodigermanes, as in the case of the reaction of diphenylgermanium dibromide,

Ph_2GeBr_2, with one equivalent of lithium amalgam in diethyl ether to give the 1,2-dibrominated digermane $BrPh_2GeGePh_2Br$, in 60% yield (**Scheme 1.3**).[90] A per-halogenated digermane, also depicted in **Scheme 1.3**, was reported in 1972 through the insertion of $GeBr_2$ into a Ge – Br bond of $GeBr_4$ to produce the hexabromodigermane, $Br_3GeGeBr_3$, in 25% yield.[91] By incorporating halogen atoms on the germanium center in these reactions, the opportunity exists to further functionalize the digermanes or to build longer chains.

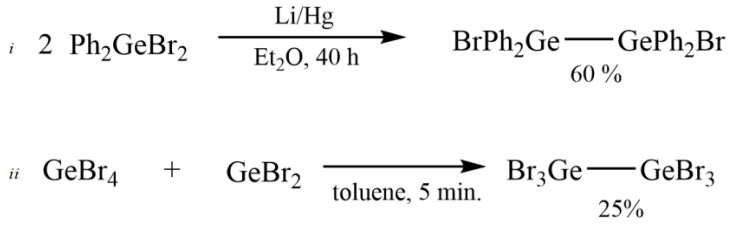

Scheme 1.3. The synthesis of halodigermanes through (*i*) a lithium amalgam reduction and (*ii*) through germylene insertion.[90,91]

LINEAR TRIGERMANES

The first reported synthesis of a trigermane occurred in 1930 through the reaction of Ph_3GeNa with Ph_2GeCl_2 producing octaphenyltrigermane $Ph_3GePh_2GeGePh_3$.[92] While no yield was reported, it is indicated that di-, tri- and polygermanes were also formed in this reaction. The synthesis of linear germanium oligomers, containing more than two germanium atoms, has a precedent of producing a mixture of compounds containing a

variable number of Ge – Ge bonds. Reactions involving anionic germanium compounds, as depicted in **Scheme 1.4**, follow this precedent. Mixtures of di-, tri- and tetragermanes are obtained in the synthesis of $Ph_3GePh_2GePh_3$, $Ph_3GeGeEt_2GePh_3$ and $Et_3GeGeMe_2GeEt_3$. Despite mixed products, good to excellent yields of the trigermanes were obtained.[74,93]

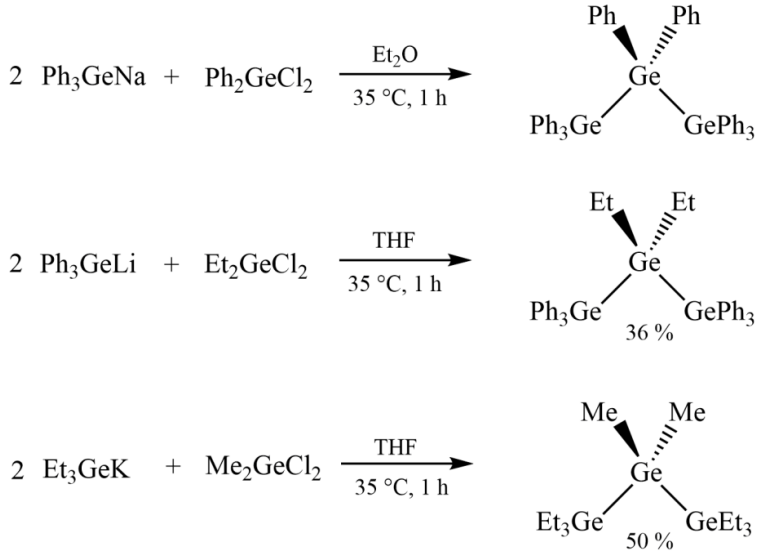

Scheme 1.4. The synthesis of trigermanes from germyl anions and R_2GeCl_2.[74,93]

In the reaction of the triphenylgermyl lithium compounds reacting with R_2GeCl_2 (R = aryl or alkyl), the yield of trigermane was successfully optimized through the use of hexamethylphosphoramide (HMPT) as the solvent. HMPT was used to suppress nucleophilic attack on the newly formed Ge – Ge bonds by the Ph_3Ge^- anion. The pathway, as depicted in **Scheme 1.5**, allows for a higher yield of the desired trigermane while decreasing the amount of larger oligogermanes formed.[19]

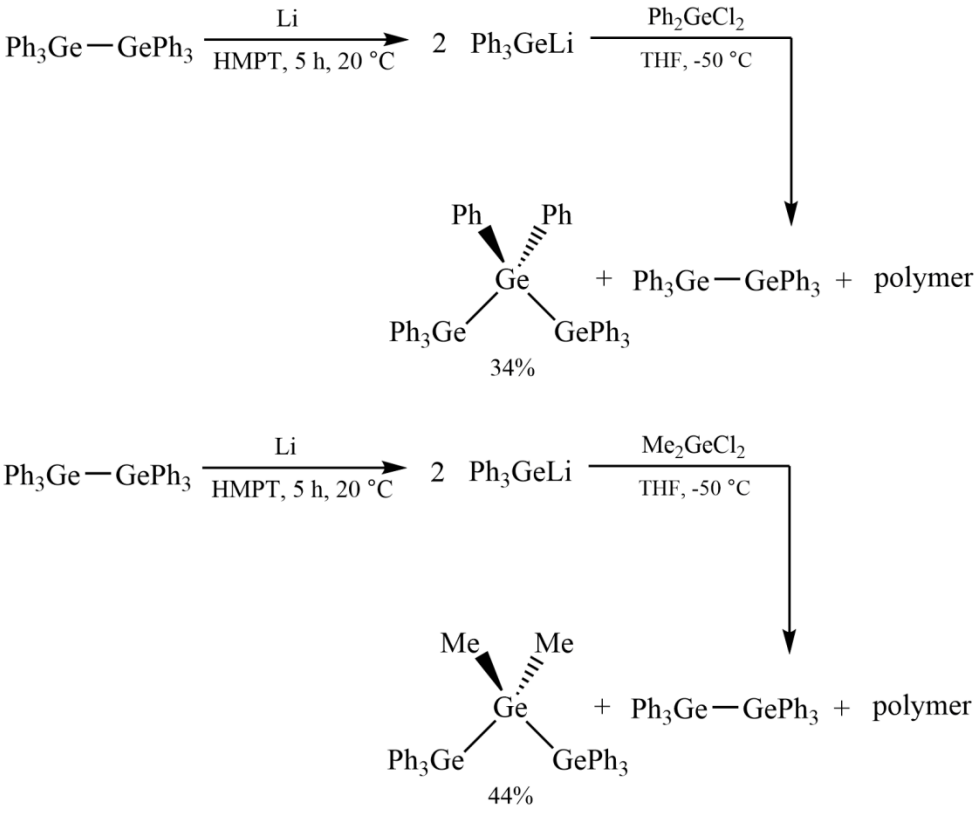

Scheme 1.5. Reaction pathway for the synthesis of trigermanes via a germyl anion in HMPT.[19]

By using HMPT as solvent, octaphenyltrigermene, $Ph_3GeGePh_2GePh_3$, was isolated in 34% yield when R = phenyl; $Ph_3GeGeMe_2GePh_3$ was obtained in 44% yield when R = methyl.[19] In both cases, hexaphenyldigermane and polymers were also detected in the products, as is common for the synthesis of longer linear germanes.

Similar to the lithium reactions reported by Dräger,[19] (diarylgermyl)lithium compounds have been reported as a means to synthesize trigermanes via a decomposition process.[94] When diarylgermanes react with *tert*-butyllithium, a (diarylgermyl)lithium compound forms which slowly decomposes in THF at room temperature over 24 hours

(**Scheme 1.6**). In the presence of an amine such as triethylamine, Et_3N, the decomposition process becomes more effective, and the nature of the resulting oligogermane obtained depends on the reaction time (**Table 1.6**).[94] Products for these reactions are di-, tri- and tetragermanes with a reactive hydrogen site on the terminal germanium atoms. The control in the number of germanium atoms in the resulting product makes (diarylgermyl)lithium reactions an opportunistic means of not only synthesizing trigermanes, but di- and tetragermanes as well.

Scheme 1.6. Synthesis of polygermanes (n = 2 – 4) via the decomposition of (diarylgermyl)lithium compounds.[94]

Table 1.6. The reaction conditions for the synthesis of di-, tri- and tetragermanes through the decomposition of (diarylgermyl)lithium as shown in **Scheme 1.6**.[94]

Time	Polygermane	Percent Yield
5 min	$H(GePh_2)_2H$	26
9.5 h	$H(GePh_2)_3H$	46
14 h	$H(GePh_2)_4H$	69

Insertion of a germylene into a germanium-halogen bond is another useful mechanism for synthesizing trigermanes. In 1986, Dräger reported that the germylene Ph_2Ge: inserting into the Ge-Cl bond of Ph_2GeHCl yielded $H(GePh_2)_nCl$.[21] The

germylene is generated from Ph_2GeHCl and Et_3N in a one-pot synthesis. Control over the length of the oligomeric chain was managed through the ratio of Ph_2GeHCl to Et_3N (**Table 1.7**). Subsequent reaction of the product with carbon tetrachloride (CCl_4) in the presence of catalytic amounts of azobisisobutyronitrile (AIBN), afforded the dichlorinated oligomeric product where the chlorine atoms are bound to the terminal germanium atoms, $Cl(GePh_2)_nCl$ (n = 2-4).[21]

Table 1.7. Ratios of Ph_2GeHCl to NEt_3 used to synthesize germanes containing 2 – 4 germanium atoms through the insertion of a germylene into a Ge – Cl bond.[21]

Ratio	**Yield**		
Ph_2GeHCl : NEt_3	**$Cl(GePh_2)_2Cl$**	**$Cl(GePh_2)_3Cl$**	**$Cl(GePh_2)_4Cl$**
3:2	60%	10%	0%
3:3	26%	40%	2%
3:6	23%	21%	36%

The last three methods described for the synthesis of trigermanes required the control of reaction conditions and reaction time in order to selectively increase the yield of the trigermane while suppressing the quantity of other oligomers. The action of Grignard reagents on germanium tetrachloride to yield oligogermanes, as mentioned earlier in the chapter (**Scheme 1.2**), is another such reaction. By removing excess magnesium metal and using THF as the reaction medium, the yield of octaphenyltrigermane was maximized (11% yield) with minimal formation of the tetragermane.[25]

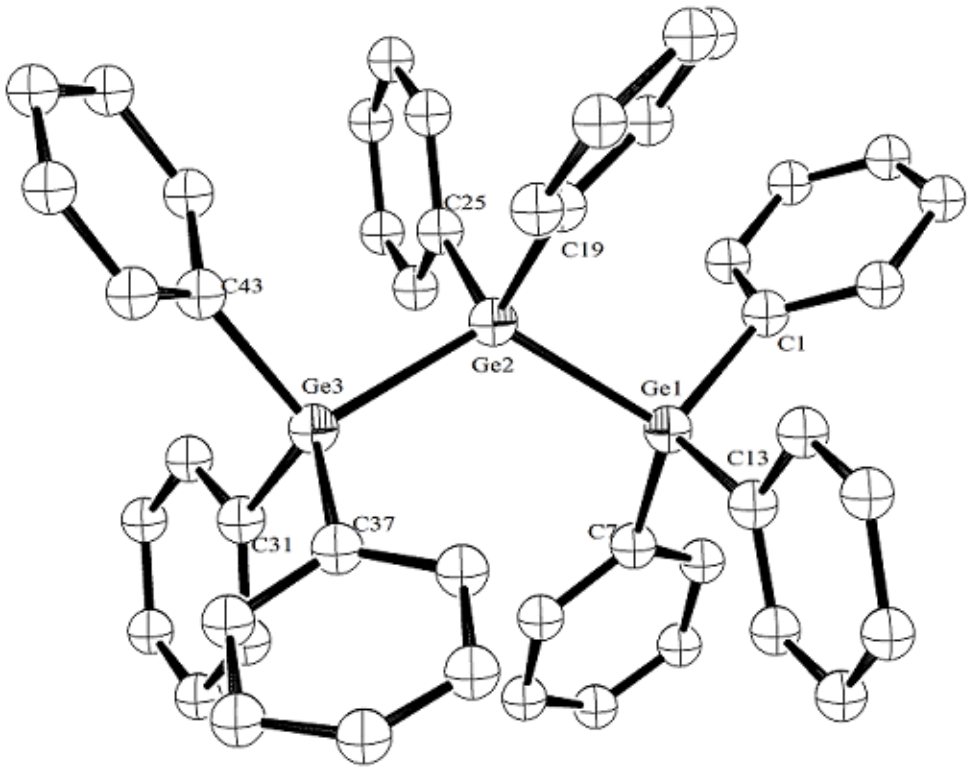

Figure 1.3. ORTEP diagram of $Ph_3GeGePh_2GePh_3$.[25]

The first structurally characterized trigermane $Ph_3GeGePh_2GePh_3$, synthesized via the process shown in **Scheme 1.2**, crystallizes in an orthorhombic space group with D_{2h} symmetry.[25] An ORTEP diagram, shown in **Figure 1.3**, illustrates the structure with a distorted tetrahedral geometry around the three germanium atoms. The angle of the Ge–Ge–Ge bond is 121.3°. The average of the Ge–Ge–C angles is 108.7°, with the most obtuse Ge–Ge–C angle being 116.0°, and the acute angle being 101.8°. The average Ge–Ge bond for $Ph_3GeGePh_2GePh_3$ is 2.440 Å, and the average Ge–C bond is 1.960 Å, which are within typical values for organogermanes.

While methods are known for synthesizing trigermanes, progress needs to be made to develop discrete molecules instead of the product mixtures observed using previously reported methods. Unlike most methods that have been described, samarium (II) iodide as detailed earlier in the chapter, is an adequate reagent for the synthesis of trigermanes.[72,73] However, costing $75.50/gram, SmI_2 is two times more expensive than solid lithium ($37.90/gram), and 85 times more expensive than sodium cubes in mineral oil ($0.89/gram) when purchased through Sigma-Aldrich.

LINEAR TETRAGERMANES

Synthesis of the first tetragermane to be structurally characterized, $Ph_3GeGePh_2GePh_2GePh_3$, was achieved by Grignard reagents acting on germanium tetrachloride in 18% yield, as a mixture with di- and trigermanes.[25] Many known syntheses of tetragermanes are the same as those used for trigermanes, but through manipulating reaction conditions and times, the yield of tetragermane product can be maximized. Triethylamine reacting with Ph_2GeHCl for the insertion of a germylene in a Ge – Cl bond[19] as well as the decomposition of Ph_2GeLi_2 in Et_3N,[94] are viable methods for the synthesis of tetragermanes. Germyl anions have also been used for the synthesis of tetragermanes as shown in **Scheme 1.7**.[74] In this reaction, Ph_3GeLi reacts with the 1,2-dichlorinated digermane to produce a perphenylated tetragermane that was isolated in 25% yield.[74]

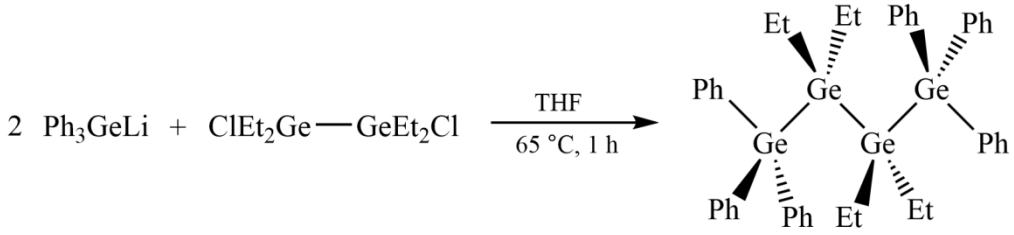

Scheme 1.7. Reaction for the synthesis of 2,2,3,3-tetraethyl-1,1,1,4,4,4-hexaphenyltetragermane.[74]

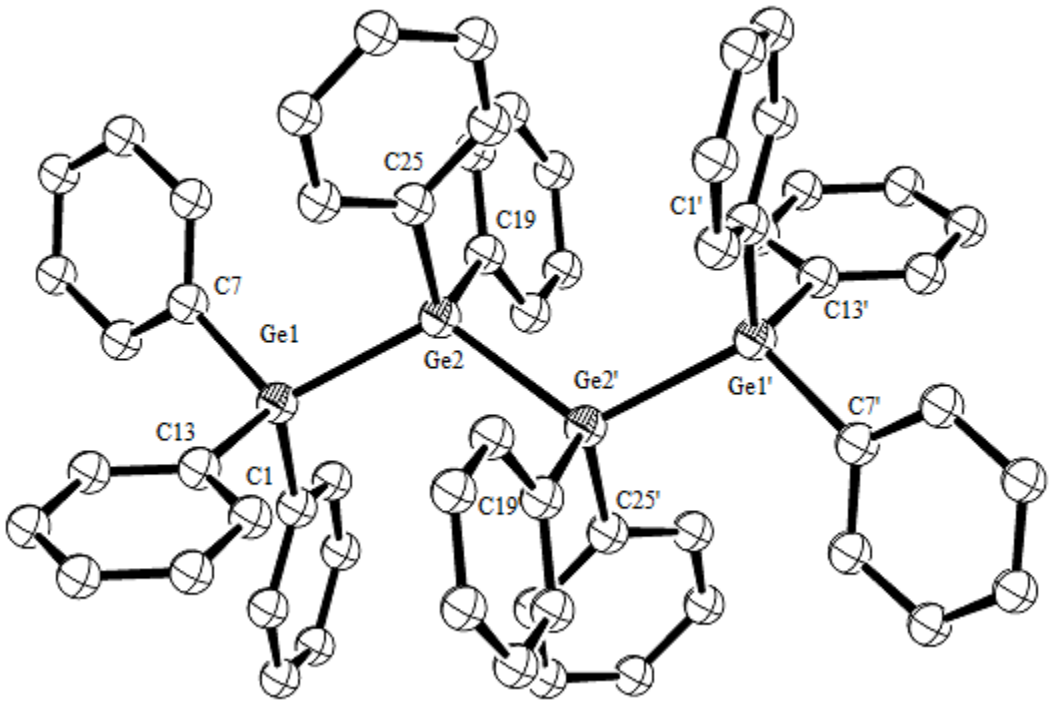

Figure 1.4. ORTEP diagram of $Ph_3GeGePh_2GePh_2GePh_3 \cdot 2\ C_6H_6$, with the benzene solvate molecules omitted.[25]

The tetragermane $Ph_3GeGePh_2GePh_2GePh_3 \cdot 2\ C_6H_6$ crystallizes in the P-1 space group with the Ge_4 backbone in a staggered conformation (**Figure 1.4**).[25] The two halves of the molecule are related by a center of inversion. The average Ge–Ge bond distance is 2.462 Å, which is slightly larger than the average Ge–Ge bond distance in $Ph_3GeGePh_2GePh_3$, and the average Ge–C bond distance is 1.968 Å. The germanium atoms were aligned in a bent fashion with the Ge–Ge–Ge angle being 117.8°. The average Ge–Ge–C and C–Ge–C angles are 109.5° and 107.1°, respectively.

LINEAR PENTAGERMANES

In 1967, Bulten and co-workers published a communication describing the synthesis of a tetragermane by a Wurtz-type coupling reaction involving 1-chloropentaethyldigermane and potassium in HMPT.[93] Two years later, the same group published a report wherein a compound that they originally thought was a tetragermane was actually the pentagermane ($Et_3GeGeEt_2GeEt_2GeEt_2GeEt_3$). Smaller quantities of hexaethyldigermane ($Et_3GeGeEt_3$), octaethyltrigermane ($Et_3GeGeEt_2GeEt_3$), and decaethyltetragermane ($Et_3GeGeEt_2GeEt_2GeEt_3$) were obtained.[95] After the pentagermane, the trigermane was isolated in the largest yield, with much smaller quantities of the di- and tetra-germane. Combustion analysis, UV/visible absorption spectroscopy and refractive index were all employed to support the claim of the successful synthesis of the pentagermane. The pathway for the synthesis as depicted in **Scheme 1.8**, is hypothesized to initially result in the formation of a tetragermane which

disproportionate upon reaction with excess potassium into triethylgermylpotassium (Et_3GeK) and $Et_3GeEt_2GeEt_2GeK$.[95] The reaction of both of these compounds with the starting material Et_3GeEt_2GeCl would result in the formation of the penta- and tri-germanes as major products. Separation of the pentagermane from the other components was accomplished through distillation.

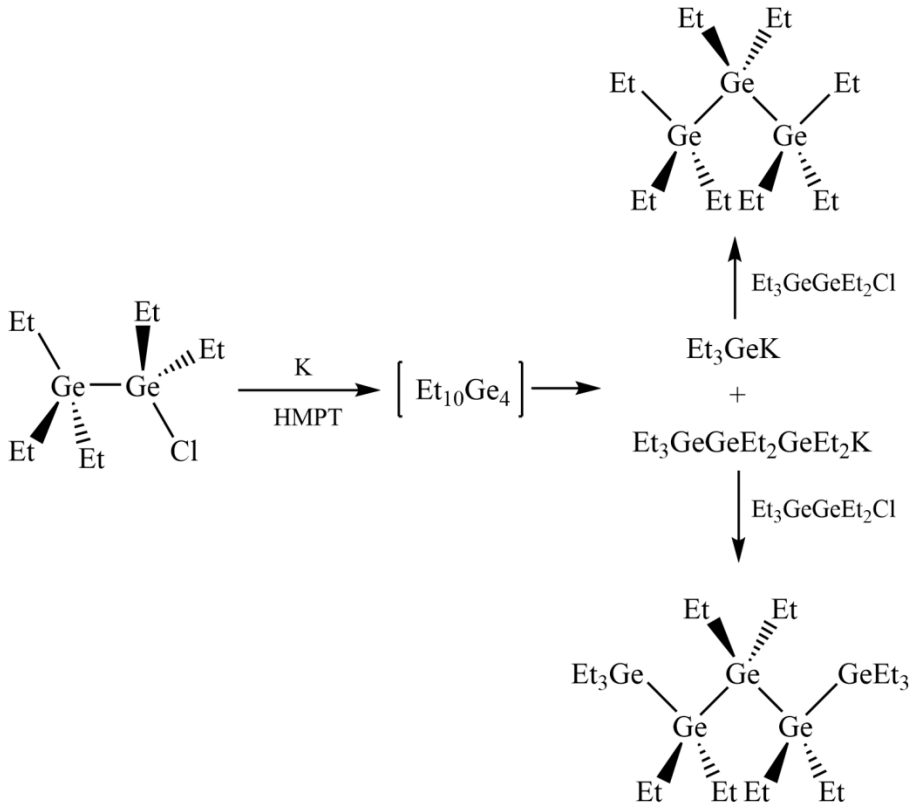

Scheme 1.8. The disproportionation of a tetragermane with excess potassium to form octaethyltrigermane and dodecaethylpentagermane.[95]

The same year that Bulten re-published his findings, another procedure was published which could prepare the perphenylated pentagermane, $Ph_3Ge(GePh_2)_3GePh_3$. The multi-step synthesis (**Scheme 1.9**) involved the reaction of pentaphenyldigermane,

Ph_3GePh_2GeH, with *n*-butyllithium, forming the digermyllithium compound Ph_3GePh_2GeLi.[24] When two equivalents of the germyllithium compound were added to diphenylgermanium dichloride (Ph_2GeCl_2) a mixture of the perphenylated germanes $Ph(GePh_2)_nPh$ (n = 2–5) was obtained.[24] The perphenylated pentagermane, although only isolated in 0.2 % yield, became the first structurally characterized pentagermane, and the longest oligogermane to be characterized by this method, to date.

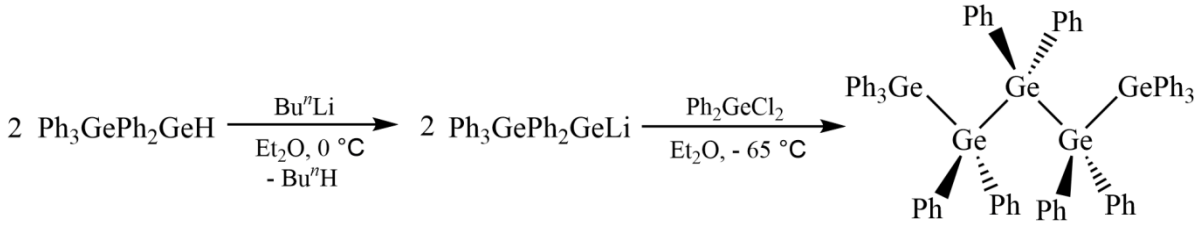

Scheme 1.9. The synthesis of dodecaphenylpentagermane from a digermyl anion and Ph_2GeCl_2.[24]

The pentagermane $Ph_3Ge(GePh_2)_3GePh_3$, as depicted in **Figure 1.5**, crystallizes in the orthorhombic space group $P2_1\ 2_1\ 2_1$.[24] As opposed to the linear tetragermane, where all four germanium atoms are coplanar, the pentagermane contains four atoms that are coplanar and one atom that is canted out of the Ge_4 plane. The environment at the germanium atoms is less distorted from the ideal tetrahedral environment than found in the analogous tri- or tetragermane. The average Ge–Ge–Ge bond angles in Ge_5Ph_{12}, Ge_4Ph_{10}, and Ge_3Ph_8 are 115.6°, 117.8°, and 121.3° respectively.[24,25] The average Ge–Ge bond in the perphenylated pentagermane is 2.460 Å; the internal Ge–Ge bonds are longer than the external Ge–Ge bonds with average values of 2.477 Å and 2.443 Å, respectively.

The bond elongation among the Ge – Ge bonds is likely due to steric effects. The average Ge–Ge–C angle measures 109.0° and the C–Ge–C angle averages 108.1°.

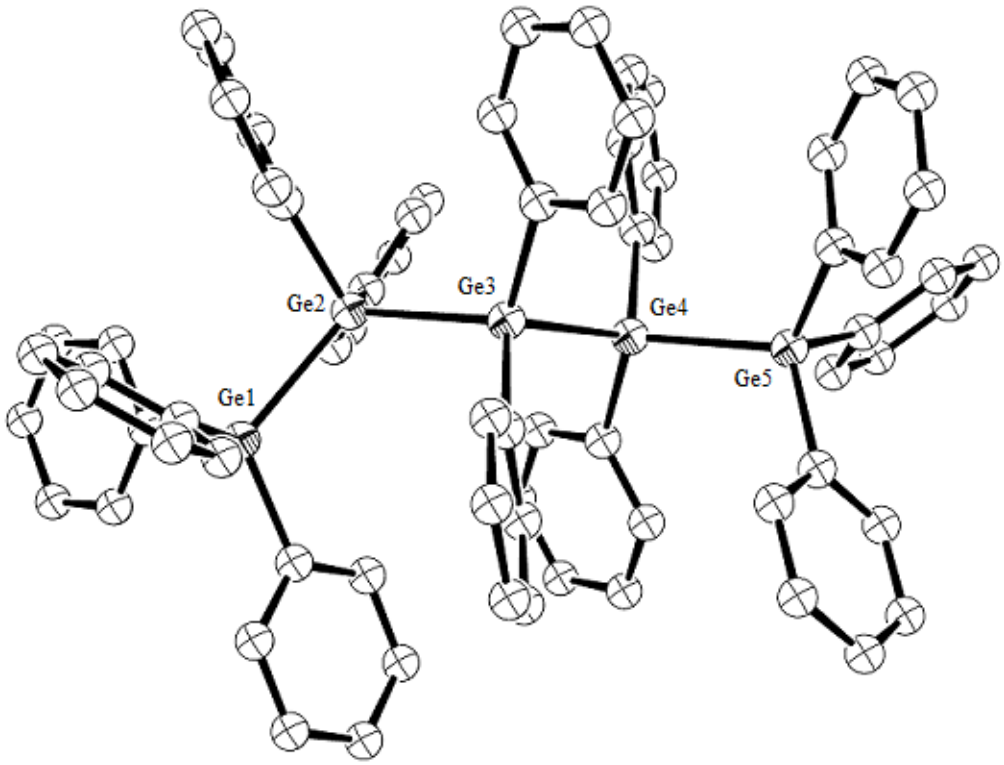

Figure 1.5. ORTEP diagram of $Ph_3Ge(GePh_2)_3GePh_3$.[24]

One of the most successful processes for synthesis of a pentagermane was reported in 1969 and consisted of step-wise metathesis reactions as depicted in **Scheme 1.10**, to yield $Ph(GeMe_2)_5Ph$.[96] The trigermane $Ph(GeMe_2)_3Ph$ was synthesized in 54% yield from the digermane $Ph(GeMe_2)_2Ph$, and the pentagermane could be obtained in 28% yield from the trigermane $Ph(GeMe_2)_3Ph$. A similar method was also successful in synthesizing the analogous 1,4-diphenyloctamethyltetragermane, $Ph(GeMe_2)_4Ph$.[96]

Germyllithium compounds were also used by Castel *et al.* when triphenylgermyllithium was added to the 1,3-dichlorinated ethyltrigermane, forming the pentagermane $Ph_3Ge(GeEt_2)_3GePh_3$,[74] where the pentagermane was isolated in 59% yield. It is of note that pentagermanes were synthesized in higher yields when the germyllithium contained just one germanium atom as in the reactions shown in **Scheme 1.10**, compared to the reaction involving a germyllithium containing two germanium atoms, as shown in **Scheme 1.9**, in which only 0.2% pentagermane was isolated.

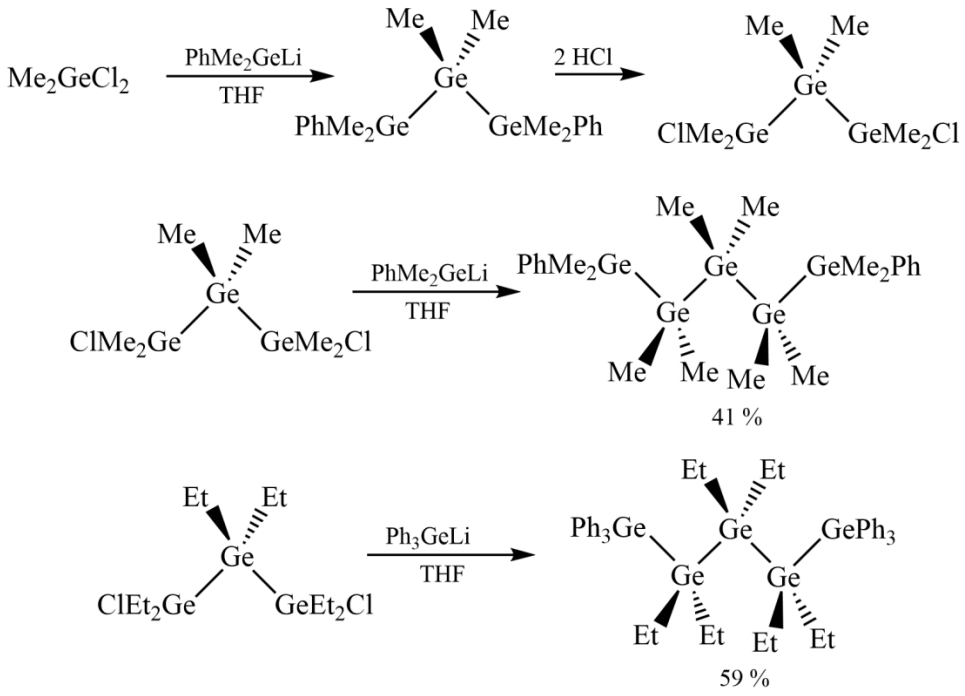

Scheme 1.10. The formation of pentagermanes via Ph_3Ge^- anions.[74,96]

The successful synthesis of pentagermanes still possesses the problem of producing multiple products, which still needs to be overcome. An increase in multiple products occurs more frequently when the synthesis of larger oligogermanes is attempted

in a one-pot procedure, making the stepwise design more appealing. Although stepwise synthesis is an effective method to tailor the makeup of the pentagermanes and allows for greater control over the substituent pattern, much lower yields are typically obtained and the formation of multiple products is still a problem. Ideally methods need to be developed to improve both the stepwise tailored control of larger oligogermanes, as well as effective, rapid processes for synthesizing larger discrete molecules.

HIGHER OLIGOGERMANES

A few examples of longer, linear oligomeric germanium species have been described.[74,95,97,98] Of the known linear germanium compounds containing six or more germanium atoms along the backbone, none have been structurally characterized. In some cases, lithium was used as a reducing agent to form compounds such as $Et_3Ge(GeEt_2)_4GeEt_3$[95] and the permethylated decagermane $Ge_{10}Me_{22}$,[98] the latter of which is an isolated side product from the Wurtz coupling of Me_3GeCl and Me_2GeCl_2 promoted by lithium metal. The permethylated species containing 2, 3, 5 and 10 germanium atoms were all detected by gas chromatography electrochemical analysis and UV/visible spectroscopy, but were not further characterized.[99]

Germanium compounds containing 6 and 7 germanium atoms were obtained when Me_3Al was reacted with a germanium halide precursor. When using 12.5 equivalents of Me_3Al with $GeCl_4$ in the presence of NaCl, the permethylated species obtained contain 3 – 6 germanium atoms along the backbone.[97] By using GeI_2 as the

source of germanium and 7 equivalents of Me_3Al, the oligogermanes $Me(MeGe_2)_nMe$, where n = 5, 6, and 7, were detected.[97] All compounds were identified by gas chromatography, but no further characterization was reported.

HYDROGERMOLYSIS

In 2006, Weinert and Subashi reported on the hydrogermolysis reaction (**Scheme 1.11**).[84] The reaction involves the use of germanium amide and a germanium hydride to form the germanium – germanium bond. Originally attempted in benzene at room temperature and refluxing benzene or toluene, the reaction did not serve to form Ge – Ge bonds. However, when using acetonitrile as the solvent, the Ge – Ge bond was successfully formed with typical product yields of 80 – 85%.[84]

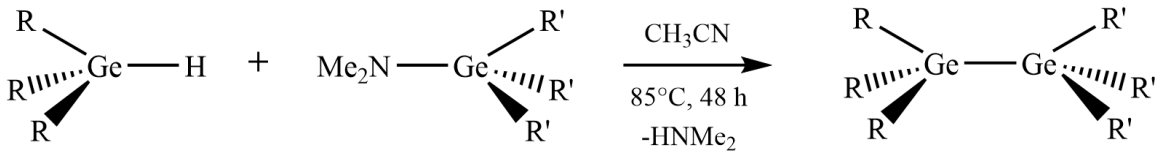

Scheme 1.11. Representative scheme for the hydrogermolysis reaction.[84]

The analogous hydrostannolysis reaction has proven to be useful in the preparation of oligostannanes.[55-57,100] However, the same reaction with germanium proved to be much more difficult to carry out. It was originally thought that highly electron withdrawing groups on the germanium containing the hydrogen precursor were necessary in order to "activate" the germanium-bound hydrogen.[101] A representative

synthesis is shown in **Scheme 1.12** in which the germanium-bound hydrogen is activated by attaching highly electron withdrawing C_6F_5 groups.

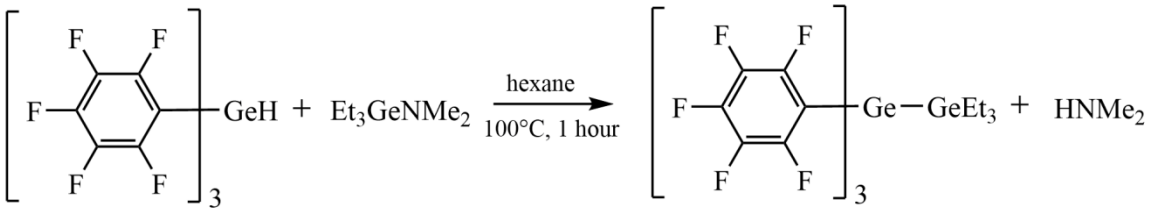

Scheme 1.12. Formation of a germanium-germanium bond using an "activated" germanium-bound hydrogen.[101]

The use of the hydrogermolysis reaction to form Ge – Ge bonds was successfully performed in a few cases using pentafluorophenyl groups as the activating ligands by refluxing the reaction mixture in hexane for one to two hours.[101,102] Known products which have successfully been produced using this method are listed in **Table 1.8**. The limitation of this reaction is the inability to vary the substituents on the germanium atoms, making the "activated" hydrogermolysis an inefficient tool for the preparation of a diverse array of oligogermane species.

Unlike the use of "activated" germanium-bound hydrogen, it was found that the hydrogermolysis reaction could proceed without the use of highly electron withdrawing groups when acetonitrile, CH_3CN, was used as the solvent. The conundrum of why the reaction would only occur in CH_3CN was elucidated by ^{1}H-NMR studies in deuterated acetonitrile.[87] The reaction was found to proceed via the formation of an α-germyl nitrile intermediate. Separate studies were completed in order to synthesize the α-germyl nitrile

independently by reacting the corresponding monochloride with $LiCH_2CN$, generated *in situ* from lithium diisopropylamide and acetonitrile (**Scheme 1.13**).[87]

Table 1.8. The synthesis of di- and trigermanes through the hydrogermolysis reaction using "activated" Ge–H bonds.

Germanium Hydrogen	Germanium Amide	Product	Yield
$(C_6F_5)_3GeH$	$(p\text{-Tol})_3GeNMe_2$	$(p\text{-Tol})_3GeGe(C_6F_5)_3$	66 %[102]
$(C_6F_5)_2GeH_2$	$(p\text{-Tol})_3GeNMe_2$	$((p\text{-Tol})_3Ge)_2Ge(C_6F_5)_2$	51 %[102]
$(C_6F_5)_3GeH$	Ph_3GeNMe_2	$Ph_3GeGe(C_6F_5)_3$	86 %[102]
$(C_6F_5)_3GeH$	Et_3GeNEt_2	$Et_3GeGe(C_6F_5)_3$	91 %[101]
$(C_6F_5)_2GeH_2$	Et_3GeNEt_2	$(Et_3Ge)_2Ge(C_6F_5)_2$	66 %[101]

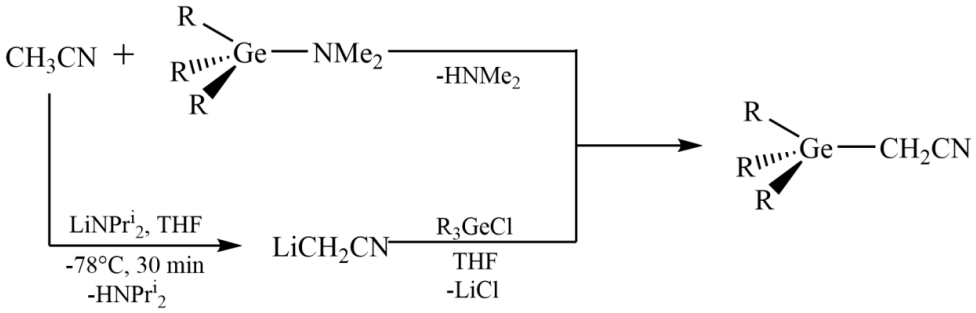

Scheme 1.13. Synthesis of α-germyl nitrile intermediate through various methods.[87]

The synthesis of three separate α-germyl nitrile species having phenyl, isopropyl, and *tert*-butyl groups on the germanium was achieved.[87] It is of note that the formation of the α-germyl nitrile was completed in as little as 6 hours *in situ* in CD_3CN, while the generation of the digermane from the α-germyl nitrile was completed in 48 hours. It is

therefore likely that the formation of the α-germyl nitrile is the fast step in the synthesis of a digermane.

Table 1.9. The synthesis of digermanes as reported in the literature via the hydrogermolysis reaction.

Reactants	**Major Product**	**Yield**	**λ_{max}**	**Ref.**
$Bu_3GeNMe_2 + Ph_3GeH$	$Bu_3GeGePh_3$	83%	232 nm	B
$Et_3GeNMe_2 + Ph_3GeH$	$Et_3GeGePh_3$	84%	231 nm	B
$Bu_3GeNMe_2 + Me_3GeH$	$Bu_3GeGeMe_3$	86%	--	B
$Pr^i_3GeNMe_2 + Ph_3GeH$	$Pr^i_3GeGePh_3$	91%	234 nm	A
$Bu^s_3GeNMe_2 + Ph_3GeH$	$Bu^s_3GeGePh_3$	81%	244 nm	C
$Me_2PhGeNMe_2 + Ph_3GeH$	$Me_2PhGeGePh_3$	76%	244 nm	C
$Bu^i_3GeNMe_2 + Ph_3GeH$	$Bu^i_3GeGePh_3$	79%	232 nm	D
$Hex^n3GeNMe_2 + Ph_3GeH$	$Hex^n_3GeGePh_3$	43%	241 nm	D
$(C_{18}H_{37})_3GeNMe_2 + Ph_3GeH$	$(C_{18}H_{37})_3GeGePh_3$	50%	236 nm	D
$Bu^tMe_2GeNMe_2 + Ph_3GeH$	$Bu^tMe_2GeGePh_3$	89%	238 nm	D

References: A,[87] B,[84] C,[103] D[85]

Since the discovery of the hydrogermolysis reaction used for the formation of germanium-germanium bonds, the preparation of approximately thirty compounds have been reported using this method, including the synthesis of digermanes (**Table 1.9**) and the synthesis of longer branched and linear oligogermanes (**Table 1.10**). Yields ranged

from good to excellent, making the hydrogermolysis reaction an effective and useful tool in synthesizing oligogermanes**.**

Table 1.10. The synthesis of branched and linear oligomeric germanium compounds (Ge ≥ 2) as reported in literature with the use of the hydrogermolysis reaction.

Reactants	**Major Product**	**Yield**	**λ_{max}**	**Ref.**
$R_2GeR'(NMe_2)$ + Ph_3GeH	Ph_3GeGeR_2R'	R = Et, 75%	--	B
		R = Bu^n, 76%	224 nm	A
		R = Ph, 92%	--	B
$R_2GeR'(NMe_2)$ + Ph_3GeR_2GeH	$Ph_3GeGeR_2GeR_2R'$	R = Et, 90%	--	B
		R = Bu^n, 94%	232 nm	B
$R_2GeR'(NMe_2)$ + $Ph_3Ge(R_2Ge)_2H$	$Ph_3Ge(GeR_2)_2GeR_2R'$	R = Et, 97%	235 nm	B
		R = Bu^n, 85%	241 nm	B
3 Ph_3GeNMe_2 + $PhGeH_3$	$PhGe(GePh_3)_3$	85%	256 nm	C
3 $Bu_2GeR'(NMe_2)$ + $PhGeH_3$	$PhGe(GeBu_2R')_3$	95%	234 nm	C

$R_2GeR'(NMe_2)$ + $PhGe(GeBu_2H)_3$	$PhGe(GeBu_2GeR_2R')_3$	R = Et, 43%	236 nm	C
		$R = Bu^n$, 89%	240 nm	C
		R = Ph, 30%	242 nm	C
2 $R_2GeR'(NMe_2)$ + Ph_2GeH_2	$R'R_2GeGePh_2GeR_2R'$	R = Et, 72%	243 nm	A
		$R = Bu^n$, 83%	243 nm	A
		R = Ph, 92%	247 nm	A
3 $Bu^n{}_3GeNMe_2$ + $PhGeH_3$	$PhGe(GeBu^n{}_3)_3$	98%	233 nm	D
2 Ph_3GeNMe_2 + $HPh_2GeGePh_2H$	$Ph_3Ge(GePh_2)_2GePh_3$	79%	269 nm	E
2 Ph_3GeNMe_2 + $HPh_2GeGePh_2GePh_2H$	$Ph_3Ge(GePh_2)_3GePh_3$	83%	295 nm	E

R' = $CH_2CH_2OCH_2CH_3$ References: A,[104] B,[84] C,[105] D,[103] E[86]

The perphenylated pentagermane was the longest linear oligomeric germanium compound synthesized and structurally characterized prior to 2013. Though originally prepared through nucleophilic substitution of $LiGePh_2GePh_3$ on Cl_2GePh_2,[24] it was also successfully synthesized in our laboratory by utilizing the hydrogermolysis reaction.[86] When one equivalent of Ph_3GeNMe_2 was added to $H(GePh_2)_3H$, the tetragermane $Ph_3Ge(GePh_2)_3H$ was formed in 79% yield. By addition of 2 equivalents of

triphenylgermanium dimethylamide to $H(GePh_2)_3H$, the perphenylated pentagermane Ge_5Ph_{12} was isolated in 83% yield.[86] A crystal of the pentagermane suitable for X-ray analysis was obtained and analyzed at 100 K as opposed to crystals previously characterized at 273 K. The average Ge–Ge bond distance and average Ge–Ge–Ge bond angle for the crystal obtained from the hydrogermolysis reaction are 2.5402(6) Å and 115.52(2)°, respectively, which are nearly identical to the structure analyzed at 273 K.[86]

The success of the hydrogermolysis reaction at synthesizing longer, discrete, linear oligomeric germanium compounds, makes it an ideal candidate for further synthetic endeavors in order to obtain even longer-chain oligogermanes. The goal of the investigations described herein is the preparation of discrete compounds containing six or more germanium atoms disposed in a linear fashion.

REFERENCES

(1) Winkler, C. *Berichte der Deutschen Chemischen Gesellschaft* **1886**, *19*, 210.

(2) Winkler, C. *Journal fur Praktische Chemie* **1886**, *142*, 177.

(3) Glockling, F. *The Chemistry of Germanium*; Academic P.: New York, London, 1969.

(4) Hayashi, T.; Uchimaru, Y.; Reddy, N. P.; Tanaka, M. *Chem. Lett.* **1992**, 647.

(5) Satge, J. *Main Group Metal Chemistry* **2004**, *27*, 301.

(6) Menchikov, L. G.; Ignatenko, M. A. *Pharmaceutical Chemistry Journal* **2013**, *46*, 635.

(7) Weinert, C. S. *Dalton Transactions* **2009**, 1691.

(8) Balaji, V.; J., M. *Polyhedron* **1991**, *10*, 1265.

(9) Miller, R. *Chem. Rev.* **1989**, *89*, 1359.

(10) Ortiz, J. V. *Polyhedron* **1991**, *10*, 1285.

(11) Pitt, C. G.; Bursey, M. M.; Rogerson, P. F. *J. Am. Chem. Soc.* **1970**, *92*, 519.

(12) Winkler, C. *Journal fur Praktische Chemie* **1887**, *36*, 177.

(13) Morgan, G. T.; Dugland, H.; Drew, K. *J. Chem. Soc., Trans.* **1925**, *127*, 1760.

(14) Dräger, M. *Z. Anorg. Allg. Chem.* **1980**, *466*, 145.

(15) Dräger, M.; Häberle, K. *J. Organomet. Chem.* **1985**, *280*.

(16) Dräger, M.; Ross, L. *Z. Anorg. Allg. Chem.* **1980**, *469*, 115.

(17) Dräger, M.; Ross, L. *Z. Anorg. Allg. Chem.* **1981**, *476*, 95.

(18) Dräger, M.; Ross, L. *Z. Anorg. Allg. Chem.* **1980**, *460*, 207.

(19) Dräger, M.; Simon, D. *J. Organomet. Chem.* **1986**, *306*, 183.

(20) Dräger, M.; Simon, D. *Z. Anorg. Allg. Chem.* **1981**, *472*, 120.

(21) Häberle, K.; Dräger, M. *J. Organomet. Chem.* **1986**, *312*, 155.

(22) Häberle, K.; Dräger, M. *Z. Anorg. Allg. Chem.* **1987**, *551*, 116.

(23) Häberle, K.; Dräger, M. *Zeitschrift fur Naturforschung* **1987**, *42*, 323.

(24) Roller, S.; Dräger, M. *J. Organomet. Chem.* **1986**, *316*, 57.

(25) Roller, S.; Simon, D.; Dräger, M. *J. Organomet. Chem.* **1986**, *301*, 27.

(26) Ross, L.; Dräger, M. *J. Organomet. Chem.* **1980**, *199*, 195.

(27) Ross, L.; Dräger, M. *J. Organomet. Chem.* **1980**, *194*, 23.

(28) Ross, L.; Dräger, M. *Z. Anorg. Allg. Chem.* **1981**, *472*, 109.

(29) Ross, L.; Dräger, M. *Z. Anorg. Allg. Chem.* **1984**, *515*, 141.

(30) Ross, L.; Dräger, M. *Zeitschrift fur Naturforschung* **1983**, *38*, 665.

(31) Ross, L.; Dräger, M. *Z. Anorg. Allg. Chem.* **1984**, *519*, 225.

(32) Simon, D.; Häberle, K.; Dräger, M. *J. Organomet. Chem.* **1984**, *267*, 133.

(33) Benfield, R. E.; Cragg, F. H.; Jones, R. G.; Swain, A. C. *J. Chem. Soc., Chem. Commun.* **1992**, 1022.

(34) Kimata, Y.; Suzuki, H.; Satoh, S.; Kuriyama, A. *Chem. Lett.* **1994**, 1163.

(35) Kimata, Y.; Suzuki, H.; Satoh, S.; Kuriyama, A. *Organomet.* **1995**, *14*, 2506.

(36) Jones, R. G.; Benfield, R. E.; Cragg, F. H.; Swain, A. C.; Webb, S. J. *Macromolecules* **1993**, *26*, 4878.

(37) Hengge, E. F. *J. Inorg. Organomet. Polym.* **1993**, *3*, 287.

(38) Miller, R. D.; Jenkner, P. K. *Macromolecules* **1995**, *27*, 5921.

(39) Lacave-Goffin, B.; Hevesi, L.; Devaux, J. *Chem Commun* **1995**, 769.

(40) Kashimura, S.; Ishifune, M.; Yamashita, N.; Bu, H.; Takebayashi, M.; Kitajima, S.; Yoshiwara, D.; Kataoka, Y.; Nishida, R.; Kawasaki, S.; Murase, H.; Shono, T. *J. Org. Chem.* **1999**, *64*, 6615.

(41) Zuev, V. V.; Skvortsov, N. K. *J. Polym. Sci. A.: Polym. Chem.* **2003**, *41*, 3761.

(42) Bratton, D.; Holder, S. J.; Jones, R. G.; Wong, W. K. C. *J. Organomet. Chem.* **2003**, *685*, 60.

(43) Imori, T.; Lu, V.; Cai, H.; Tilley, T. D. *J. Am. Chem. Soc.* **1995**, *117*, 9931.

(44) Imori, T.; Tilley, T. D. *J. Chem. Soc., Chem. Commun.* **1993**, 1607.

(45) Thompson, S. M.; Schubert, U. *Inorgan. Chim. Acta* **2004**, *357*, 1959.

(46) Choffat, F.; Smith, P.; Caseri, W. *J. Mat. Chem.* **2005**, *15*, 1789.

(47) Lu, V.; Tilley, T. D. *Macromolecules* **1996**, *29*, 5763.

(48) Lu, V.; Tilley, T. D. *Macromolecules* **2000**, *33*, 2403.

(49) Deacon, P. R.; Devylder, N.; Hill, M. S.; Mahon, M. F.; Molloy, K. C.; Price, G. J. *Journal of Organometallic Chemistry* **2003**, *687*, 46.

(50) Okano, M.; Matsumoto, N.; Arakawa, M.; Tsuruta, T.; Hamano, H. *Chem Commun* **1998**, 1799.

(51) Babcock, J. R.; Sita, L. R. *J. Am. Chem. Soc.* **1996**, *118*, 12481.

(52) Mochida, K.; Hayakawa, M.; Tsuchikawa, T.; Yokoyama, Y.; Wakasa, M.; Hayashi, H. *Chem. Lett.* **1998**, 91.

(53) Adams, S.; Dräger, M. *J. Organomet. Chem.* **1985**, *288*, 295.

(54) Adams, S.; Dräger, M.; Mathiasch, B. *J. Organomet. Chem.* **1987**, *326*, 173.

(55) Sita, L. R. *Adv. Organomet. Chem.* **1995**, *38*, 189.

(56) Sita, L. R. *Acc. Chem. Res.* **1994**, *27*, 191.

(57) Sita, L. R. *Organomet.* **1992**, *11*, 1442.

(58) Sita, L. R.; Terry, K. W.; Shibata, K. *J. Am. Chem. Soc.* **1995**, *117*, 8049.

(59) Cross, R. J.; Glockling, F. *J. Organomet. Chem.* **1965**, *146*, 146.

(60) Gilman, H.; Melvin, H. W. *J. Am. Chem. Soc.* **1949**, *71*, 4050.

(61) Johnson, O. H.; Harris, D. M. *J. Am. Chem. Soc.* **1950**, *72*, 5566.

(62) West, R. *J. Am. Chem. Soc.* **1953**, *75*, 6080.

(63) Lesbre, M.; Mazerolles, P.; Satge, J. *The Organic Compounds of Germanium*; John Wiley & Sons: New York, 1971.

(64) Amadoruge, M. L.; Weinert, C. S. *Chem. Rev.* **2008**, *108*, 4253.

(65) Bauer, H.; Burschkies, K. *Berichte der Deutschen Chemischen Gesellschaft* **1934**, *67B*, 1041.

(66) Johnson, O. H.; Nebergall, W. H. *J. Am. Chem. Soc.* **1948**, *70*, 1706.

(67) Shackelford, J. M.; De Schmertzing, H.; Heuther, C. H.; Podall, H. *J. Org. Chem.* **1963**, *28*, 1700.

(68) Neumann, W. P.; Kuhlein, K. *Tetrahedron Lett.* **1963**, 1541.

(69) Neumann, W. P.; Kuhlein, K. *Liebigs Ann. Chem.* **1965**, *683*, 1.

(70) Carrick, A.; Glockling, F. *J. Chem. Soc. A.* **1966**, 623.

(71) Semlyen, J. A.; Walker, G. R.; Phillips, C. S. G. *J. Chem. Soc.* **1965**, 1197.

(72) Azemi, T.; Yokoyama, Y.; Mochida, K. *J. Organomet. Chem.* **2005**, *690*, 1588.

(73) Yokoyama, Y.; Hayakawa, M.; Azemi, T.; Mochida, K. *J. Chem. Soc., Chem. Commun* **1995**, 2275.

(74) Castel, A.; Riviere, P.; Saint-Roch, B.; Satge, J. *J. Organomet. Chem.* **1983**, *247*.

(75) Tamborski, C.; Ford, F. E.; Lehn, W. L.; Moore, G. L.; Soloski, E. J. *J. Org. Chem.* **1962**, *27*, 619.

(76) Bulten, E. J.; Noltes, J. G. *Tetrahedron Lett.* **1966**, *7*, 4389.

(77) *CRC Handbook of Chemistry and Physics*; 87th ed.; Lide, D. R., Ed.; CRC Press: Boca Raton, FL, 2006.

(78) Kraus, C. A.; Flood, E. A. *J. Am. Chem. Soc.* **1932**, *54*, 1635.

(79) Brown, M. P.; Fowles, G. W. A. *J. Chem. Soc.* **1958**, 2811.

(80) Triplett, K.; Curtis, M. D. *J. Organomet. Chem.* **1976**, *107*, 23.

(81) Seyferth, D. *J. Am. Chem. Soc.* **1957**, *79*, 2738.

(82) Glockling, F.; Hooton, K. A. *J. Chem. Soc.* **1962**, 3509.

(83) Harris, D. M.; Nebergall, W. H.; Johnson, O. H.; Rochow, E. E.; Tolivaisa, N. *Inorg. Synth.* **1957**, *5*, 72.

(84) Subashi, E.; Rheingold, A. L.; Weinert, C. S. *Organometallics* **2006**, *25*, 3211.

(85) Schrick, E. K.; Forget, T. J.; Roewe, K. D.; Schrick, A. C.; Moore, C. E.; Golen, J. A.; Rheingold, A. L.; Materer, N. F.; Weinert, C. S. *Organometallics* **2013**, *32*, 2245.

(86) Samanamu, C. R.; Amadoruge, M. L.; Schrick, A. C.; Chen, C.; Golen, J. A.; Rheingold, A. L.; Materer, N. F.; Weinert, C. S. *Organometallics* **2012**, *31*, 4374.

(87) Amadoruge, M. L.; DiPasquale, A. G.; Rheingold, A. L.; Weinert, C. S. *J. Organomet. Chem.* **2008**, *693*, 1771.

(88) Parkanyi, L.; Kalman, A.; Sharma, S.; Nolen, D. M.; Pannell, K. H. *Inorg. Chem.* **1994**, *33*, 180.

(89) Weidenbruch, M.; Grimm, F.-T.; Herrndorf, M.; Schafer, A.; Peters, K.; von Schnering, H. G. *J. Organomet. Chem.* **1988**, *341*, 335.

(90) Metlesics, W.; Zeiss, H. *J. Am. Chem. Soc.* **1960**, *82*, 3321.

(91) Curtis, M. D.; Wolber, P. *Inorg. Chem.* **1972**, *11*, 431.

(92) Kraus, C. A.; Brown, C. L. *J. Am. Chem. Soc.* **1930**, *52*, 4031.

(93) Bulten, E. J.; Noltes, J. G. *Tetrahedron Lett.* **1967**, *16*, 1443.

(94) Castel, A.; Riviere, P.; Satge, J.; Ko, H. Y. *Organometallics* **1990**, *9*, 205.

(95) Bulten, E. J.; Noltes, J. G. *J. Organomet. Chem.* **1969**, *16*, 8.

(96) Kumada, M.; Sakamoto, S.; Ishikawa, M. *J. Organomet. Chem.* **1969**, *17*, 235.

(97) Glockling, F.; Light, J. R. C. *J. Chem. Soc. A.* **1967**, 623.

(98) Mochida, K.; Hodota, C.; Hata, R.; Fukuzumi, S. *Chem. Lett.* **1998**, 263.

(99) Okano, M.; Mochida, K. *Chem. Lett.* **1990**, 701.

100) Shibata, K.; Weinert, C. S.; Sita, L. R. *Organometallics* **1998**, *17*, 2241.

(101) Bochkarev, M. N.; Vyazankin, N. S.; Bochkarev, L. N.; Razuvaev, G. A. *J. Organomet. Chem.* **1976**, *110*, 149.

(102) Zaitsev, K. V.; Kapranov, A. A.; Churakov, A. V.; Poleshchuk, O. K.; Oprunenko, Y. F.; Tarasevich, B. N.; Zaitseva, G. S.; Karlov, S. S. *Organometallics* **2013**, *32*, 6500.

(103) Amadoruge, M. L.; Yoder, C. H.; Conneywerdy, J. H.; Heroux, K.; Rheingold, A. L.; Weinert, C. S. *Organometallics* **2009**, *28*, 3067.

(104) Amadoruge, M. L.; Gardinier, J. R.; Weinert, C. S. *Organometallics* **2008**, *27*, 3753.

(105) Amadoruge, M. L.; Golen, J. A.; Rheingold, A. L.; Weinert, C. S. *Organometallics* **2007**, *27*, 1979.

CHAPTER II

PROTECTION/DEPROTECTION STRATEGIES FOR SYNTHESIZING LINEAR OLIGOGERMANE

INTRODUCTION

A potentially useful method for the preparation of long-chain oligogermanes is synthesis via the selective stepwise construction of a compound by adding one or two germanium atoms to the chain at a time in a single reaction. Through stepwise synthesis, it would be possible to vary the substituents at each germanium atom allowing for greater variation and control over the physical properties of the compounds. The stepwise synthesis of oligogermanes involving the addition of the germanium atoms one at a time was achieved using the synthons $R_2Ge(NMe_2)CH_2CH_2OEt$ (R = Et, Bu^n, Ph) as shown in **Scheme 2.1**.[1] The synthons contain a reactive amide group and a protected hydride site, which are both located on a single germanium atom. After the hydrogermolysis reaction is complete, the resulting oligogermane is then treated with diisobutylaluminum hydride (DIBAL-H) to remove the protecting ethoxyethyl group and introduce a Ge – H bond for further reaction with an additional equivalent of the synthon. While the analogous

oligostannanes readily lose the protecting group upon addition of DIBAL-H[2] to yield a Sn – H group, the corresponding germanium compounds require more vigorous reaction conditions for successful conversion to the hydride. In order to synthesize the oligomeric germanium compounds using this stepwise method, purification of the crude reaction product by washing the crude mixture on a silica gel column to remove residual DIBAL-OEt is required.[1,3] In an attempt to stream-line the process to obtain longer oligomeric germanium chains with fewer steps, the addition of two germanium atoms to the chain at one time was investigated.

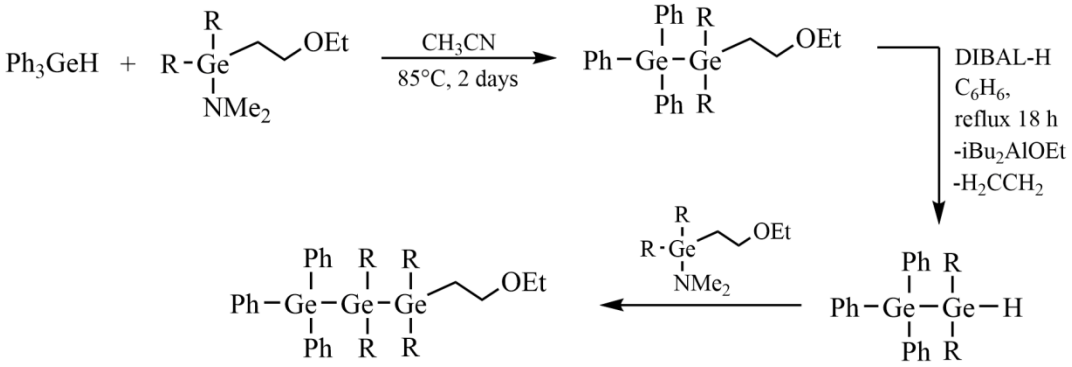

Scheme 2.1. Synthesis of oligogermanes using a protection/deprotection strategy.

RESULTS AND DISCUSSION

Synthesis of the Butyl Synthon, $Bu_2Ge(NMe_2)CH_2CH_2OEt$

The synthons for the hydrogermolysis reaction are prepared in four steps starting with the germane R_2GeH_2. As shown in **Scheme 2.2**, Bu_2GeHCl (**2**) can be prepared from

commercially available Bu_2GeCl_2, which was first converted to Bu_2GeH_2 (**1**) using lithium aluminum hydride, $LiAlH_4$, via literature methods.[4] Subsequently, $CuCl_2$ was employed to selectively replace one hydrogen with a chloride.[5] Then in the hydrogermylation reaction, the hydrochloride **2** was added across the double bond of ethyl vinyl ether in an anti-Markovnikov fashion, and azobisisobutyronitrile, (AIBN, $[(CH_3)_2C(CN)]_2N_2$), was used as a radical initiator for the hydrogermylation reaction. The ^1H nuclear magnetic resonance (NMR) spectrum of $Bu_2Ge(Cl)CH_2CH_2OCH_2CH_3$ (**3**) no longer contained the peaks corresponding to the septet arising from the hydrogen atom of **2** at 5.46 ppm, and new peaks corresponding to the ethoxyethyl group were present at 3.41 ppm (triplet) and 3.15 ppm (quartet) for the methylene protons adjacent to the oxygen, 1.17-1.11 ppm (multiplet) for the methylene protons adjacent to the germanium, and 1.01 ppm (triplet) for the CH_3 protons of the $–CH_2CH_2OCH_2CH_3$ group.

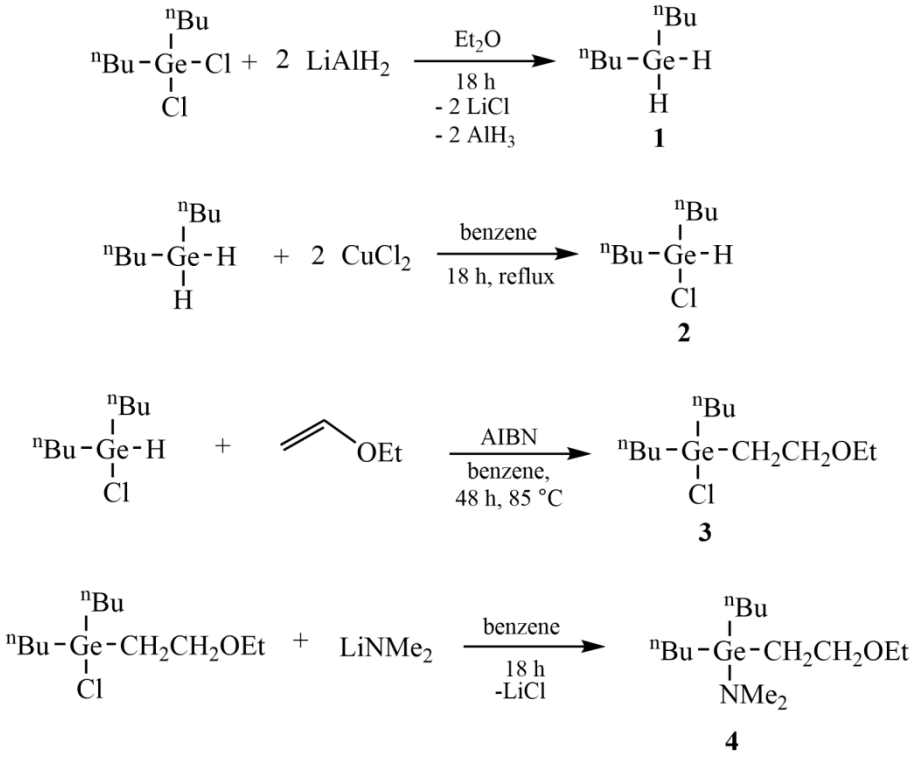

Scheme 2.2. Synthesis of the butyl synthon starting from Bu_2GeCl_2.

The last step in the synthesis of the butyl synthon involved the reaction of **3** with lithium dimethylamide, $LiNMe_2$, in benzene solvent for 18 hours at room temperature. Filtration of the resulting suspension removed the insoluble lithium chloride salt byproduct and the benzene was subsequently removed *in vacuo*. The butyl synthon, $Bu_2Ge(NMe_2)CH_2CH_2OEt$ (**4**), was isolated in 91% yield from **3** as a brown oil. The ^1H NMR spectrum of the resulting compound showed the presence of a new singlet at 2.59 ppm for the protons attached to the methyl carbons of the amide group, indicating a successful metathesis reaction (**Figure 2.1**).

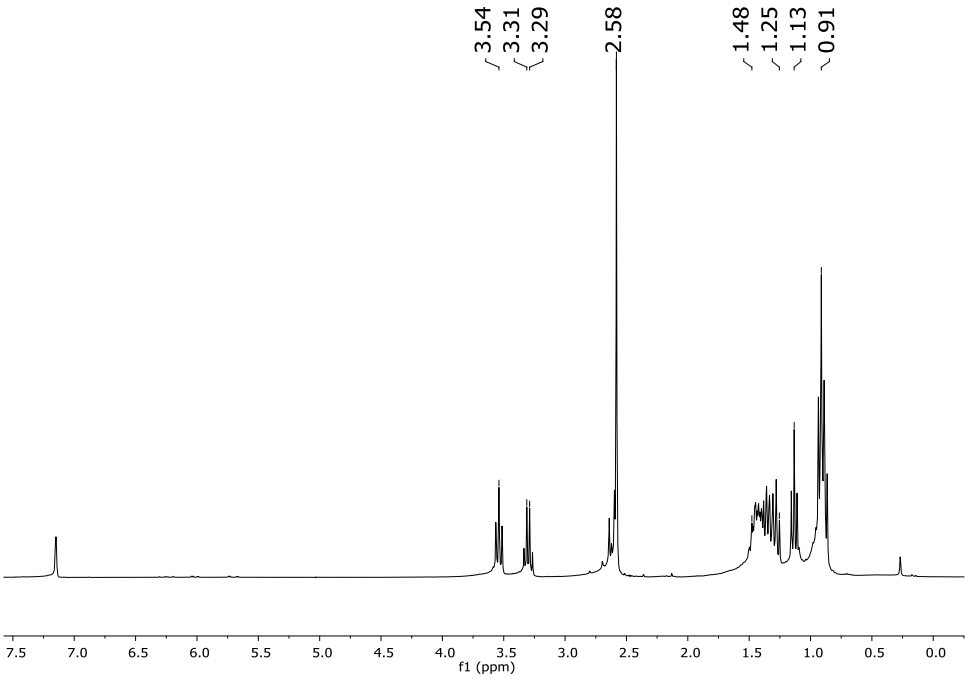

Figure 2.1. ^{1}H NMR spectrum of $Bu_2Ge(NMe_2)CH_2CH_2OEt$ (**4**) in benzene-d_6.

Synthesis of the Trigermane $EtOCH_2CH_2(Bu_2Ge)(GePh_2)(GeBu_2)CH_2CH_2OEt$

The hydrogermolysis reaction was utilized in synthesizing the trigermane **5** starting with the butyl synthon. Two equivalents of **4** were added to one equivalent of Ph_2GeH_2 in CH_3CN in a Schlenk tube that was then sealed (**Scheme 2.3**). The reaction was heated at 90 °C for 3 days, at which time the volatiles were removed *in vacuo* to produce the trigermane **5** in 69 % yield as a pale yellow liquid. The H^1 NMR spectrum of **5** is shown in **Figure 2.2**. Protons at the methylene groups neighboring the oxygen atoms were shifted slightly upfield compared to those in the synthon, as expected due to the loss

of the electron withdrawing –NMe_2 group. The ^{1}H and ^{13}C NMR spectra were compared to the reported literature data and thus confirmed the successful synthesis of trigermane **5**.[1]

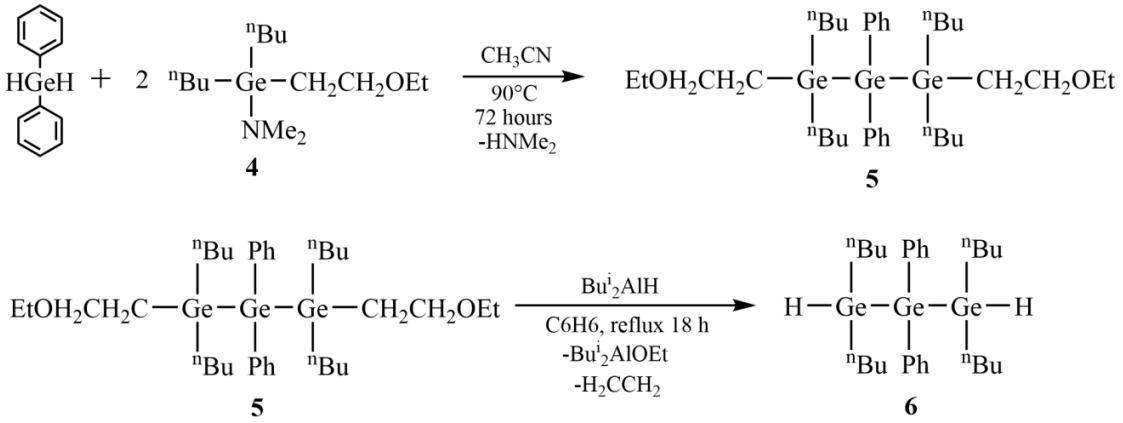

Scheme 2.3. Synthesis of the trigermane **5** followed by cleavage of Ge–C bond to form Ge–H bond.

To achieve further chain growth of the trigermane, **5** was refluxed with a slight excess of DIBAL-H in benzene overnight, followed by evaporation of the benzene solvent and ethylene byproduct *in vacuo*. The ^{1}H NMR spectrum of the trigermane product showed two broad peaks at 2.2 and 3.5 ppm that most likely correspond to polymerized $^{i}Bu_2AlOCH_2CH_3$ product.

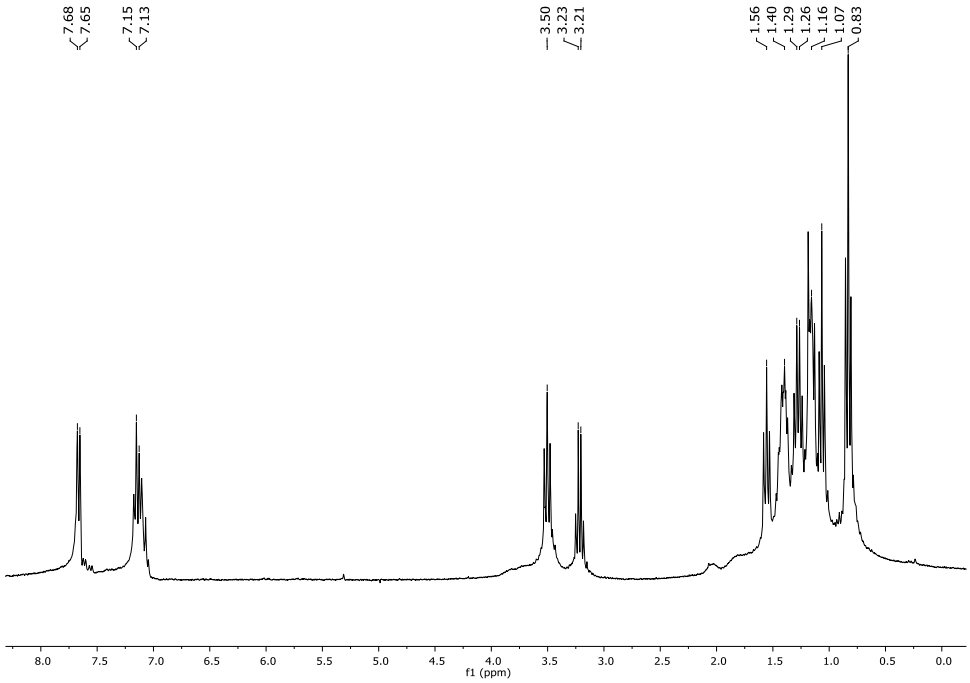

Figure 2.2. ^{1}H NMR spectrum of trigermane **5** in benzene-d_6**.**

Cleavage of the germanium–carbon bond is thought to occur through formation of a six-membered ring intermediate involving attachment of the aluminum atom of DIBAL-H to the oxygen atom of the ethoxyethyl group, and also the formation of a hydride bridge between the aluminum and germanium atoms, as depicted in **Scheme 2.4**. The aluminum-hydrogen bond is then broken leaving a germanium bound hydrogen atom. The germanium-carbon and an oxygen-carbon bonds are also broken, resulting in the formation of $Bu^{i}_{2}AlOEt$ and ethylene gas.

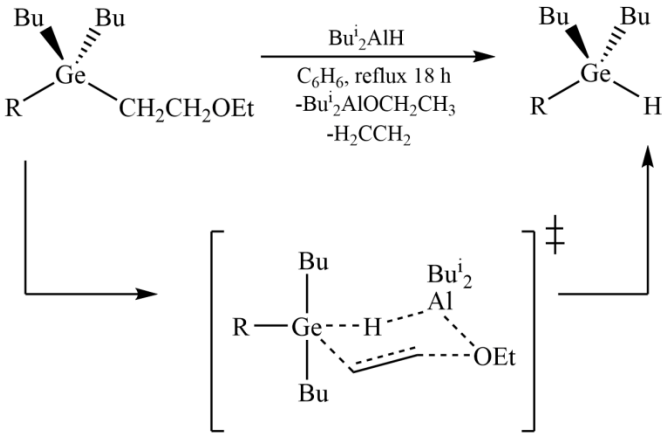

Scheme 2.4. Suggested reaction mechanism for cleavage and subsequent hydride addition using DIBAL-H.

Synthesis of the Pentagermane

$EtOCH_2CH_2(Bu_2Ge)(GeBu_2)(GePh_2)(GeBu_2)(GeBu_2)CH_2CH_2OEt$

The pentagermane $EtOCH_2CH_2(GeBu_2)_2(GePh_2)(GeBu_2)_2CH_2CH_2OEt$ (**7**) was synthesized from the trigermane **6** via the hydrogermolysis reaction involving treatment of **6** with two equivalents of the butyl synthon **4** in acetonitrile, as depicted in **Scheme 2.5**. The pentagermane **7** was obtained in 17% yield as a yellow oil after flash column chromatography and distillation using the Kugelrohr oven to remove any residual butyl synthon. The ^1H NMR spectrum of the pentagermane product showed a slight downfield shift of the protons of the methylene groups adjacent to the oxygen atoms compared to those of **5**, as expected with the lengthening of the germanium backbone. The alkyl

region of the ^{1}H NMR spectrum also displayed increased complexity with the overlapping signals of the butyl groups, as shown in **Figure 2.3**.

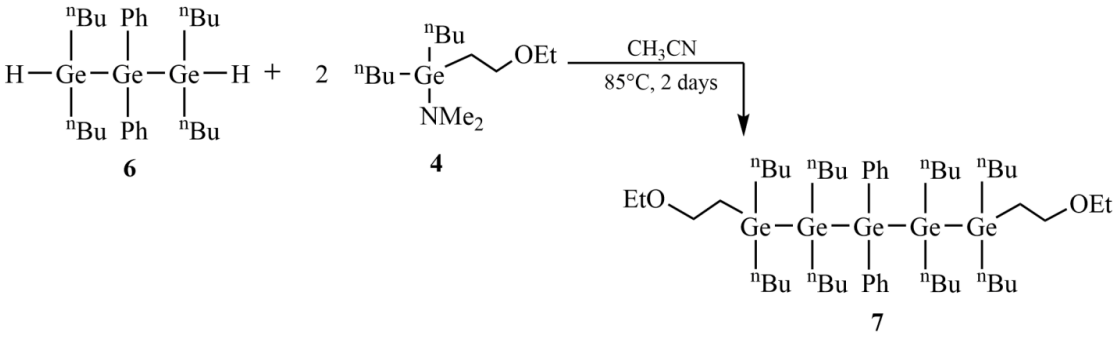

Scheme 2.5. Hydrogermolysis reaction for the synthesis of **7**.

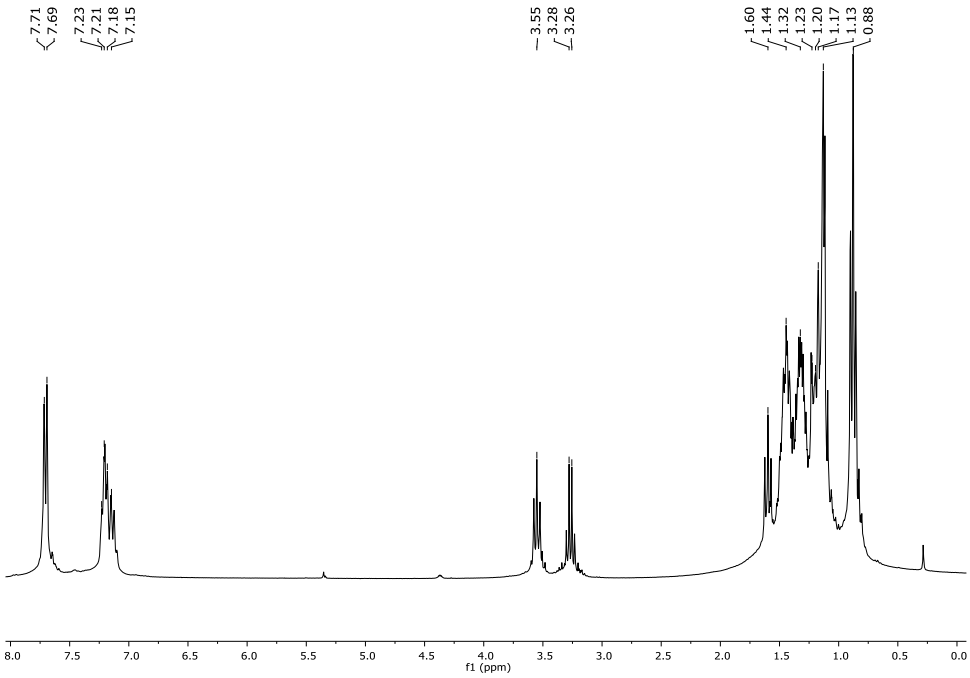

Figure 2.3. ^{1}H NMR spectrum of **7** in benzene-d_6.

Synthesis of Longer Oligogermanes

The synthesis of longer-chain oligogermanes was attempted using these protection/deprotection strategies. When two equivalents of DIBAL-H were reacted with **7**, a peak corresponding to a germanium bound hydrogen atom in the ^{1}H NMR spectrum of the product, typically observed at 4 to 4.5 ppm, was not visible. In all attempts to deprotection, the very broad ^{1}H NMR peak corresponding to the aluminum polymer overlapped with this region making it difficult to confirm a successful reaction. The product of the DIBAL-H reaction was then combined with two equivalents of the butyl synthon in an attempt to form the heptagermane. The ^{1}H NMR spectrum of the hydrogermolysis product suggested that reaction did not occur, as the protons of the methylene groups neighboring the oxygen atoms gave resonances with chemical shifts nearly identical to those in **7**, and the region associated with the protons of the butyl groups remained consistent with **7**. The ^{13}C NMR spectrum of the product contained only 12 resonances for the aliphatic carbons, not the expected 16 resonances for the heptagermane. Ultraviolet/visible spectroscopy and electrochemistry, which will be discussed in a later chapter, were also used to indicate unsuccessful formation of the heptagermane.

With the unsuccessful attempts at forming a heptagermane utilizing butyl synthons, new synthetic methods needed to be explored. Oligomers containing butyl substituents were also liquid and this made it impossible to obtain crystal structures to confirm the composition of the compounds and to ascertain their solid-state geometry. The next logical move would be to attempt chain building using the

protection/deprotection strategy with phenyl substituted synthons. While the synthesis of the trigermane $EtOCH_2CH_2(GePh_2)(GePh_2)(GePh_2)CH_2CH_2OEt$ has been accomplished, the synthesis of higher oligomers was halted when DIBAL-H failed to remove the protecting group.[3] A new plan, as discussed in the next chapter, was developed in which long-chain oligogermanes were synthesized using phenyl substituents at the central germanium atoms and isopropyl substituents on the terminal germanium atoms, to yield solid products that allowed for the possibility of characterization using X-ray crystallography.

EXPERIMENTAL

General Considerations

All manipulations were carried out under an inert atmosphere of nitrogen gas using standard Schlenk, syringe, and glovebox techniques. All solvents were purified using a Glass Contour solvent purification system. The starting material Ph_2GeH_2 and Bu_2GeCl_2 were purchased from Gelest. The reagents $LiAlH_4$, ethyl vinyl ether, AIBN, DIBAL-H (1.0 M in hexanes) and $LiNMe_2$ were purchased from Sigma-Aldrich and $CuCl_2$ was purchased from VWR. All starting materials and reagents were used as received with no further purification. Bu_2GeH_2 was synthesized using two equivalents of $LiAlH_4$ and Bu_2GeCl_2, and the hydrochloride Bu_2GeHCl was prepared using literature

methods.[5] All NMR spectra were collected on a Gemini 2000 NMR spectrometer and were reference to benzene-d_6 solvent.

Synthesis of $Bu_2Ge(Cl)CH_2CH_2OCH_2CH_3$, 3

To a Schlenk tube, 1.761 g (7.886 mmol) of Bu_2GeHCl in 40 mL benzene and 0.032 g (0.19 mmol) of AIBN were added. Ethyl vinyl ether (1.7 mL, 18 mmol) was then syringed into the reaction tube. The reaction was sealed and placed in an 85 °C oil bath for 65 hours. After cooling to room temperature, the solvent was removed *in vacuo*, yielding 2.072 g (89%) $Bu_2Ge(Cl)CH_2CH_2OEt$. ^1H NMR (C_6D_6, 25 °C): δ 3.39 (t, J = 6.9 Hz, 2H, -$GeCH_2CH_2O$), 3.13 (q, J = 7.0 Hz, 2H, -OCH_2CH_3), 1.59 – 1.50 (m, 4H, $GeCH_2CH_2CH_2CH_3$), 1.45 (t, J = 7.0 Hz, 4H, -$GeCH_2CH_2CH_2CH_3$), 1.30 (sext, J = 7.3 Hz, 4H, $GeCH_2CH_2CH_2CH_3$), 1.16 – 1.10 (m, 2H, $GeCH_2CH_2O$-), 1.00 (t, J = 7.0 Hz, 3H, -OCH_2CH_3), 0.86 (t, J = 7.3 Hz, 6H, $GeCH_2CH_2CH_2CH_3$) ppm. ^{13}C NMR (C_6D_6, 25 °C): δ 66.9 (-OCH_2CH_3), 66.1 ($GeCH_2CH_2O$-), 22.6, 26.1, 21.1, 20.0, 15.3, 13.8 (aliphatic carbons) ppm.

Synthesis of $Bu_2Ge(NMe_2)CH_2CH_2OCH_2CH_3$, 4

$Bu_2Ge(Cl)CH_2CH_2OEt$ (2.037 g, 6.896 mmol) and $LiNMe_2$ (0.422 g, 8.27 mmol) were combined in 50 mL benzene. The reaction was allowed to stir for 18 hours at room temperature. A solid precipitate of LiCl was filtered out using a medium frit and a 1/8”

layer of celite to give a clear, yellow solution. The solvent was removed *in vacuo* to afford 1.785 g (5.871 mmol, 84% yield) $Bu_2Ge(NMe_2)CH_2CH_2OEt$ as a clear, pale yellow liquid. ^{1}H NMR (C_6D_6, 25 °C): δ 3.54 (t, *J* = 7.8 Hz, 2H, $GeCH_2CH_2O$-), 3.30 (q, *J* = 7.0 Hz, 2H, $-OCH_2CH_3$), 2.58 (s, 6H, $N(CH_3)_2$), 1.50-1.33 (m, 6H), 1.28, (t, *J* = 8.0 Hz, 3H, $-OCH_2CH_3$), 1.13 (t, *J* = 7.0 Hz, 6H, $GeCH_2CH_2CH_2CH_3$), 0.91 (t, *J* = 7.0 Hz, 4H, $GeCH_2CH_2CH_2CH_3$) ppm. ^{13}C NMR (C_6D_6, 25 °C): δ 68.0 ($-OCH_2CH_3$), 65.8 ($GeCH_2CH_2O$-), 41.4 ($-N(CH_3)_2$), 27.3, 26.9, 15.6, 15.0, 14.0, 13.6 (aliphatic carbons) ppm.

Synthesis of $EtOCH_2CH_2(Bu_2Ge)(GePh_2)(GeBu_2)CH_2CH_2OEt$, 5

A Schlenk tube was charged with 1.512 g (6.607 mmol) of Ph_2GeH_2, 4.017 g (13.21 mmol) of $Bu_2Ge(NMe_2)CH_2CH_2OEt$ in 50 mL of CH_3CN. The tube was sealed and placed in a 95 °C oil bath for 72 hours. After transferring to a Schlenk flask via cannula, the volatiles were removed *in vacuo* to produce a brown oil. The crude product was then placed on the Kugelrohr (T = 180 °C, P = 0.205 mmHg) to remove remaining starting material, affording 2.676 g (3.584 mmol) of **5** as a brown liquid in 54% yield. ^{1}H NMR (C_6D_6, 25 °C): δ 7.67 (d, *J* = 6.6 Hz, 4H, *m*-H), 7.17-7.05 (m, 6H, *p*- and *o*-H), 3.35 (t, *J* = 7.8 Hz, 4H, $GeCH_2CH_2O$-), 3.22 (q, *J* = 7.0 Hz, 4H, $-OCH_2CH_3$), 1.56 (t, *J* = 7.8 Hz, 6H, $-OCH_2CH_3$), 1.45-1.37 (m, 8H, $Ge(CH_2CH_2CH_2CH_3)_2$), 1.28 (hex, *J* = 7.3 Hz, 8H, $Ge(CH_2CH_2CH_2CH_3)_2$), 1.17 (m, 8H, $Ge(CH_2CH_2CH_2CH_3)_2$), 1.07 (t, J = 7.0 Hz, 6H, $-OCH_2CH_3$), 0.83 (t, *J* = 6.8, 12H, $Ge(CH_2CH_2CH_2CH_3)_2$) ppm. ^{13}C NMR (C_6D_6, 25

°C): δ 140.5 (*ipso*-C), 136.1 (*o*-C), 128.4 (*m*-C), 128.1 (*p*-C), 68.9 (-O*C*$H_2$$CH_3$), 65.7 (Ge$CH_2$*C*$H_2$O-), 28.8 (-O$CH_2$*C*$H_3$), 27.0 (Ge($CH_2CH_2CH_2$*C*$H_3$)$_2$), 16.6 (Ge($CH_2CH_2$*C*$H_2CH_3$)$_2$), 15.6 (Ge($CH_2$*C*$H_2CH_2CH_3$)$_2$), 15.5 (Ge*C*$H_2CH_2$O-), 13.9 (Ge(*C*$H_2CH_2CH_2CH_3$)$_2$) ppm. UV/visible: λ_{max} 237 nm (v br, ε = 5.42 x 10^4 mol^{-1} cm^{-1})**.**

Synthesis of EtOCH_2CH_2(Bu_2Ge)($GeBu_2$)($GePh_2$)($GeBu_2$)($GeBu_2$)CH_2CH_2OEt (7) by formation of H(Bu_2Ge)($GePh_2$)($GeBu_2$)H (6)

A solution of **5** (2.579 g, 3.454 mmol), 1.0 M DIBAL-H (7.6 mL, mmol) and 100 mL benzene were refluxed for 18 hours. Volatiles were removed *in vacuo*. The crude product from the DIBAL-H reaction was combined with 2.100 g (6.907 mmol) of $Bu_2Ge(NMe_2)CH_2CH_2OEt$ and 40 mL CH_3CN in a Schlenk tube. The reaction was sealed and placed in a 90 °C oil bath for 72 hours. Volatiles were removed *in vacuo*. The pentagermane was purified by flash chromatography through silica gel, using hexane to put the product on the column, and then a solution of 10% Et_2O in hexane to remove the product from the column. After removing the solvent *in vacuo*, residual impurities were removed via Kugelrohr (T = 100 °C, P = 0.05 mmHg) to afford 0.659 g (0.588 mmol, 17.0% yield) of **7** as a yellow oil. ^{1}H NMR (C_6D_6, 25 °C): δ 7.70 (d, *J* = 6.7 Hz, 4H, *m*-H), 7.23-7.10 (m, 6H, *p*- and *o*-H), 3.55 (t, *J* = 7.8 Hz, 4H, $GeCH_2C$*H*$_2$O-), 3.27 (q, *J* = 7.0 Hz, 4H, -OC*H*$_2$$CH_3$), 1.60 (t, *J* = 7.8 Hz, 4H, GeC*H*$_2$$CH_2$O-), 1.50-1.09 (m, 52H), 0.88 (t, J = Hz, 24H, Ge($CH_2CH_2CH_2C$*H*$_3$)$_2$) ppm. ^{13}C NMR (C_6D_6, 25 °C): δ 140.4 (*ipso*-C), 136.1 (*o*-C), 128.6 (*m*-C), 128.1 (*p*-C), 68.9 (-O*C*$H_2$$CH_3$), 65.7 (Ge$CH_2$*C*$H_2$O-),

28.8, 27.0, 16.6, 15.6, 15.5, 14.8, 14.6, 13.9, 10.4, 7.5 (aliphatic carbons) ppm.

UV/visible: λ_{max} 243 nm (v br, $\varepsilon = 1.10 \times 10^4$ mol^{-1} cm^{-1})**.**

REFERENCES

(1) Subashi, E.; Rheingold, A. L.; Weinert, C. S. *Organometallics* **2006**, *25*, 3211.

(2) Sita, L. R. *Organometallics* **1992**, *11*, 1442.

(3) Amadoruge, M. L.; Gardinier, J. R.; Weinert, C. S. *Organometallics* **2008**, *27*, 3753.

(4) Glockling, F. *The Chemistry of Germanium*; Academic P.: New York, London, 1969.

(5) Ohshita, J.; Toyoshima, Y.; Iwata, A.; Tang, H.; Kunai, A. *Chemistry Letters* **2001**, 886.

CHAPTER III

REACHING NEW LENGTHS

INTRODUCTION

With the discovery of the limitations of the protection/deprotection strategy for the synthesis of long chain oligogermanes, it was evident that new synthetic methodology needed to be employed. Ideally, the goal of obtaining a longer linear oligogermane was sought in order to develop an oligogermane which could mirror the properties observed in polymeric germanium compounds such as thermochromism, conductivity, and luminescence. It was desired to achieve solid products that could be crystallized for structural characterization. Thus, attempts were made to synthesize an oligomeric germanium compound containing more crystalline organic groups such as phenyl and isopropyl substituents.

It was established that instead of building larger molecules by the addition of one or two germanium atoms at a time, it was desirable to quickly obtain molecules containing several germanium atoms. As described in Chapter 1, many existing methods for the development of larger oligomers of germanium produced mixtures of germanium

compounds that included oligogermanes with various chain lengths. These methods would be ineffective at synthesizing discrete molecules, particularly long-chain germanium oligomers. Reactions that form compounds containing multiple germanium atoms that could be easily isolated were thought to proceed by the use of cyclic compounds as precursors. In this chapter, the synthesis of a new hexagermane will be discussed which was easily achieved through the use of cyclic germanium compounds in three steps in a good overall yield.

RESULTS AND DISCUSSION

The Hexagermane

Prior to this work, the longest oligomeric germanium compound structurally characterized was the perphenylated pentagermane Ge_5Ph_{12}, but this species failed to exhibit any physical properties displayed by polygermanes, such as luminescence and/or thermochromism.[1] It was then our goal to synthesize and crystallize a linear hexagermane. Original attempts to synthesize a perphenylated hexagermane, $Ph_3Ge(GePh_2)_4GePh_3$, were directed towards addition of groups either in a 2 + 2 + 2 or a 1 + 3 + 2 fashion. In this context, the 2 + 2 + 2 method describes a strategy where three groups, each containing two germanium atoms, are combined. This method can be carried out in two ways, the first of which involves the addition of two equivalents of $Ph_3GeGePh_2H$ to one equivalent of $Me_2N(GePh_2)_2NMe_2$. The hydrogermolysis reaction was attempted using these two compounds obtained using a variety of synthetic methods,

but never resulted in an isolable hexagermane product. The compound $Ph_3GeGePh_2H$ often contained the perphenylated trigermane $Ph_3GeGePh_2GePh_3$ or the compound $HPh_2GeGePh_2H$ as impurities, and attempts at the synthesis of the diamide typically resulted in an incoherent mixture of compounds with the ^1H NMR containing multiple proton signals in the range typical of the $–NMe_2$ group. Thus, the inability to obtain pure starting materials rendered this synthetic method unsuccessful. A second attempt at a 2 + 2 + 2 addition used the hydrogermolysis reaction of two equivalents of $Ph_3Ge(GePh_2)NMe_2$ with one equivalent of $HPh_2GeGePh_2H$ as depicted in **Scheme 3.1**. Depending on the method used for synthesizing the starting material, the product obtained by the hydrogermolysis reactions was inconsistent to a varying degree. The hydrogermolysis reaction carried out using the starting materials as shown in **Scheme 3.1**, in acetonitrile solvent at 90 °C for 72 hours produced the cleanest product. The product of this reaction was typically a thick, viscous mixture and was white to light yellow in color. After reaction, Kugelrohr distillation was attempted in order to remove some impurities. The ^1H NMR spectrum of the product did not confirm formation of Ge_6Ph_{12}, as it contained multiple overlapping peaks in the phenyl region. The ^{13}C NMR spectrum contained the correct number of peaks corresponding to the 12 magnetically non-equivalent carbons corresponding to the three different sets of phenyl rings attached to the Ge_6 backbone. Analyzing the product using electrochemistry, which will be discussed in a later chapter, gave some evidence of a product containing six germanium atoms. However, characterization of the compound using ultraviolet/visible spectroscopy resulted in a spectrum that contained an absorbance maximum of 285 nm. The published absorbance maximum for Ge_5Ph_{12} is 295 nm.[2] Lengthening of the germanium backbone

should result in a red-shift in the maximum absorbance of the compounds, however this was not observed in the UV/visible spectrum of the product shown in **Scheme 3.1**. Crystallization of the product was attempted, but a crystal suitable for X-ray diffraction was not obtained. With insufficient evidence for the successful preparation of Ge_6Ph_{12} via UV/visible and NMR spectroscopy and the lack of suitable crystals for X-ray diffraction, it was necessary to find other means for the synthesis of a hexagermane.

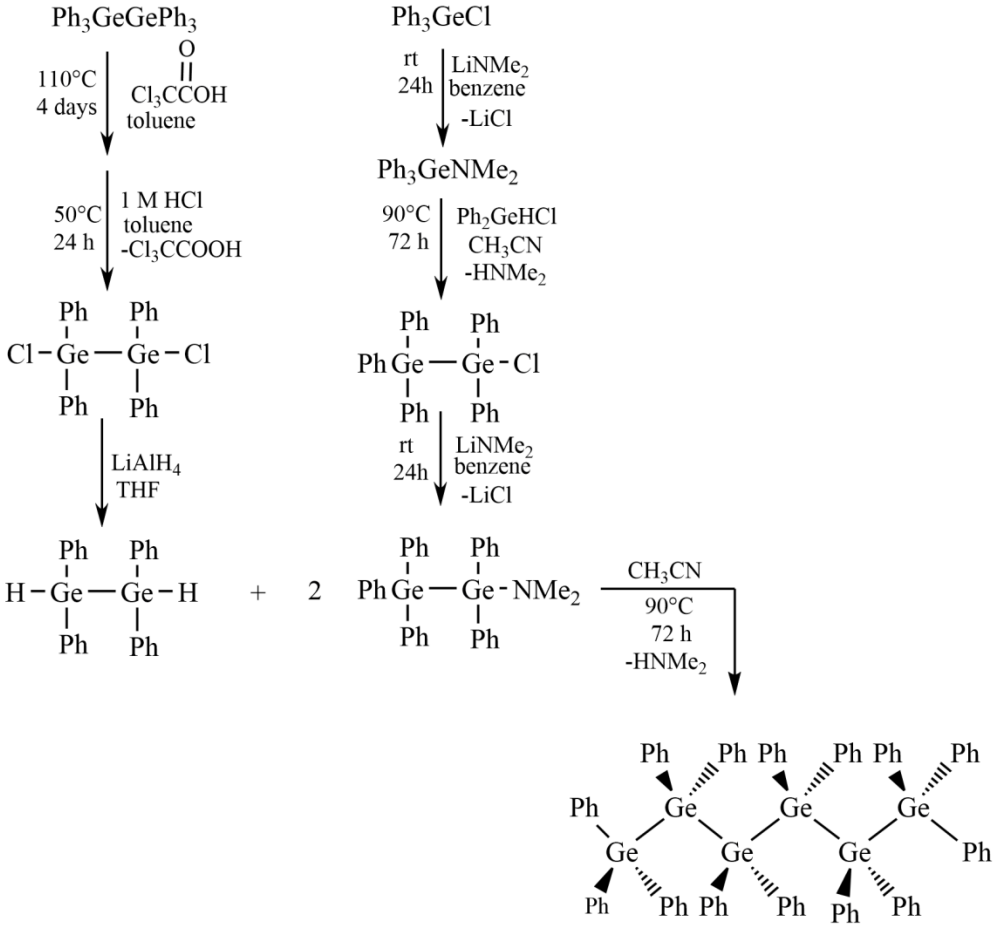

Scheme 3.1. Attempted synthesis of a perphenylated hexagermane in a 2 + 2 + 2 fashion.

In order to synthesize a linear hexagermane using a 2 + 3 + 1 strategy, the synthesis of a trigermane with hydrogens on the terminal germanium atoms,

$HPh_2GeGePh_2GePh_2H$ was required. Attempts were made to synthesize this compound by adding two equivalents of $Ph_2Ge(NMe_2)Cl$ to Ph_2GeH_2, and also via the decomposition of (diarylgermyl)lithium compounds with *tert*-butyllithium as described in Chapter 1.[3] To the trigermane starting material obtained by either method, a single equivalent of either Ph_3GeNMe_2 or $Ph_3GePh_2GeNMe_2$ was added in attempts to synthesize either the tetragermane $Ph(GePh_2)_4H$ or pentagermane $Ph(GePh_2)_5H$, respectively, with a hydrogen bonded to one of the terminal germanium atoms. Attempts at synthesizing the hexagermane by these strategies were unsuccessful, often resulting in an intractable mixture of products.

The next attempt at synthesizing a hexagermane was carried out using a cyclic tetragermane as the starting material. Octaphenylcyclotetragermane (**8)**, $(GePh_2)_4$, was obtained using the procedure reported by Ross and Dräger in 1980[4] via a Wurtz-type coupling as depicted in **Scheme 3.2**, where Ph_2GeCl_2 was refluxed for one hour with sodium chunks in boiling toluene. After work-up, **8** was obtained in 44% yield as a white crystalline solid. The ^{1}H NMR spectrum of **8** recorded in benzene-d_6, as shown in **Figure 3.1a**, contained a doublet of doublets at 7.54 ppm ($J_{1,3}$ = 7.3, $J_{1,4}$ = 2.0), corresponding to the *meta*-protons of the phenyl groups and a multiplet between 7.02 and 6.96 ppm corresponding to the o*rtho*- and *para*-protons on the phenyl rings. The ^{13}C NMR spectrum for **8**, shown in **Figure 3.1b**, contained four peaks at 138.45 (*ipso*), 136.57 (*ortho*), 128.73 (*para*), and 128.51 (*meta*) ppm for the phenyl carbons. The ^{13}C NMR of the cyclic tetragermane was also recorded in deuterated chloroform ($CDCl_3$), and the observed resonances were nearly identical to the values at 137.3 (*ipso*), 135.5 (*o*), 128.2 (*m*), and 128.7 (*p*) reported by Dräger.[4]

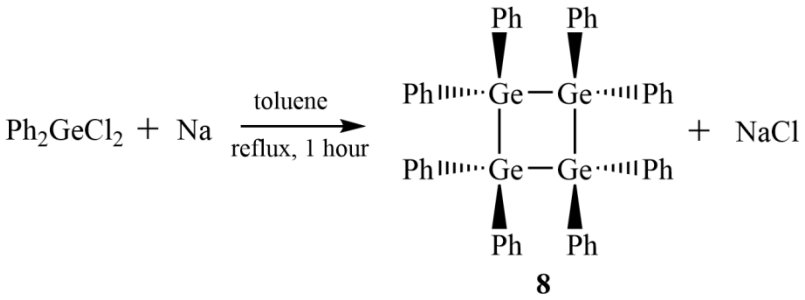

8

Scheme 3.2. Synthesis of **8** via Wurtz-type coupling.

A crystal of **8** suitable for X-ray diffraction was obtained from diffusion of hexane into benzene and is depicted in **Figure 3.2**. The X-ray crystal structure for **8** obtained at 298 K has been previously reported[5], while data for **8** was obtained at 100 K. A comparison of select bond angles and distances of the crystals obtained at the two different temperatures are shown in **Table 3.1**. The bond lengths and angles of the two crystal structures are similar. For both crystals the average bond lengths for the Ge – C and Ge – Ge bonds are 1.96 and 2.464 Å, respectively. Average bond angles for the C – Ge – Ge were 114.73° and 114.9° for the crystals characterized at 100 K and 298 K and the average bond angles for Ge – Ge – Ge were 89.953° and 90.0°, respectively. The values that differed the most significantly among the two structures were the average C – Ge – C angle and the deviation from planarity of the Ge_4 ring. The average C – Ge – C angle for **8** characterized at 100 K was 107.44°, while that of the structure characterized at 298 K was 106.9°. Between the two structures, the Ge_4 ring for the structure characterized at 100 K was puckered by 4.6°, while the structure characterized at 298 K had a less distorted pucker angle of 3.9°.

a)

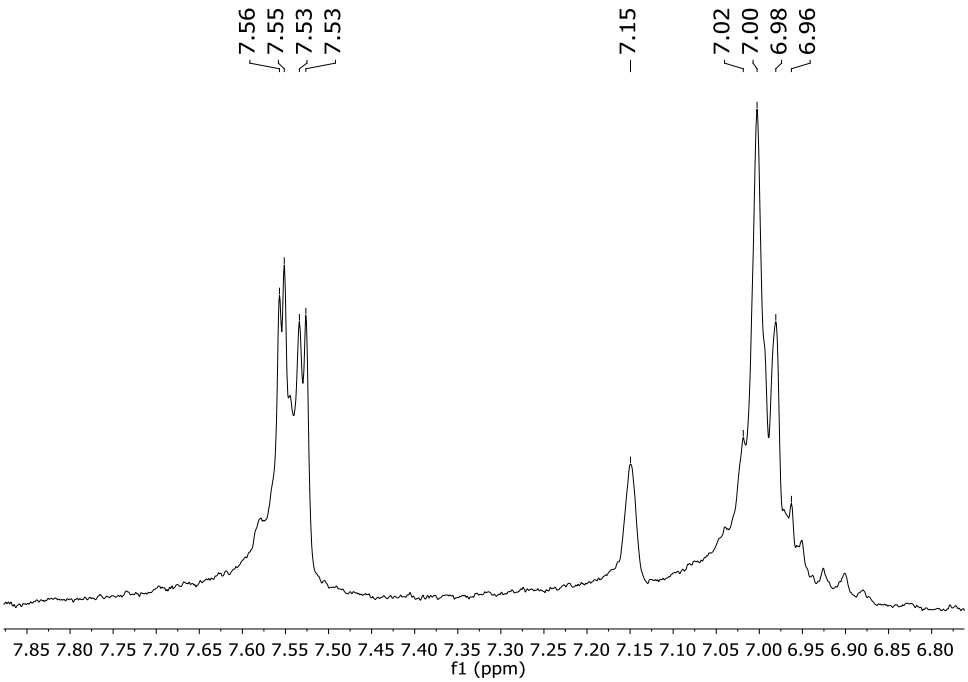

b)

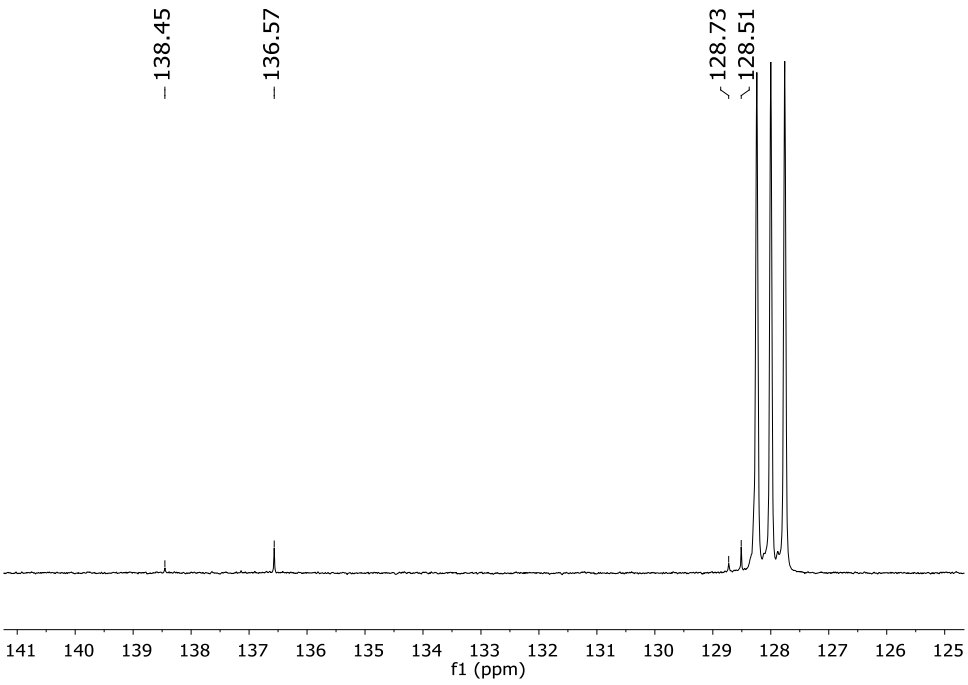

Figure 3.1. Aromatic region of the NMR spectra for compound **8**, in benzene-d_6. a) ^{1}H NMR; b) ^{13}C NMR

The X-ray structures for several other cyclic tetragermanes have also been reported, including $(GeTol_2)_4$ (Tol = *p*-$CH_3C_6H_4$)[6], $Ge_4Bu^t_4Cl_4$[7] and $Ge_4Pr^i_8$.[8] The species $(GeTol_2)_4$, like **8**, is C_2 symmetric. The average Ge-Ge bond distance in $(GeTol_2)_4$ is 2.4610(7) Å, which is shorter than the corresponding bond distances in **8**, and this has been observed in other compounds containing tolyl, rather than phenyl, substituents.[9] The average Ge – Ge bond lengths in $Ge_4Bu^t_4Cl_4$ and $Ge_4Pr^i_8$ were 2.465(2) and 2.4745(9) Å, respectively. The average Ge – Ge – Ge bond angles for the compounds $(GeTol_2)_4$, $Ge_4Bu^t_4Cl_4$ and $Ge_4Pr^i_8$ are 89.02(5)°, 89.09(6)° and 89.38(3)°, respectively. All of these angles are less than the average Ge – Ge – Ge bond in compound **8** characterized at either 100 or 298 K. Average Ge – Ge bond distances for **8** and $Ge_4Bu^t_4Cl_4$ are nearly identical despite the presence of the large *t*-butyl groups, due to the four *tert*-butyl substituents being located on opposite sides of the Ge_4 plane in an alternating fashion, thus alleviating steric strain. Unlike the bond angles, the pucker angles of the Ge_4 plane for the compounds of $(GeTol_2)_4$, $Ge_4Bu^t_4Cl_4$ and $Ge_4Pr^i_8$ were all significantly larger than that of **8**. Pucker angles for the compounds $Ge_4Bu^t_4Cl_4$ and $Ge_4Pr^i_8$ were 14.6° and 11.9°, respectively, while that of the $(GeTol_2)_4$ species was 21.1°. The oligogermane $(GePh_2)_4$ was less distorted due to the efficient packing of the phenyl substituents, as the phenyl rings on either side of the Ge_4 ring all align in a parallel fashion.

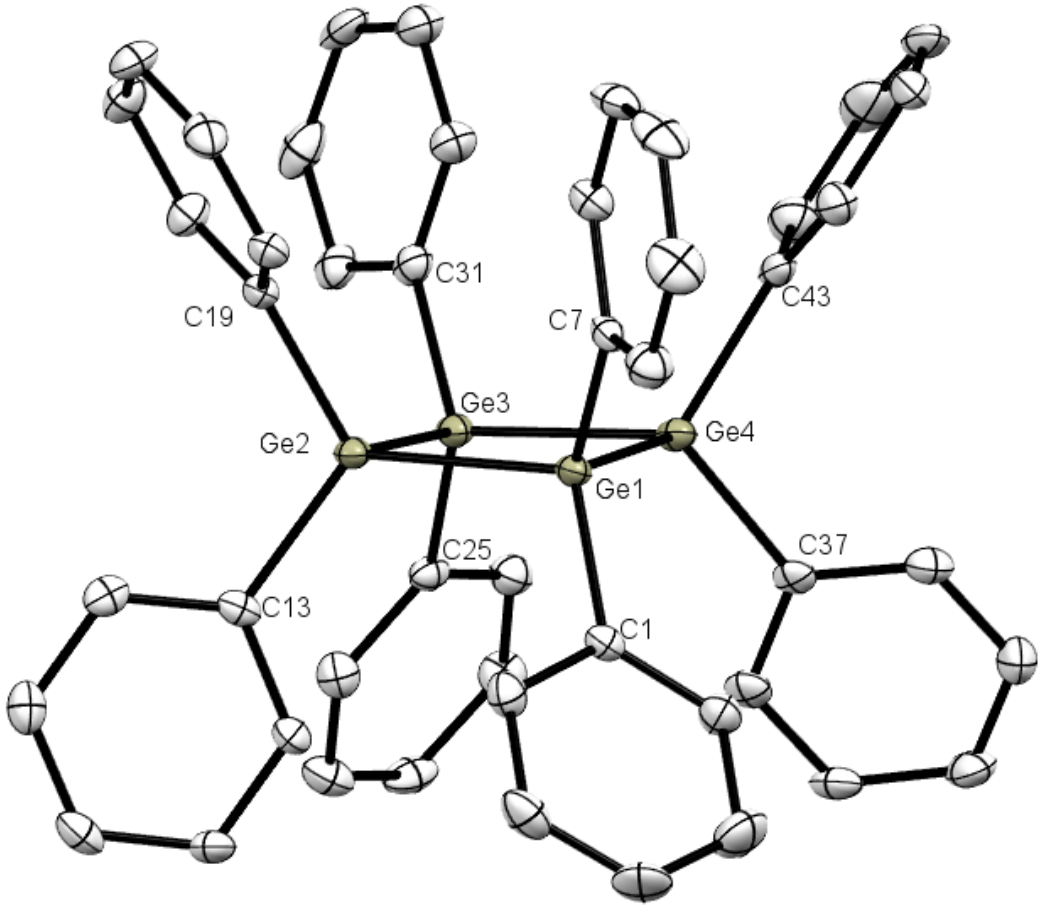

Figure 3.2. ORTEP diagram of **8** with hydrogen atoms omitted. Thermal ellipsoids are drawn at 50 % probability.

Table 3.1. Select bond angles (degrees) and bond lengths (Å) for **8** characterized at 100 K. A complete list of bond angles, distances and torsional angles are listed in the appendix.

Ge(1)-C(1)	1.950(3)	Ge(2)-Ge(3)	2.4730(4)
Ge(1)-C(7)	1.952(3)	Ge(3)-C(31)	1.955(3)
Ge(1)-Ge(2)	2.4534(4)	Ge(3)-C(25)	1.956(3)
Ge(1)-Ge(4)	2.4580(4)	Ge(3)-Ge(4)	2.4713(4)
Ge(2)-C(13)	1.956(3)	Ge(4)-C(37)	1.952(3)
Ge(2)-C(19)	1.958(3)	Ge(4)-C(43)	1.958(3)
C(1)-Ge(1)-C(7)	107.62(11)	C(31)-Ge(3)-C(25)	106.36(11)
C(1)-Ge(1)-Ge(2)	113.03(8)	C(31)-Ge(3)-Ge(4)	114.48(8)
C(7)-Ge(1)-Ge(2)	113.42(8)	C(25)-Ge(3)-Ge(4)	113.20(8)
C(1)-Ge(1)-Ge(4)	116.46(8)	C(31)-Ge(3)-Ge(2)	114.71(8)
C(7)-Ge(1)-Ge(4)	115.87(8)	C(25)-Ge(3)-Ge(2)	118.70(8)
Ge(2)-Ge(1)-Ge(4)	89.789(13)	Ge(4)-Ge(3)-Ge(2)	89.031(13)
C(13)-Ge(2)-C(19)	110.33(11)	C(37)-Ge(4)-C(43)	105.45(11)
C(13)-Ge(2)-Ge(1)	114.56(8)	C(37)-Ge(4)-Ge(1)	114.81(7)
C(19)-Ge(2)-Ge(1)	111.43(8)	C(43)-Ge(4)-Ge(1)	116.78(8)
C(13)-Ge(2)-Ge(3)	115.85(7)	C(37)-Ge(4)-Ge(3)	115.64(8)
C(19)-Ge(2)-Ge(3)	112.90(8)	C(43)-Ge(4)-Ge(3)	113.75(8)
Ge(1)-Ge(2)-Ge(3)	90.531(13)	Ge(1)-Ge(4)-Ge(3)	90.464(13)

Table 3.2. Average bond lengths (Å), bond angles (°) and pucker angles (°) for structures of **8** characterized at 100 K and 298 K.

Average Bond Length (Å)	**8** at 100 K	**8** at 298 K[5]
Ge-C	1.954	1.962
Ge-Ge	2.4639	2.465
Average Bond Angles (°)		
C-Ge-C	107.44	106.9
C-Ge-Ge	114.73	114.9
Ge-Ge-Ge	89.953	90.0
Avg Torsional Angle (°)		
Ge-Ge-Ge-Ge	3.255	3.9

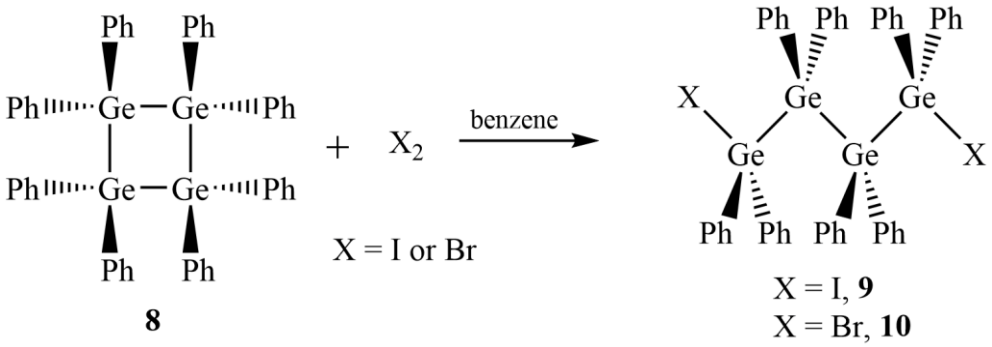

Scheme 3.3. Ring-opening of a cyclic germanium compound using X_2 (X = Br or I).[10]

The next step in the synthesis of the desired hexagermane involved the ring-opening of **8**. Dräger reported the ring-opening of the tetragermane **8** using molecular iodine, as depicted in **Scheme 3.3**.[10] The crystal structure of the 1,4-diiodide-1,1,2,2,3,3,4,4-octaphenyltetragermane was obtained at 298 K and the average bond

distances and angles are listed in **Table 3.4**. Compound **8** was converted to 1,4-dibromo-1,1,2,2,3,3,4,4-octaphenyltetragermane, **10**, via ring opening using molecular bromine. The completion of the ring-opening reaction of Br_2 with **8** could be easily ascertained and the addition of the Br_2 was stopped when a faint yellow color remained. The reaction is very favorable and proceeds quickly due to the alleviation of ring strain which occurs as the reaction proceeds. In the structure of **8**, the average Ge – Ge – Ge bond angle is 89.953°. This angle, which is much more acute than the idealized angle of 109.5° for a tetrahedral germanium, is highly strained. By relieving this strain, the ring-opening reaction proceeds rapidly.

The ^{1}H and ^{13}C NMR spectra of **10**, as shown in **Figure 3.3**, clearly indicates only one species present in the product. The ^{1}H NMR spectrum contains two singlets at 7.60 and 7.41 ppm (J = 7.8 and 7.5, respectively) for the hydrogen atoms located *meta* to the germanium on the two magnetically non-equivalent phenyl rings. The multiplet located between 7.06 and 6.90 ppm represents the 24 *ortho* and *para* protons present in **10**. The ^{13}C NMR spectrum of **10** contains 8 signals at 137.87 (*ipso*), 136.78 (*ortho*), 135.73 (*ipso*), 134.74 (*ortho*), 129.99 (*para*), 129.44 (*para*), 128.78 (*meta*) and 128.67 (*meta*) ppm, all of which are shifted downfield with respect to the carbon resonances present in **8** due to the electron withdrawing bromine atoms terminating the germanium chain.

a)

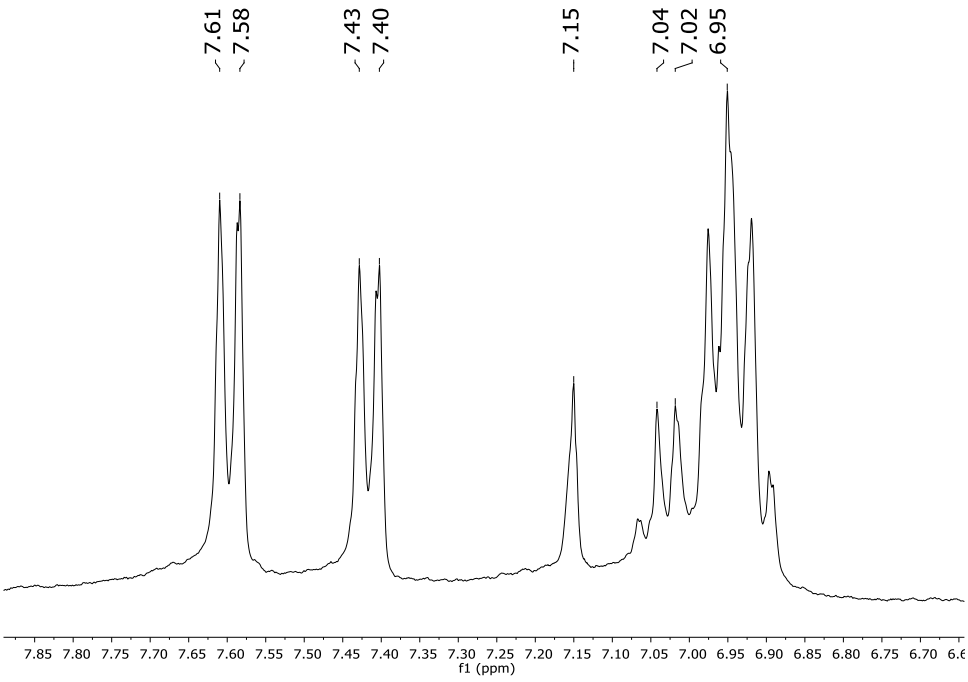

b)

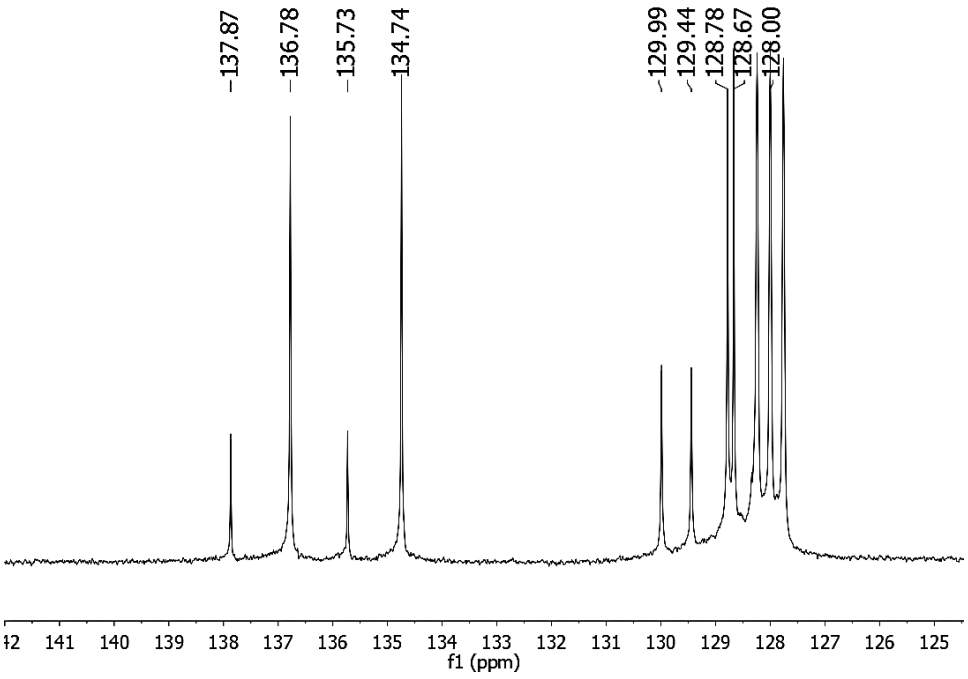

Figure 3.3. Aromatic regions of the NMR spectra of **10** in benzene-d_6. a.) ^{1}H NMR; b.) ^{13}C NMR

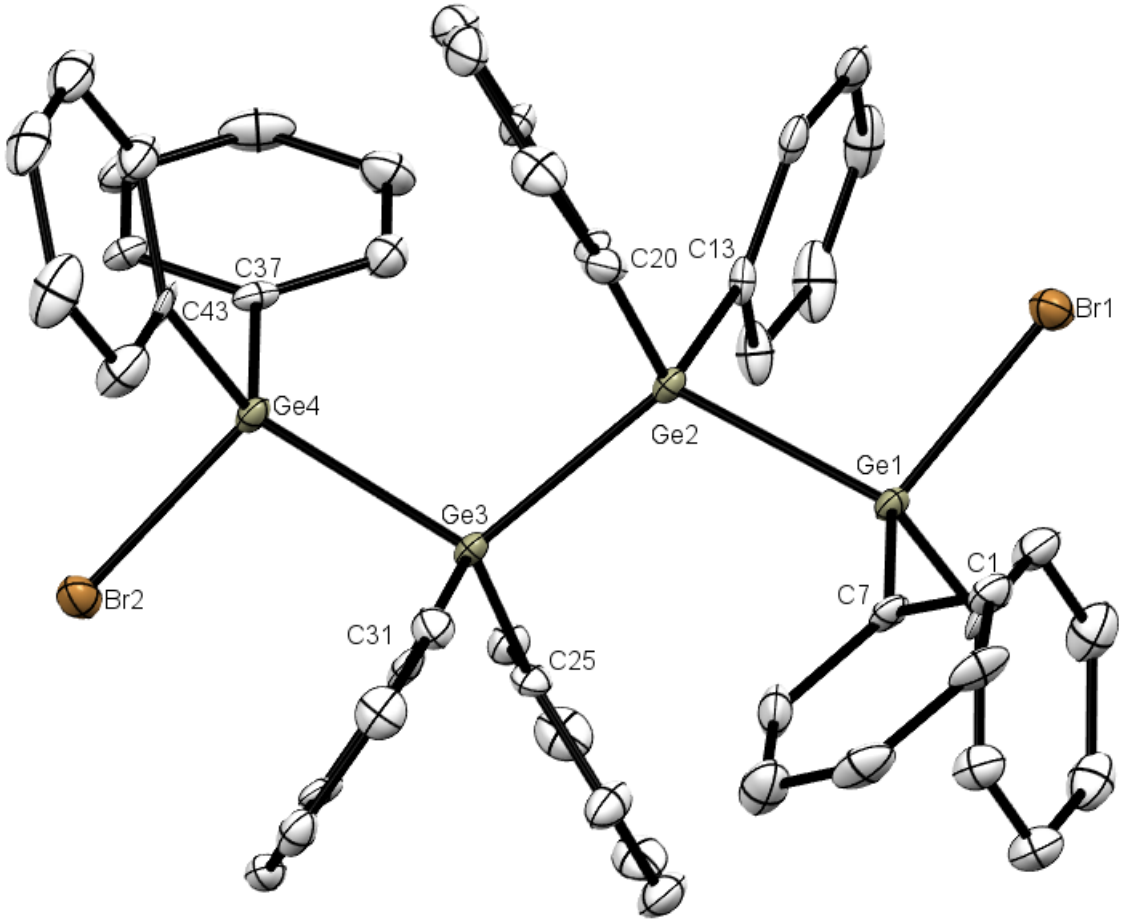

Figure 3.4. ORTEP diagram of **10** with hydrogen atoms omitted. Thermal ellipsoids are drawn at 50 % probability.

A crystal of **10** suitable for X-ray diffraction was obtained by diffusion of hexane into benzene and is shown in **Figure 3.4**. Compound **10** crystallized in the monoclinic space group P2(1) and select bond distances and angles for **10** are collected in **Table 3.4**. Two similar structures to that of **10** have been determined, including the iodine terminated tetragermane **9**, shown in **Scheme 3.3**.[10] The chlorine terminated tetragermane $Cl(GePh_2)_4Cl$, synthesized through germylene insertion of Ph_2Ge into Ph_2GeHCl followed by subsequent chlorination, has also been structurally analyzed.[11] The average bond distances and angles for the three halogen terminated tetragermanes are listed in **Table 3.3**. Similar to **10**, the iodine terminated species **9** crystallizes in a monoclinic space group $P2_1/n$, while the chlorine terminated analogue crystallizes in the triclinic space group P-1. Similarities also exist between $Cl(GePh_2)_4Cl$ and **9** in that both structures contain an inversion center located between the two central germanium atoms while the bromine terminated compound **10** does not. The average Ge – Ge and Ge – X bond distances increase as the covalent radius of the halogen atom increase. The average Ge – Ge – Ge bond angles for **9** and **10** are similar and measure 114.2(1)° and 113.29(3)°, respectively while the chlorine terminated tetragermane contained an average Ge – Ge – Ge bond angle of 116.24(8)°. All of the germanium atoms in all three compounds are present in a distorted tetrahedral geometry. In addition to the average Ge – Ge – Ge bond angles, the average Ge – Ge – X (X = Cl, Br, I) bond angles exhibit a trend as **9** and **10** are similar in value at 103.4(1) and 103.65(3)°, respectively, and $Cl(GePh_2)_4Cl$ possessed an average Ge – Ge – Cl bond able of 100.3(2)°.

Table 3.3. Average bond angles (Å) and bond angles (°) for the compounds $X(GePh_2)_4X$ (X = Cl, Br, I).[10,11]

Bond or Angle	**$Cl(GePh_2)_4Cl$**	**$Br(GePh_2)_4Br$ (10)**	**$I(GePh_2)_4I$**
d_{avg} Ge – Ge	2.445(3)	2.4473(7)	2.4549(5)
d_{avg} Ge – X	2.134(7)	2.3540(8)	2.5594(4)
d_{avg} Ge – C_{ispo}	1.97(7)	1.953(0)	1.95(2)
$\angle_{avg}$ Ge – Ge – Ge	116.24(8)	113.29(3)	114.2(1)
$\angle_{avg}$ Ge – Ge – X	100.3(2)	103.65(3)	103.4(1)

Table 3.4. Select bond distances (Å) and angles (°) for **10**. A complete list of bond angles and distances are listed in the appendix.

Br(1)-Ge(1)	2.3468(8)	C(19)-Ge(2)-C(13)	109.4(2)
Br(2)-Ge(4)	2.3612(8)	C(19)-Ge(2)-Ge(1)	112.86(14)
Ge(1)-C(7)	1.944(5)	C(13)-Ge(2)-Ge(1)	100.54(14)
Ge(1)-C(1)	1.952(5)	C(19)-Ge(2)-Ge(3)	107.96(15)
Ge(1)-Ge(2)	2.4470(7)	C(13)-Ge(2)-Ge(3)	110.49(15)
Ge(2)-C(19)	1.957(5)	Ge(1)-Ge(2)-Ge(3)	115.33(3)
Ge(2)-C(13)	1.959(5)	C(31)-Ge(3)-C(25)	108.3(2)
Ge(2)-Ge(3)	2.4548(6)	C(31)-Ge(3)-Ge(4)	102.61(15)
Ge(3)-C(31)	1.948(5)	C(25)-Ge(3)-Ge(4)	111.30(14)
Ge(3)-C(25)	1.964(5)	C(31)-Ge(3)-Ge(2)	111.85(16)
Ge(3)-Ge(4)	2.4401(7)	C(25)-Ge(3)-Ge(2)	111.24(15)
Ge(4)-C(37)	1.950(5)	Ge(4)-Ge(3)-Ge(2)	111.25(3)
Ge(4)-C(43)	1.952(5)	C(37)-Ge(4)-C(43)	109.6(2)

Average Ge-C	1.953(5)	C(37)-Ge(4)-Br(2)	104.83(15)
Average Ge-Ge	2.4473(7)	C(43)-Ge(4)-Br(2)	102.78(17)
Average Ge-Br	2.3540(8)	C(37)-Ge(4)-Ge(3)	118.39(16)
C(7)-Ge(1)-C(1)	111.6(2)	C(43)-Ge(4)-Ge(3)	115.28(14)
C(7)-Ge(1)-Br(1)	105.99(16)	Br(2)-Ge(4)-Ge(3)	103.94(3)
C(1)-Ge(1)-Br(1)	104.68(17)	Average C-Ge-C	109.7(6)
C(7)-Ge(1)-Ge(2)	119.15(15)	Average C-Ge-Br	104.57(5)
C(1)-Ge(1)-Ge(2)	110.62(14)	Average Ge-Ge-Br	103.65(3)
Br(1)-Ge(1)-Ge(2)	103.36(3)	Average Ge-Ge-Ge	113.29(3)

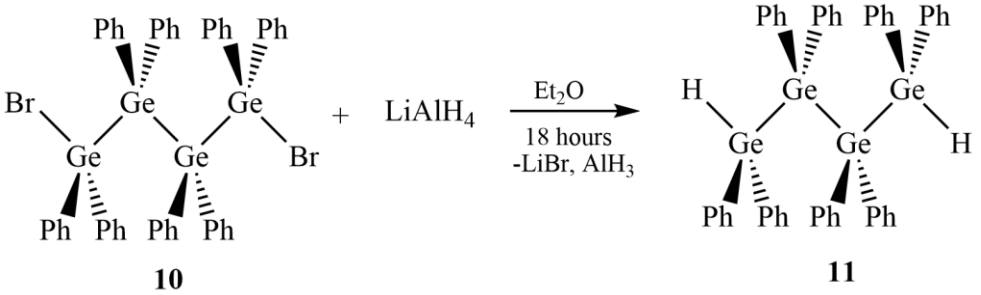

Scheme 3.4. Reduction of the bromine terminated tetragermane **10** to **11** using $LiAlH_4$.

The compounds **9** and **10** were both converted to the hydrogen terminated tetragermane, however when attempting the reaction in **Scheme 3.4** using the iodine terminated tetragermane **9**, several intractable products we obtained. Successful conversion of the bromine terminated tetragermane **10** to the 1,1,2,2,3,3,4,4-octaphenyltetragermane (**11)**, $H(GePh_2)_4H$, was achieved through the action of $LiAlH_4$ on **10** in Et_2O at room temperature for 18 hours and **11** was isolated, as shown in **Scheme**

3.4. The solution was quenched with de-gassed deionized water. Filtration of the reaction followed by drying of the ether layer over magnesium sulfate removed any residual water. Subsequent filtration to remove hydrated magnesium sulfate and then removal of the ether *in vacuo* produced **11** as a white solid in 84 % yield. The ^{1}H NMR spectrum of **11** exhibits a singlet at 5.63 ppm, arising from the two equivalent germanium-bound protons (**Figure 3.5a**). In comparison to the reported literature values for the germanium-bound hydrogen in the analugous compounds $H(GePh_2)H$ and $H(GePh_2)_2H$, which contain resonances at 5.15 and 5.57 ppm, respectively, the signal for **11** arises at 5.63 ppm. This is expected as the proton becomes less shielded with the increased number of consecutive formally Ge(II) atoms, and thus becomes shifted downfield with respect to the shorter compounds. The ^{13}C NMR spectra exhibited carbon signals for the two magnetically separate phenyl peaks at 140.53 (*ipso*-C_6H_5), 137.78 (*ipso*-C_6H_5), 136.49 (*ortho*-C_6H_5), 136.03 (*ortho*-C_6H_5), 128.88 (*para*-C_6H_5), 128.75 (*para*-C_6H_5), 128.56 (*meta*-C_6H_5) and 128.13 (*meta*-C_6H_5) ppm.

a)

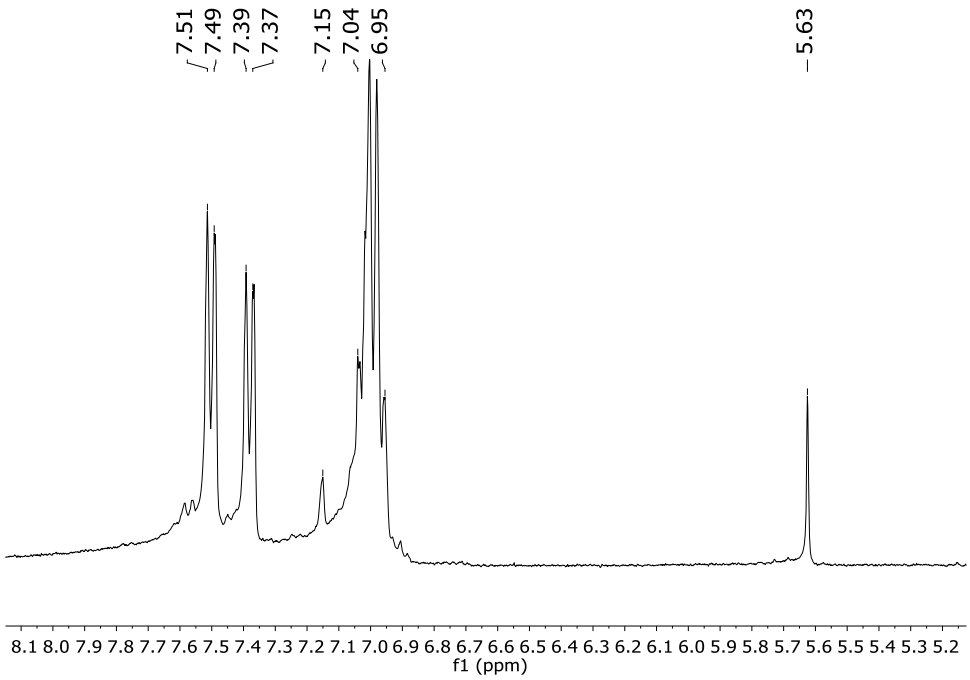

b)

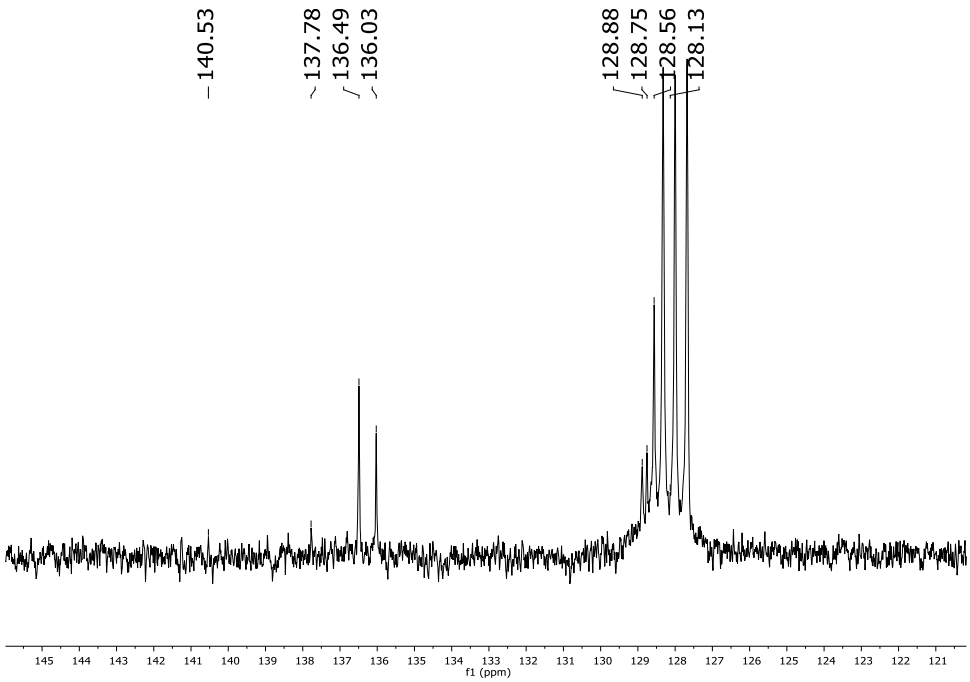

Figure 3.5. Aromatic regions of the NMR spectra of **11** in benzene-d_6. a.) ^{1}H NMR; b.) ^{13}C NMR

The infrared spectrum of the compound **11** was obtained. The stretching band for the germanium-hydrogen bond was observed at 2000 cm^{-1}. This value was similar to the stretching frequency for comparable compounds with the formula $H(GePh_2)_nH$ that were observed at 2024 (n = 1), 2028 (n = 2), and 2034 cm^{-1} (n = 3), and similar to values previously reported for $H(GePh_2)_4H$.[3,12]

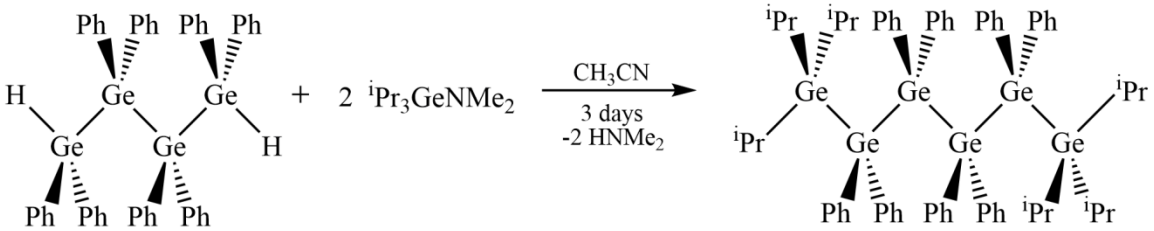

11 **12**

Scheme 3.5. The hydrogermolysis reaction to the isopropyl terminated hexagermane **12**.

The synthesis of the hexagermane was achieved via the hydrogermolysis reaction of the tetragermane **11** and two equivalents of tri-isopropylgermanium dimethylamide, $Pr^i_3GeNMe_2$. Unlike other examples of the hydrogermolysis reaction, **11** was only partially soluble in CH_3CN, even upon heating. Despite low solubility, the reaction was completed using conditions typical for the hydrogermolysis reaction, namely heating the reaction mixture at 90 °C for 72 hours. The product 1,1,1,6,6,6-hexaisopropyl-2,2,3,3,4,4,5,5-octaphenylhexagermane (**12**), $Pr^i_3Ge(GePh_2)_4GePr^i_3$, was only poorly soluble in hot CH_3CN, therefore **12** was filtered out of solution and washed using room temperature hexanes. Upon removal of the remaining volatiles *in vacuo*, **12** was collected as a white solid in 40% yield. Compound **12** exhibited a melting point range of 208-212 °C.

The ^{1}H NMR spectrum of **12**, shown if **Figure 3.5a**, did not contain the resonances associated with the protons attached to the germanium atom in **11** at 5.63 ppm, or the protons located on the amide methyl groups of the $Pr^{i}_{3}GeNMe_2$ starting material at 2.66 ppm. The resonances due to the methine and methyl protons of the isopropyl ligands were observed at 1.48 ppm as a septet (J = 7.2 Hz) and a doublet at 0.89 ppm (J = 7.2 Hz), respectively. Resonances for the *ortho*-protons on the phenyl rings were doublets observed at 7.39 (J = 7.5 Hz) and 7.34 (J = 7.5 Hz) ppm, both representing 8 hydrogens upon integration. Multiplets overlapping between 7.15 and 6.96 ppm were integrated to 24 hydrogens for the *meta*- and *para*-protons located on the phenyl rings of compound **12**. The ^{13}C NMR spectrum of **12**, as shown in **Figure 3.6b**, contained resonances for the carbons of the phenyl rings at 140.56, 139.73, 137.32, 137.02, 136.93, 136.56, 128.16 and 127.90 ppm. Resonances located at 21.2 and 18.2 ppm correspond to the methyl and methine carbons of the isopropyl groups, respectively.

A crystal of **12** suitable for X-ray diffraction was obtained through evaporative diffusion of hexanes into dichloromethane, CH_2Cl_2. An ORTEP depiction of **12** is shown in **Figure 3.7**. Selected bond distances and angles of **12** are listed in **Table 3.5**. The compound, which crystallizes in a P-1 space group contains a center of inversion located at the center of the innermost Ge-Ge single bond. The central bond was the longest of the three germanium-germanium bonds with a distance of 2.4710(3) Å, and the two terminal Ge-Ge bond distances each measured 2.4670(2) Å. All Ge – Ge bond distances are elongated in comparison to the typical distance of ca. 2.45 Å due to the presence of three sterically encumbering isopropyl groups on each terminal germanium atom. The two unique Ge – Ge – Ge bond angles were greater than the ideal tetrahedral angle of 109.5°

with an average value of 115.74(1)°. The most obtuse of the Ge – Ge – Ge bond angles were at the termini of the molecule due to the steric effects of the large isopropyl substituents. The average C – Ge – C bond angles at the terminal germanium atoms were close to ideal at 108.74(7)°, while the angles for internal C – Ge – C measured more acute, 107.95(6)° and 105.92(6)°, at Ge(2) and Ge(3), respectively. The geometric environment around the terminal germanium atoms were closer to an ideal tetrahedral environment than the internal germanium atoms, and this has been observed when three relatively large substituents need to be accomodated at a single germanium atom.

a)

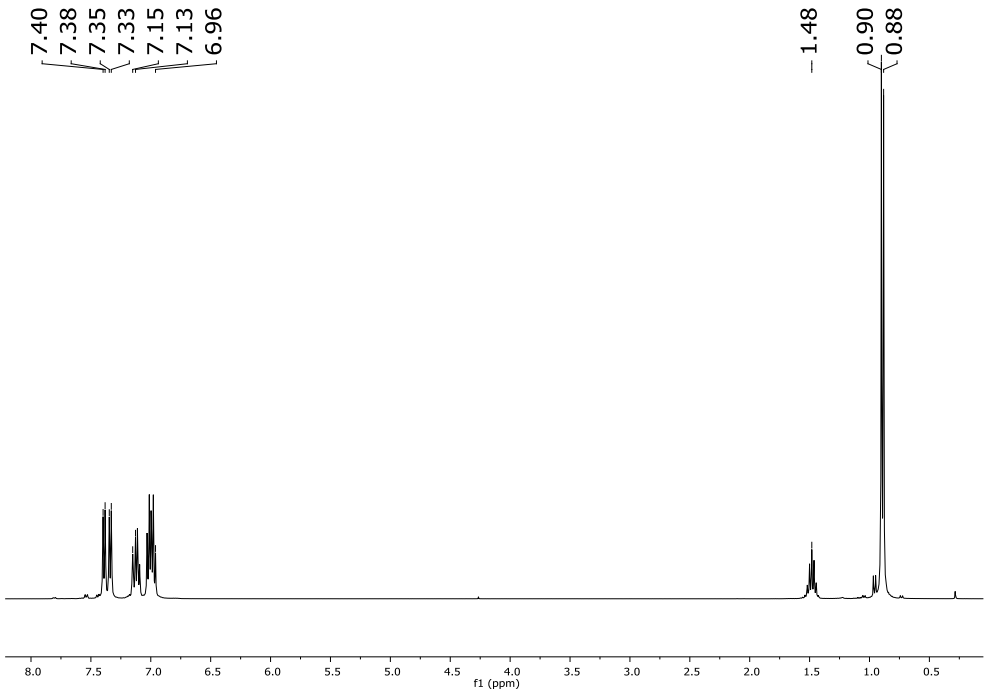

b)

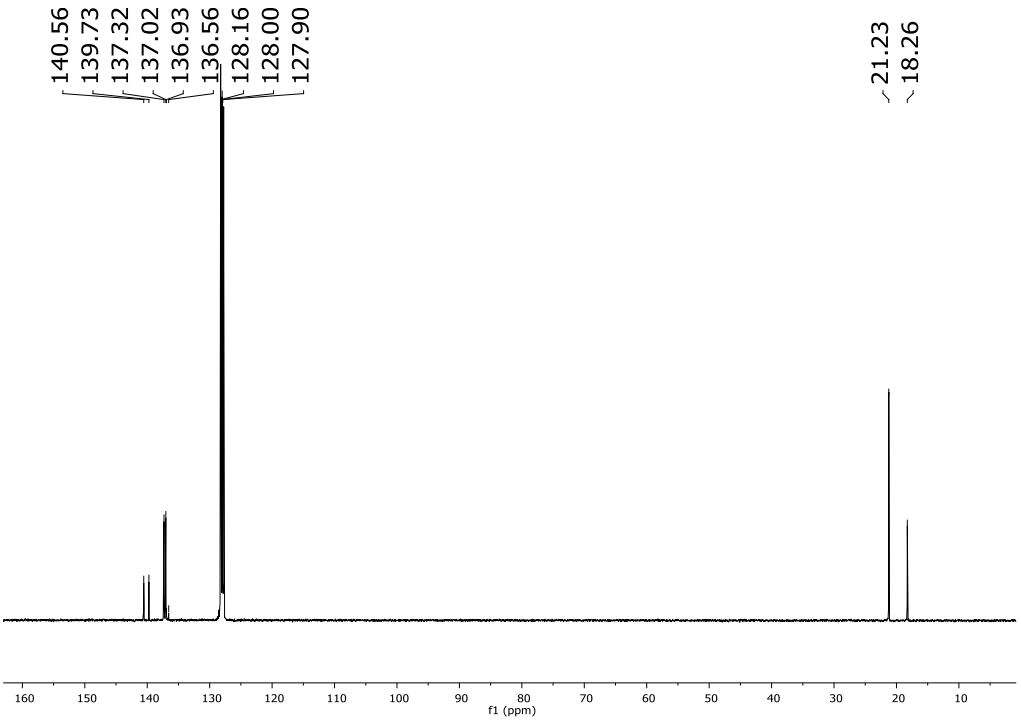

Figure 3.6. a) ^{1}H NMR spectrum of **12** in benzene-d_6. b) ^{13}C NMR spectrum of **12** in benzene-d_6.

The overall geometry of the crystal packing for **12** can be considered through two different perspectives, which are shown in **Figure 3.8**. One perspective contains two sets of three *trans*-coplanar germanium atoms. However, a second perspective can also be obtained in which the four central germanium atoms are coplanar and arranged in a *trans*-fashion. In this second perspective, one terminal atom is canted above the Ge_4 plane while the opposite terminal atom is canted below the Ge_4 plane. This second perspective, thus, shows a similar disposition for four of the five germanium atoms in Ge_5Ph_{12}.

The hexagermane **12** is, to date, the longest structurally characterized linear oligomeric germanium compound to be reported. The intriguing physical properties of **12** will be discussed in Chapter 4. We also endeavored to synthesize the related smaller

oligomers $Pr^{i}_{3}Ge(GePh_2)_nGePr^{i}_{3}$, where n = 2, 3 and 4, such that their structures and properties could be compared to compound **12**.

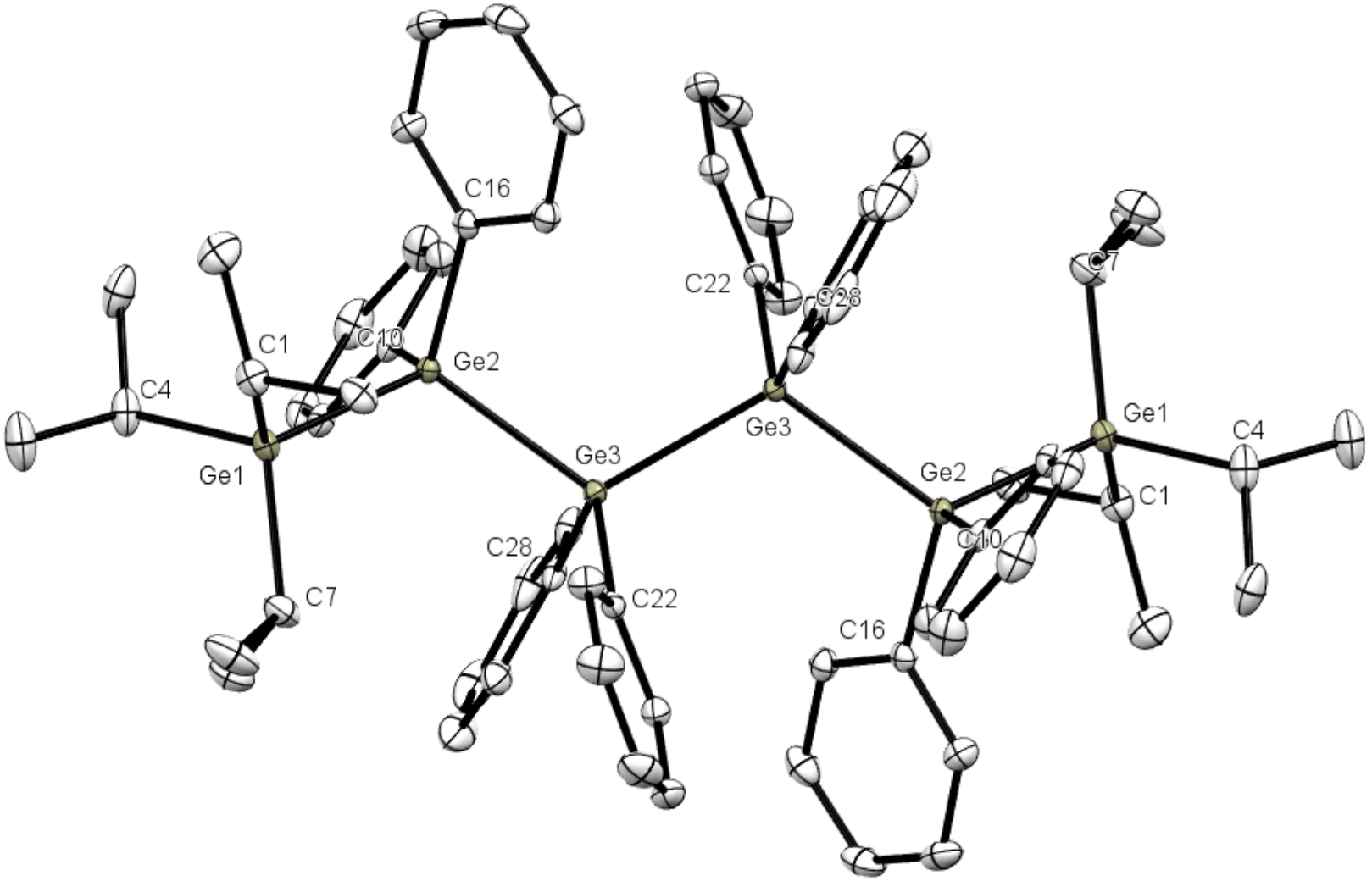

Figure 3.7. ORTEP diagram of **12** with the hydrogen atoms omitted. Thermal ellipsoids are drawn at 50% probability.

Table 3.5. Select bond distances (Å) and angles (°) for **12**. A complete list of bond angles and distances are listed in the appendix.

Ge(1)-C(4)	1.9892(16)	C(22)-Ge(1)-C(28)	105.92(6)
Ge(1)-C(7)	1.9948(16)	C(4)-Ge(1)-Ge(2)	109.19(5)
Ge(1)-C(1)	1.9952(16)	C(7)-Ge(1)-Ge(2)	109.49(5)
Ge(2)-C(16)	1.9552(15)	C(1)-Ge(1)-Ge(2)	111.91(4)
Ge(2)-C(10)	1.9697(15)	C(16)-Ge(2)-Ge(1)	107.71(4)
Ge(3)-C(22)	1.9666(15)	C(10)-Ge(2)-Ge(1)	110.80(4)
Ge(3)-C(28)	1.9682(15)	C(16)-Ge(2)-Ge(3)	111.71(4)
Ge(1)-Ge(2)	2.4670(2)	C(10)-Ge(2)-Ge(3)	100.93(4)
Ge(2)-Ge(3)	2.4715(3)	C(22)-Ge(3)-Ge(2)	115.68(4)
Ge(3)-Ge(3#)	2.4745(3)	C(28)-Ge(3)-Ge(2)	99.69(4)
C(4)-Ge(1)-C(7)	108.99(7)	C(22)-Ge(3)-Ge(3#)	108.47(4)
C(4)-Ge(1)-C(1)	108.74(7)	C(28)-Ge(3)-Ge(3#)	112.43(4)
C(7)-Ge(1)-C(1)	108.48(7)	Ge(1)-Ge(2)-Ge(3)	117.330(8)
C(16)-Ge(1)-C(10)	107.95(6)	Ge(2)-Ge(3)-Ge(3#)	114.153(10)

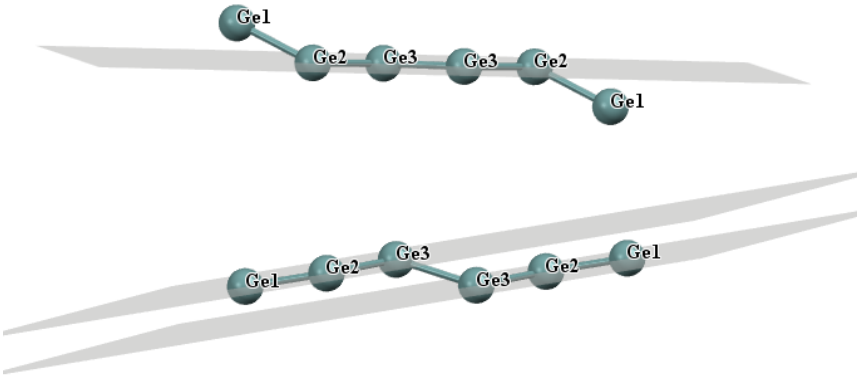

Figure 3.8. MERCURY diagram of the germanium backbone of **12** through as viewed through two separate planes.

The Pentagermane

Synthesis of 1,1,1,5,5,5-hexaisopropyl-2,2,3,3,4,4-hexaphenylpentagermane (**14**), $Pr^{i}_{3}Ge(GePh_2)_3GePr^{i}_{3}$, first required the preparation of a trigermane containing a germanium-hydrogen bond on both the terminal germanium atoms, to which the capping $Pr^{i}_{3}Ge$- groups could be attached. Previous syntheses indicated this task would be difficult to perform while still achieving a discrete molecule.

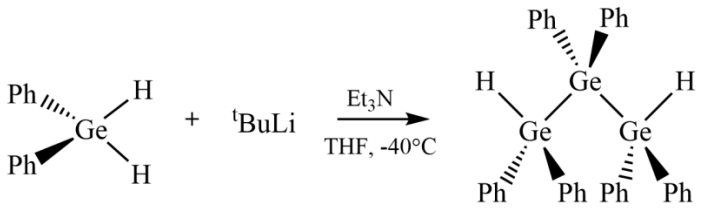

13

Scheme 3.6. Synthesis of **13** via a (diarylgermyl)lithium compound.[3]

The synthesis of hexaphenyltrigermane, $H(GePh_2)_3H$ (**13**), was accomplished through decomposition of (diarylgermyl)lithium compounds, as reported by Castel *et al*.[3] This reaction, as shown in **Scheme 3.6**, was previously used with the subsequent hydrogermolysis reaction in order to synthesize $Ph_3Ge(GePh_2)_3GePh_3$ in excellent yields.[2] When *tert*-butyllithium is added in slight excess to diphenylgermane at -40 °C, the (diarylgermyl)lithium, Ph_2GeHLi, is generated. The lithium compound slowly decomposes in THF at 20 °C, and the decomposition becomes more efficient in the presence of an amine such as triethylamine, Et_3N. By controlling the reaction time in the presence of Et_3N, the selective synthesis of the di-, tri- and tetragermyllithium will occur with limited amounts of unwanted oligomers. Further reaction of the decomposition product with water provides the oligogermanes $H(Ph_2Ge)_nH$. To achieve **13**, the

decomposition was allowed to react for 9.5 hours, at which time quenching was performed. After filtration and removal of volatiles *in vacuo*, a crude product was collected as a milky viscous liquid.

The ^{1}H NMR spectrum of this crude product mixture indicated that there were two different germanium-bound hydrogens giving resonances at 5.68 and 5.15 ppm. The most upfield signal contained a shift identical to that of Ph_2GeH_2.[2] Purification was attempted via distillation on a high vacuum line using a Kugelrohr oven, but the two species could not be separated.

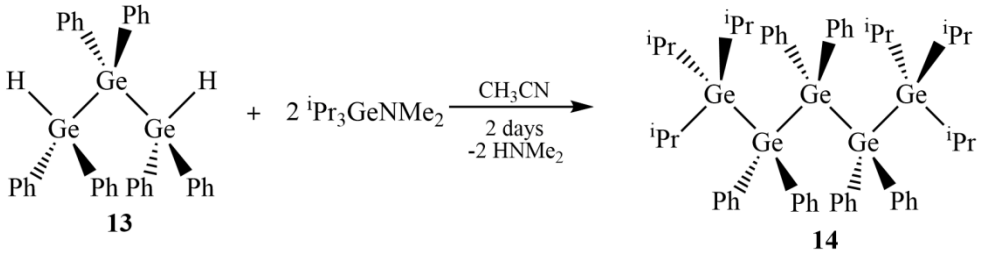

Scheme 3.7. Hydrogermolysis reaction to the pentagermane **14**.

A decision was made to proceed despite the presence of a product mixture, with the anticipation that the products obtained after hydrogermolysis could be separated by crystallization. Synthesis of **14** via the hydrogermolysis reaction using the mixture containing **13** and two equivalents of $Pr^{i}_{3}GeNMe_2$, as shown in **Scheme 3.7**, was performed in CH_3CN solvent with a reaction time of 72 hours. After reaction a solid precipitate formed, which was filtered from the solvent and washed with hexanes to remove any smaller oligomers resulting from the hydrogermolysis reaction of the amide with Ph_2GeH_2. Compound **14** was collected as a white solid in 23 % yield.

Despite starting with a mixture of hydrogen-terminated oligogermanes, the ^{1}H NMR spectrum of the product indicated **14** formed a clean product. The ^{1}H NMR spectrum of **14** contained a doublet at 0.96 ppm (J = 7.4 Hz) for the methyl protons of the isopropyl groups and a septet at 1.54 ppm (J = 7.4 Hz) for the methine protons of the isopropyl groups. The phenyl region of the ^{1}H NMR spectrum consisted of two doublets at 7.81 ppm (J = 7.1 Hz) and 7.43 ppm (J = 7.9 Hz) for the *ortho*-phenyl protons, and a multiplet at 7.11 – 6.98 ppm for the *meta*- and *para*-phenyl protons. Attempts at obtaining a crystal suitable for X-ray diffraction were unsuccessful.

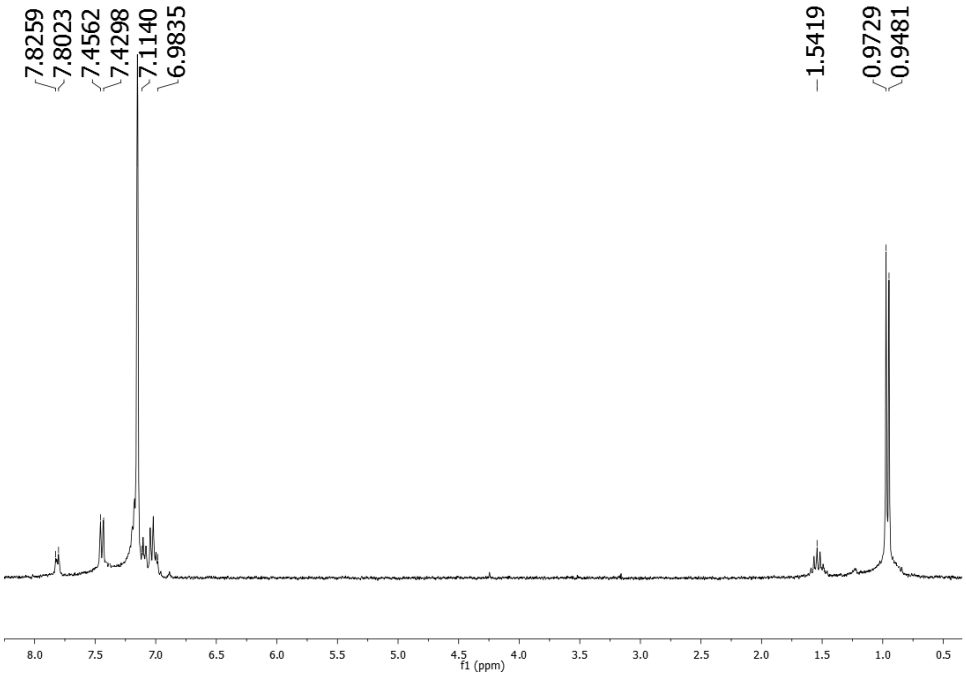

Figure 3.9. ^{1}H NMR spectrum of **14** in benzene-d_6.

SYNTHESIS OF THE LINEAR TETRA- AND TRIGERMANES

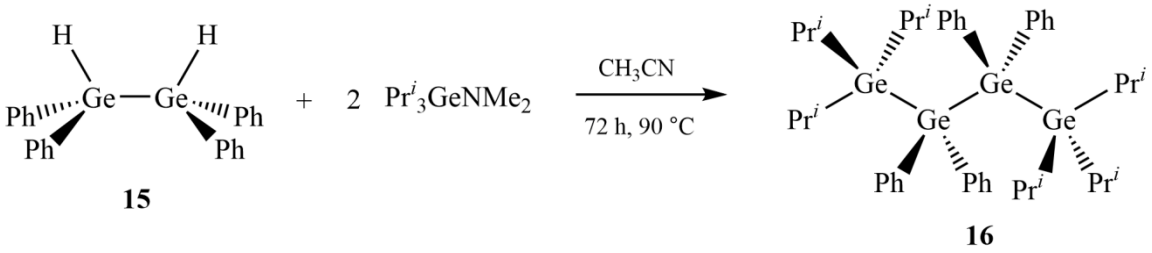

Scheme 3.8. Attempted hydrogermolysis reaction of **15** with two equivalents of $Pr^i_3GeNMe_2$.

The synthesis of the linear tetragermane and trigermane of the series $Pr^i_3Ge(GePh_2)_nGePr^i_3$ (n = 1 or 2) proved a much more difficult task than the larger oligomers. To prepare the linear tetragermane $Pr^i_3Ge(GePh_2)_2GePr^i_3$ (**16)**, two equivalents of $Pr^i_3GeNMe_2$ were reacted with $HPh_2GeGePh_2H$ (**15**) in CH_3CN for 72 hours at 90 °C, as shown in **Scheme 3.8**. A solid yellow precipitate formed that was initially collected through filtration and washed with hexanes. This means of work-up was not effective as **16** is sparingly soluble in hexanes at room temperature, which was shown by recording the ^1H NMR of both the solid collected through filtration and of the material collected from the dried hexane wash layer.

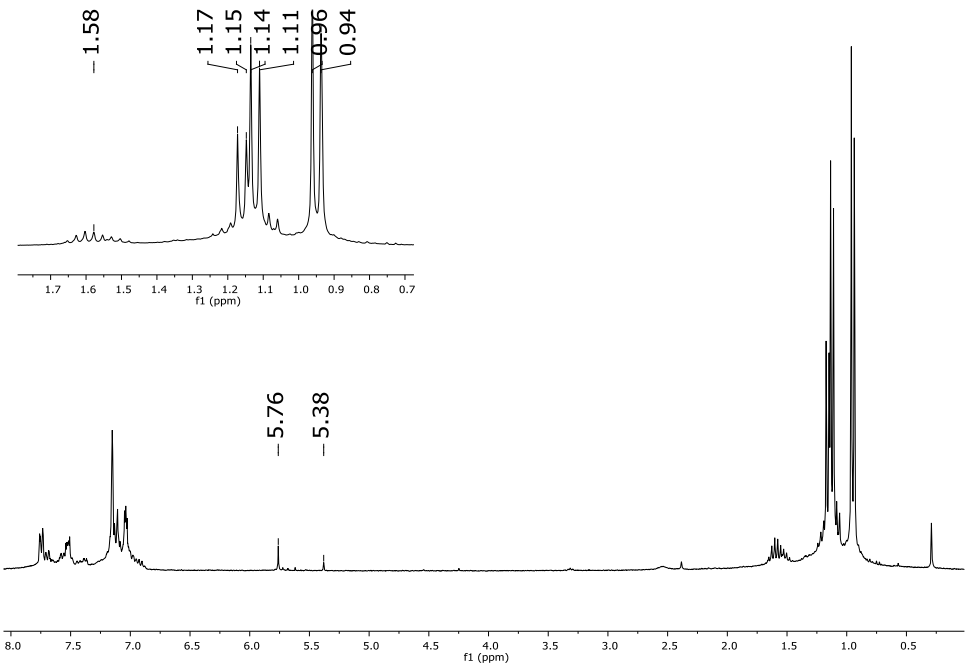

Figure 3.10. ^{1}H NMR spectrum of the reaction of two equivalents of $Pr^{i}_{3}GeNMe_2$ with one equivalent of $HPh_2GeGePh_2H$, in benzene-d_6.

The ^{1}H NMR spectrum shown in **Figure 3.10**, of the product obtained via **Scheme 3.8**, contained three separate sets of doublets corresponding to the methyl protons of three magnetically non-equivalent isopropyl groups (1.16, 1.13 and 0.95 ppm). A multiplet between 1.40 and 1.70 ppm as well as a multiplet visible among the doublets between 1.00 and 1.30 ppm indicated the presence of methyl protons of three different sets of isopropyl groups. Besides suggesting the presence of multiple isopropyl groups, the ^{1}H NMR spectrum also contained two singlet resonances at 5.76 and 5.38 ppm. These resonances are within the range typical for germanium-bound hydrogen atoms. The phenyl region of the spectrum also indicated that multiple species were present in the product of **Scheme 3.8**.

Multiple attempts were made to synthesize **16** as a clean product, all resulting in a similar NMR spectrum. It was decided that the hydrogermolysis reaction of two equivalents of $Pr^{i}_{3}GeNMe_2$ with one equivalent of $HPh_2GeGePh_2H$, did not effectively proceed to completion. Based on the ^{1}H NMR spectrum of the product, it was hypothesized that the species present in the product are $Pr^{i}_{3}GeCH_2CN$, **15**, $H(GePh_2)_2GePr^{i}_{3}$ and **16**. This mixture of compounds accounted for the three chemically distinct isopropyl groups, as well as the two separate resonances for the germanium-bound hydrogens. The resonance located at 5.76 ppm was close to the Ge – H proton resonance in **15** at 5.62 ppm, to indicate the presence of **15** in the product mixture, and the resonance observed at 5.38 ppm was attributed to the compound $H(GePh_2)_2GePr^{i}_{3}$.

Attempts were made to separate **16** from the other compounds in the product mixture. One such attempt was by utilizing distillation under high vacuum with a Kugelrohr oven. Temperatures up to 160 °C at 0.05 mmHg were applied to the solution, but no separation occurred. Heating of the sample to higher temperatures resulted in the pyrolysis of the sample.

Purification of the product mixture through crystallization was also attempted. Though bulk crystallization was ineffective, a crystal suitable for X-ray diffraction was obtained through slow evaporative diffusion of hexane into benzene, and the structure obtained is shown in **Figure 3.11**. Select bond distances and angles for **16** are listed in **Table 3.6**. Compound **16** crystallized in the triclinic crystal system in the P-1 space group. The tetragermane has an inversion center located between the central two germanium atoms, which is also the longest Ge – Ge bond in the compound. The average Ge – Ge bond for **16** is 2.4696(4) Å, which is similar to the average Ge – Ge bond for **12**

that measures 2.4703(2) Å. The average Ge – C bond lengths of 1.974(5) Å at the terminal germanium atoms were longer than the Ge – C bond lengths of the internal germanium atom bound to phenyl at 1.991(5) and 1.968(5) Å, respectively. The C – Ge – C bond angles of the –$GePr^{i}_{3}$ groups were also more obtuse than the corresponding bond angle at the phenyl-substituted germanium atoms with angles of 108.4(8)° and 104.9(2)°, respectively. This trend, which is also present in the hexagermane **12**, is attributed to the three relatively large substituents on the terminal atoms, which force a nearly tetrahedral environment at the terminal germanium atoms.

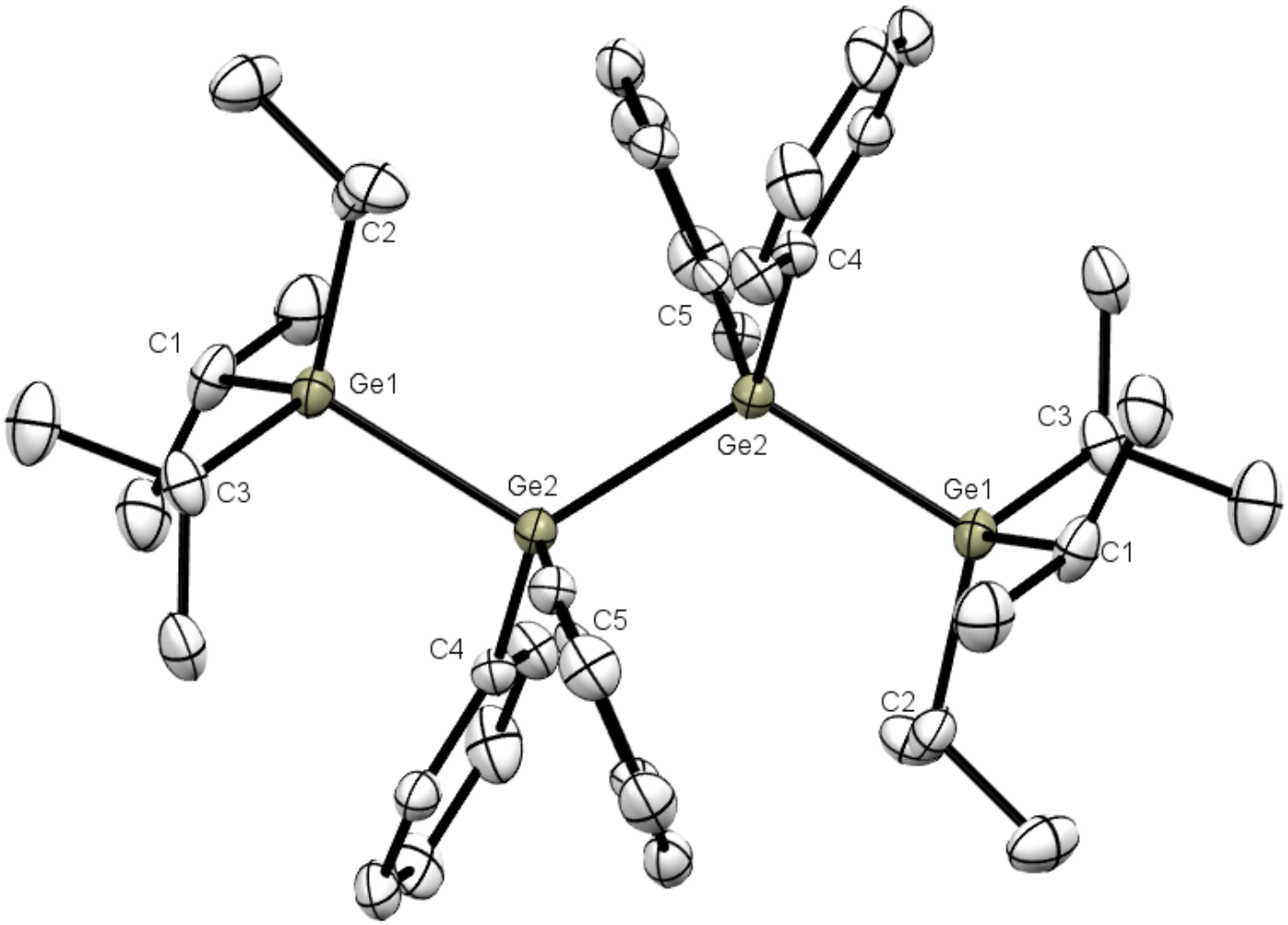

Figure 3.11. ORTEP diagram of **16** with the hydrogen atoms omitted. Thermal ellipsoids are drawn at 50 % probability.

Table 3.6. Select bond distances (Å) and angles (°) for **16**. A complete list of bond angles and distances are listed in the appendix.

Ge(1) – Ge(2)	2.4669(7)	C(3) – Ge(1) – Ge(2)	110.22(15)
Ge(2) – Ge(2#)	2.4723(10)	C(4) – Ge(2) – Ge(1)	105.10(13)
Ge(1) – C(1)	1.985(5)	C(4) – Ge(2) – Ge(2#)	109.50(14)
Ge(1) – C(2)	1.955(5)	C(5) – Ge(2) – Ge(1)	111.22(14)
Ge(1) – C(3)	1.993(5)	C(5) – Ge(2) – Ge(2#)	108.89(12)
Ge(2) – C(4)	1.962(5)	C(1) – Ge(1) – C(2)	107.6(2)
Ge(2) – C(5)	1.974(5)	C(1) – Ge(1) – C(3)	109.6(2)
Ge(1) – Ge(2) – Ge(2#)	116.51(3)	C(3) – Ge(1) – C(2)	108.2(2)
C(1) – Ge(1) – Ge(2)	110.61(15)	C(4) – Ge(2) – C(5)	104.9(2)
C(2) – Ge(1) – Ge(2)	110.49(13)		

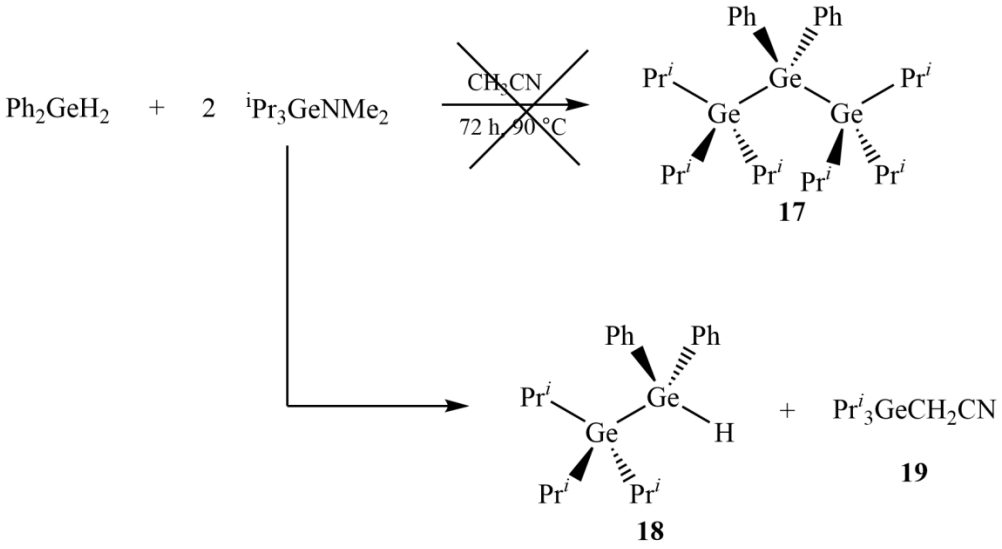

Scheme 3.9. Attempted synthesis of **17** via the hydrogermolysis reaction.

The synthesis of 1,1,1,3,3,3-hexaisopropyl-2,2-diphenyltrigermane (**17**), $Pr^{i}_{3}GeGePh_2GePr^{i}_{3}$ also proved to be difficult. Like the previous reactions, the hydrogermolysis reaction was carried out using two equivalents of $Pr^{i}_{3}GeNMe_2$ and one equivalent of Ph_2GeH_2, as shown in **Scheme 3.9**, in an attempt to synthesize the trigermane $Pr^{i}_{3}GeGePh_2GePr^{i}_{3}$. After reaction time of 72 hours at 90 °C and evaporation of the CH_3CN solvent *in vacuo*, a ^1H NMR spectrum was recorded of the clear resulting liquid (**Figure 3.12**). The product contained a resonance within the typical range of germanium-bound hydrogen atom at 5.34 ppm, which is shifted downfield from the germanium bound hydrogen in Ph_2GeH_2, typically observed at 5.15 ppm. The presence of the resonance for the Ge – H indicates that the reaction had not gone to completion. The spectrum also contained two sets of doublets and two septets for the methyl and methine protons of two magnetically non-equivalent isopropyl groups. Only one set of phenyl resonances were visible in the spectrum, indicating that only one species containing phenyl groups was present, and a singlet is also visible at 1.20 ppm. The ^1H NMR spectrum indicated that two compounds are present in the product, $Pr^{i}_{3}GePh_2GeH$ and $Pr^{i}_{3}GeCH_2CN$, where the former gives rise to the phenyl resonances, the doublet at 1.16 ppm (methyl) and the septet at 1.76 ppm (methine). The CH_2 (methylene) of the α-nitrile species is responsible for the singlet at 1.20, the ISOPROPYL doublet at 0.97 ppm and the septet at 1.53 ppm. The resonances for the α-nitrile species correspond to the values reported previously.[13]

The reaction was repeated and stirred at 90 °C for 10 days. After removal of the solvent *in vacuo*, the ^1H NMR spectrum looked identical to the spectrum taken after 72 hours. The reaction was also attempted at a temperature of 110 °C, but the ^1H NMR data

indicated the reaction was again unsuccessful. Unlike the synthesis of the tetragermane, there was no evidence for the formation of the desired product in the attempted synthesis of the trigermane. The compound **18** was synthesized separately by reacting Ph_2GeH_2 with one equivalent of $Pr^i_3GeNMe_2$. After removing the volatiles *in vacuo*, **18** was isolated as a colorless oil in 87% yield. The ^{1}H NMR spectrum of **18** contained a doublet at 1.13 (J = 7.2 Hz) and a septet at1.50 (J = 7.2 Hz) ppm for the methyl and methine protons, respectively. The phenyl region contained two multiplet regions at 7.67 – 6.40 ppm and 7.16 – 7.07 ppm for the *meta*- and overlapping *ortho*- and *para*-phenyl protons, respectively. A singlet was present at 5.34 ppm for the germanium-bound hydrogen, which is identical to the germanium-bound hydrogen resonance found in the product shown in **Figure 3.12**.

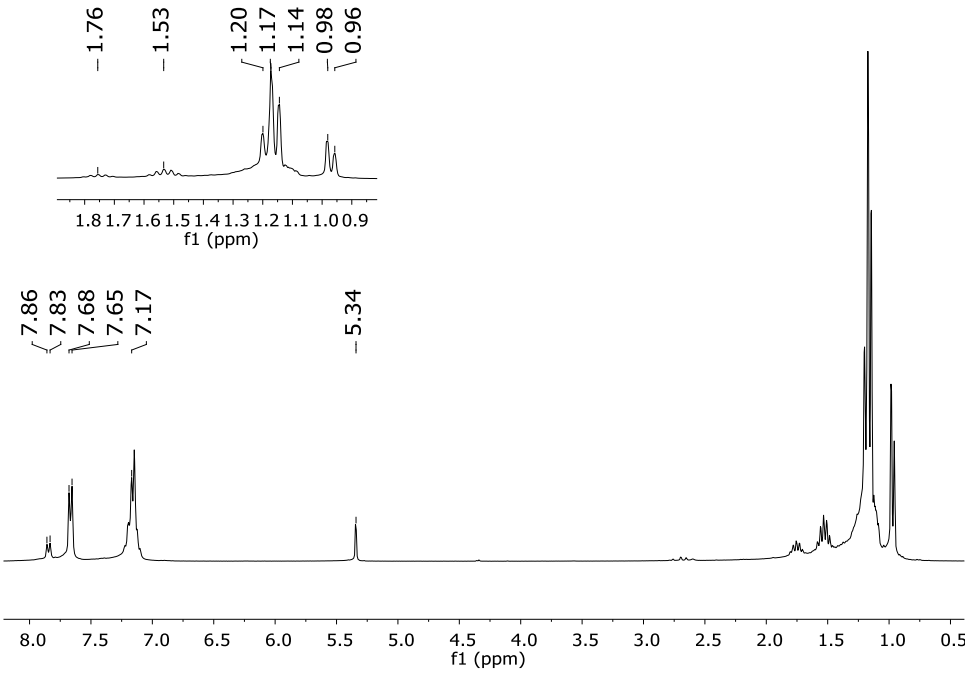

Figure 3.12. ^{1}H NMR spectrum of the hydrogermolysis reaction of two equivalents of $Pr^i_3GeNMe_2$ with one equivalent of Ph_2GeH_2, in benzene-d_6.

The ability to perform a single addition of a trialkyl germanium to a germanium species containing two germanium-bound hydrogens is a very unique quality of this reaction. The hydrogermolysis reaction rarely proceeds with such selectivity where only one germanium-bound hydrogen is replaced. Other examples of similar reactivity occurring often proceeded when single addition occurred on a longer chain of germanium atoms, where the extended chain length makes the germanium-bound hydrogen less reactive.[2] Both the attempted synthesis of the trigermane and the synthesis of the tetragermane are unique systems for the hydrogermolysis, as many tri- and tetragermanes have been successfully synthesized using the hydrogermolysis reaction, none of those reported however contain isopropyl groups. It was then pertinent to ask if qualities of the isopropyl group were affecting the reactive nature of the germanium-bound hydrogen to perform electrophilic attack on the carbon of the α-germyl nitrile.

Previous experiments implementing the hydrogermolysis reaction in our research lab has revealed a correlation between the use of alkyl and phenyl substituents and the success of the reaction. When alkyl substituents were bound to the same germanium atom as the hydrogen atom, the reaction was stalled or completely hindered. This is typically seen as reactions using R_3GeH (R = Bu, Pr, Et, Me) produced no yield or low yield for the hydrogermolysis reaction in comparison to Ar_3GeH (Ar = phenyl, tolyl) when reacted with Ph_3GeNMe_2. The inductively donating alkyl groups cause the germanium-bound hydrogen atom to be less electropositive, preventing the hydrogermolysis reaction from effectively occurring.

In the attempted synthesis of **16** and **17**, a similar correlation can be made. In these reactions, a stepwise addition of the terminal germanium atoms occurs. The

addition of the first $-GePr^{i}_{3}$ group readily proceeds and the product from this addition is observed in the ^{1}H NMR spectra of the reactions shown in both **Scheme 3.8** and **Scheme 3.9**. The addition of the second $-GePr^{i}_{3}$ group does not add in the case of the attempted synthesis of the trigermane $Pr^{i}_{3}GeGePh_{2}GePr^{i}_{3}$ and only partially adds in the attempted synthesis of the tetragermane $Pr^{i}_{3}Ge(GePh_{2})_{2}GePr^{i}_{3}$. Comparing these compounds with the observed reactivity of $R_{3}GeH$ for hydrogermolysis, the inductive donating ability of the isopropyl groups continues to have a significant impact on the electronic nature of the remaining germanium-bound hydrogen atom even when not located on the same germanium atom. When the isopropyl groups were on the germanium atom β to the germanium-bound hydrogen as in the case of the attempted synthesis of **17**, the trigermane products were not observed through NMR spectroscopy. When the isopropyl groups were positioned on the germanium atom γ to the hydrogen atom, as in the synthesis of **16**, the reaction occur but failed to proceed to completion. In the synthesis of the pentagermane **14**, where the isopropyl groups were located on the germanium atom δ to the hydrogen, the reaction proceeded with no observable difficulty. Thus the inductively donating isopropyl group has a significant impact on the success of the hydrogermolysis reaction and the effects of the electron donating alkyl are diminished when the alkyl substituents are located on germanium atoms farther from the participating germanium-bound hydrogen.

CONCLUSION

The first hexagermane to be structurally characterized was obtained in four steps from Ph_2GeCl_2, where the final two germanium atoms were added to the chain using the hydrogermolysis reaction in good yields. The related pentagermane was also synthesized in low yields from $H(GePh_2)_3H$. Upon attempted synthesis of the linear tri- and tetragermane, a limit to the success of the hydrogermolysis reaction was realized. The presence of isopropyl groups β or γ to the reactive hydrogen atom appeared to inhibit the formation of the Ge – Ge bonds using the hydrogermolysis reaction.

EXPERIMENTAL

General Considerations

All manipulations were carried out under an inert atmosphere of nitrogen gas using standard Schlenk, syringe, and glovebox techniques. All solvents were purified using a Glass Contour solvent purification system. The starting materials Ph_2GeH_2 and Pr^i_3GeCl were purchased from Gelest. The reagents $LiAlH_4$, $LiNMe_2$, sodium, Br_2, I_2, Bu^tLi, and Et_3N were purchased from Sigma-Aldrich. All starting materials and reagents were used as received with no further purification. The compounds $Pr^i_3GeNMe_2$[13] and $H(GePh_2)(GePh_2)H$[9] were synthesized using previously reported methods. All NMR spectra were collected on either an INOVA Gemini 2000 NMR spectrometer or the INOVA UNITY 400 NB spectrometer and were referenced to benzene-d_6 solvent. IR

spectra were obtained using a Perkin-Elmer 1720 infrared spectrometer. Elemental analyses were conducted by Galbraith Laboratories.

All single crystal X-ray diffraction studies were carried out at the UCSD Crystallography Lab using a Bruker Kappa APEX-II CCD diffractometer equipped with Mo Kα radiation. Crystals were mounted on a Cryoloop with Paratone oil and data were collected in a nitrogen gas stream at 100(2) K. Crystal-to-detector distance was 35 mm and exposure time was 20 seconds per frame using a scan width of 1.0°. The data were integrated using the Bruker SAINT Software program and scaled using the SADABS software programs. Nonhydrogen atoms were refined anisotropically by full-matrix least-squares (SHELXL-2013). Hydrogen atoms were placed using a riding model and constrained relative to their parent atoms using HFIX command in SHELXL-2013.

Synthesis of $Br(GePh_2)(GePh_2)(GePh_2)(GePh_2)Br$ (10)

A suspension of Ge_4Ph_8 (0.30 g, 0.33 mmol) in benzene (50 mL) was titrated with a 0.059 M solution of bromine in benzene until the solution remained clear with a slight yellow color. Volatiles were removed *in vacuo* and the resulting solid was washed with cold Et_2O (3 x 5 mL). Product was dried *in vacuo* to yield **10** (0.31 g, 89% yield) as a white solid. ^{1}H NMR (C_6D_6, 25 °C) δ 7.60 (d, J = 7.8 Hz, 8 H, *m*-C_6H_5), 7.41 (d, J = 7.5 Hz, 8 H, *m*-C_6H_5), 7.06 – 6.90 (m, 24 H, *o*-C_6H_5 and *p*-C_6H_5) ppm. ^{13}C NMR (C_6D_6, 25 °C) δ 136.87 (*ipso*-C_6H_5), 136.78 (*ortho*-C_6H_5), 135.73 (*ipso*-C_6H_5), 134.74 (*ortho*-C_6H_5), 129.99 (*para*-C_6H_5), 129.44 (*para*-C_6H_5), 128.78 (*meta*-C_6H_5), 128.67 (*meta*-

C_6H_5) ppm. UV/Vis (CH_2Cl_2): λ_{max} 281 nm (ε 8.4 x 10^4 M^{-1} cm^{-1}). *Anal*. Calcd. For $C_{48}H_{40}Br_2Ge_4$: C, 54.00; H, 3.78. Found: C, 53.87; H, 3.83.

Synthesis of H($GePh_2$)($GePh_2$)($GePh_2$)($GePh_2$)H (11)

To a solution of **10** (1.05 g, 0.984 mmol) in Et_2O (60 mL) was added $LiAlH_4$ (0.08 g, 2 mmol) while in a -78 °C bath. The reaction mixture was allowed to come to room temperature and was stirred for 18 hours. The solution was quenched with 5 mL de-gassed deionized water, and subsequently filtered. The remaining clear solution was dried over $MgSO_4$ and filtered. The solvent was removed *in vacuo* to yield **11** (0.75 g, 84% yield) as a white solid. ^{1}H NMR (C_6D_6, 25 °C) δ 7.50 (d, *J* = 6.3 Hz, 8 H, *o*-C_6H_5). 7.38 (d, *J* = 6.3 Hz, 8 H, *o*-C_6H_5), 7.04 – 6.95 (m, 24 H, *m*-C_6H_5 and *p*-C_6H_5), 5.63 (s, 2H, -Ge-*H*) ppm. ^{13}C NMR (C_6D_6, 25 °C) δ 140.53 (*ipso*-C_6H_5), 137.78 (*ipso*-C_6H_5), 136.49 (*ortho*-C_6H_5), 136.03 (*ortho*-C_6H_5), 128.88 (*para*-C_6H_5), 128.75 (*para*-C_6H_5), 128.56 (*meta*-C_6H_5), 128.13 (*meta*-C_6H_5) ppm. *Anal*. Calcd. For $C_{48}H_{42}Ge_4$: C, 63.37; H, 4.66. Found: C, 63.26: H, 4.59.

Preparation of $Pr^i_3Ge(GePh_2)(GePh_2)(GePh_2)(GePh_2)GePr^i_3$, (12)

To a solution of $Pr^i_3GeNMe_2$ (0.22 g, 0.90 mmol) in CH_3CN (15 mL) was added a solution of **11** (0.40 g, 0.45 mmol) in CH_3CN (15 mL). The reaction mixture was sealed in a Schlenk tube and was stirred in an oil bath at 90 °C for 72 h, after which time a white precipitate was present. The reaction mixture was cooled and the solid was collected by

filtration and washed with hexane (3 x 5 mL) to yield **12** (0.23 g, 40%) as a white solid. ^{1}H NMR (C_6D_6, 25 °C) δ 7.39 (d, J = 7.5 Hz, 8H, *ortho*-C_6H_5), 7.34 (d, J = 7.5 Hz, 8H, *ortho*-C_6H_5), 7.15 – 6.96 (m, 24H, *meta*-C_6H_5 and *para*-C_6H_5), 1.48 (septet, J = 7.2 Hz, 6H, -C*H*$(CH_3)_2$), 0.89 (d, J = 7.2 Hz, 36H, -CH(C*H*$_3)_2$) ppm. ^{13}C NMR (C_6D_6, 25 °C) δ 140.56 (*ipso*-C_6H_5), 139.73 (*ipso*-C_6H_5), 137.32 (*ortho*-C_6H_5), 137.02 (*ortho*-C_6H_5), 136.93 (*para*-C_6H_5), 136.56 (*para*-C_6H_5), 128.16 (*meta*-C_6H_5), 127.90 (*meta*-C_6H_5), 21.2 (-CH(*C*$H_3)_2$), 18.2 (-*C*$H(CH_3)_2$) ppm. *Anal*. Calcd. For $C_{66}H_{82}Ge_6$: C, 60.44; H, 6.31. Found: C, 60.36; H, 6.36.

Synthesis of H(GePh$_2$)$_3$H (13)

Ph_2GeH_2 (1.00 g, 4.37 mmol) and 1.7 M Bu^{t}Li (3.1 mL, 5.27 mmol) was combined in 10 mL Et_3N at -40 °C. After stirring for 5 minutes, the reaction was brought to room temperature and stirred for 9.5 hours. Volatiles were removed in vacuo to yield a white solid. The crude product was placed under high vacuum to remove volatile impurities. Product **13** was isolated in 0.41 g (41 % yield) as a crude product.

Synthesis of Pr$^i_3$Ge(GePh$_2$)(GePh$_2$)(GePh$_2$)GePr$^i_3$ (14)

A Schlenk tube was charged with the crude product **13** (0.41 g, 0.60 mmol), Pr$^i_3$GeNMe$_2$ (0.33 g, 1.3 mmol) and 10 mL CH_3CN. The tube was sealed and stirred for 72 hours and 90 °C. A solid precipitate formed which was collected through filtration and washed with hexanes. Remaining solvent was removed *in vacuo* and the pentagermane

14 was isolated in 23% yield (0.15 g, 0.14 mmol). ^{1}H NMR (C_6D_6, 25 °C) δ 7.81 (d, J = 7.08 Hz, 12H, *meta*-C_6H_5), 7.44 (d, J = 7.9 Hz, 12H, *meta*-C_6H_5), 7.11-6.98 (m, 24H, *ortho*- and *para*-C_6H_5), 1.54 (septet, J = 7.4 Hz, 6H, -C*H*$(CH_3)_2$), 0.96 (d, J = 7.4 Hz, 36H, -CH(C*H*$_3)_2$) ppm. ^{13}C NMR (C_6D_6, 25 °C) δ 143.93 (*meta*-C_6H_5), 142.43 (*meta*-C_6H_5), 140.83 (*meta*-C_6H_5), 137.22 (*ortho*-C_6H_5), 136.89 (*ortho*-C_6H_5), 135.37 (*ortho*-C_6H_5), 128.54 (*para*-C_6H_5), 128.05 (*para*-C_6H_5), 127.22 (*para*-C_6H_5), 21.35 (-*C*H$(CH_3)_2$), 18.38 (-CH(*C*H$_3)_2$) ppm.

Attempted synthesis of $Pr^{i}_3Ge(GePh_2)(GePh_2)GePr^{i}_3$ (16)

A Schlenk tube was charged with $H(GePh_2)(GePh_2)H$ (0.39 g, 0.085 mmol), $Pr^{i}_3GeNMe_2$ (0.42 g, 1.7 mmol) and 10 mL CH_3CN. The tube was sealed and stirred at 90 °C for 72 hours. Volatiles were removed *in vacuo*. A yellow solid was collected (0.35 g). ^{1}H NMR (C_6D_6, 25 °C) δ 7.80 – 7.35 (-C_6H_5), 7.15 – 6.88 (-C_6H_5), 5.76 (s, *H*$Ph_2GeGePh_2H$), 5.38 (s, *H*$Ph_2GeGePh_2GePr^{i}_3$), 1.70-1.40 (m, -CH$(CH_3)_2$ of *H*$Ph_2GeGePh_2GePr^{i}_3$ and $Pr^{i}_3GePh_2GeGePh_2GePr^{i}_3$), 1.16 (d, J = 6.5 Hz, ((C*H*$_3$)CH)$_3GeCH_2CN$), 1.12 (d, J = 7.2 Hz, -CH(C*H*$_3)_2$ of $HPh_2GeGePh_2GePr^{i}_3$), 0.95 (d, J = 6.8 Hz, -CH(C*H*$_3)_2$ of $Pr^{i}_3GePh_2GeGePh_2GePr^{i}_3$) ppm.

Attempted synthesis of $Pr^{i}_3Ge(GePh_2)GePr^{i}_3$ (17)

A Schlenk tube was charged with Ph_2GeH_2 (0.51 g, mmol), $Pr^{i}_3GeNMe_2$ (1.09 g, mmol) and 30 mL CH_3CN. The tube was sealed and stirred for 72 hours at 90 °C. The

volatiles were removed *in vacuo* to yield 0.61 g of a clear oil. ^{1}H NMR (C_6D_6, 25 °C) δ 7.85 (d, *J* = 7.7 Hz), 7.67 (d, J = 7.4 Hz), 7.17 (m), 5.34 (s, *H*GePh$_2$GePr$^{i}_3$), 1.76 (sept, *J* = 7.4 Hz, ((CH$_3$)$_2$C*H*)$_3$GeCH$_2$CN), 1.53 (sept, *J* = 7.4 Hz, HPh$_2$GeGe(C*H*(CH$_3$)$_2$)$_3$), 1.20 (s, Pr$^{i}_3$GeC*H*CN), 1.16 (d, *J* = 7.6 Hz, ((C*H*$_3$)$_2$CH)$_3$GeCH$_2$CN), 0.97 (d, *J* = 8.3 Hz, ((CH$_3$)$_2$C*H*)$_3$GePh$_2$GeH) ppm.

Synthesis of Pr$^{i}_3$GePh$_2$GeH (18)

A Schlenk tube was charged with Ph$_2$GeH$_2$ (0.72 g, 3.1 mmol), Pr$^{i}_3$GeNMe$_2$ (0.77 g, 3.1 mmol) and 20 mL CH$_3$CN. The tube was sealed and stirred for 72 hours at 90 °C. The volatiles were removed *in vacuo* to yield **18** (1.18 g, 87% yield) as a clear oil. ^{1}H NMR (C_6D_6, 25 °C) δ 7.66 (dd, $J^{1,3}$ = 8.0 Hz, $J^{1,4}$ = 1.6 Hz, 2H, *meta*-C$_6$H$_5$), 7.16 – 7.07 (m, 3H, *ortho*- and *para*-C$_6$H$_5$), 5.34 (s, 1H, Ge-*H*), 1.50 (septet, *J* = 7.2 Hz, 3H, -C*H*(CH$_3$)$_2$), 1.13 (d, *J* = 7.2 Hz, 18H, -CH(C*H*$_3$)$_2$) ppm. ^{13}C NMR (C_6D_6, 25 °C) δ 138.54 (*ispo*-C$_6$H$_5$), 135.91 (*meta*-C$_6$H$_5$), 128.56 (*ortho*-C$_6$H$_5$), 128.52 (*para*-C$_6$H$_5$), 21.25 (-*C*H(CH$_3$)$_2$), 16.64 (-*C*H(CH$_3$)$_2$) ppm. IR ν(Ge-H) 1996 cm^{-1}.

REFERENCES

(1) Roller, S.; Dräger, M. *J. Organomet. Chem.* **1986**, *316*, 57.

(2) Samanamu, C. R.; Amadoruge, M. L.; Schrick, A. C.; Chen, C.; Golen, J. A.; Rheingold, A. L.; Materer, N. F.; Weinert, C. S. *Organometallics* **2012**, *31*, 4374.

(3) Castel, A.; Riviere, P.; Satge, J.; Ko, H. Y. *Organometallics* **1990**, *9*, 205.

(4) Ross, L.; Dräger, M. *J. Organomet. Chem.* **1980**, *194*, 23.

(5) Ross, L.; Dräger, M. *J. Organomet. Chem.* **1980**, *199*, 195.

(6) Rupar, P. A.; Jennings, M. C.; Baines, K. M. *Organomet.* **2008**, *27*, 5043.

(7) Sekiguchi, A.; Yatabe, T.; Naito, H.; Kabuto, C.; Sakurai, H. *Chem. Lett.* **1992**, 1697.

(8) Mochida, K.; Kawajiri, Y.; Goto, M. *Bull. Chem. Soc. Jpn.* **1993**, *66*, 2773.

(9) Amadoruge, M. L.; Short, E. K.; Moore, C.; Rheingold, A. L.; Weinert, C. S. *J. Organomet. Chem.* **2010**, *695*, 1813.

(10) Dräger, M.; Simon, D. *Z. Anorg. Allg. Chem.* **1981**, *472*, 120.

(11) Häberle, K.; Dräger, M. *J. Organomet. Chem.* **1986**, *312*, 155.

(12) Marchand, A.; Gerval, P.; Riviere, P.; Satge, J. *J. Organomet. Chem.* **1978**, *162*, 365.

(13) Amadoruge, M. L.; DiPasquale, A. G.; Rheingold, A. L.; Weinert, C. S. *J. Organomet. Chem.* **2008**, *693*, 1771.

CHAPTER IV

PHYSICAL PROPERTIES OF LINEAR OLIGOGERMANES

INTRODUCTION

Oligomeric and polymeric group 14 compounds exhibit interesting optical and electronic properties such as luminescence, thermochromism, polychroism, and conductivity. In oligomeric germanium species, these properties are observed when the germanium atoms are arranged in a *trans*-coplanar configuration, allowing for the σ-delocalization to occur as discussed in Chapter 1. While a number of polymeric group 14 catenates have been prepared and characterized, the exact composition of these species are unknown since they have a distribution of molecular weights.[1-7] It is postulated, however, that polymeric species contain multiple arrays of *trans*-coplanar atoms which are terminated by strong out-of-plane twists and so can be regarded as having regions of short-range order that are disrupted by regions of disorder.[1] Of the group 14 polymeric systems, those containing silicon or tin have been most extensively studied while only a few germanium-containing polymers have been reported.

The known polymeric germanium compounds include [(*p*-$(MeO)_3Si(C_6H_4)MeGe]_n$[8], $H(GeMe_2)_nMe$[9], $H(GeMeAr)_nMe$ (Ar = Ph, *p*-Tol, *p*-FC_6H_4, *p*-$F_3CC_6H_4$, *m*-$Me_2C_6H_3$, *p*-$(H_3CO)C_6H_4$)[3], $(R_2Ge)_n$ (R = Me, Bu^n, Ph)[10], and *m*-(*S*)-2-methylbutylphenyldimethylpolygermane[11]. Some of these systems exhibit fluorescence and/or conductivity. These properties allow for the possibility of germanium-based polymers being used as new optical or conductive materials, especially as the limitations of silicon-based materials begin to be realized.

Similar to the polymeric species, oligogermanes, which are discrete compounds with a defined composition and structure, serve as small-molecule models for the larger polygermane system.[12-16] Oligogermanes are postulated to exhibit physical properties similar to those of the polygermanes, provided a sufficient number of catenated germanium atoms are present in the Ge – Ge backbone. A few long-chain methyl substituted oligogermanes have been reported, including Ge_6Me_{14}[4] and $Ge_{10}Me_{22}$.[17] However, these systems were not fully characterized having only been investigated by GC/mass spectroscopy and UV/visible spectroscopy. Consequently the pentagermane Ge_5Ph_{12} represented the longest, fully characterized oligogermane reported.[18,19] Though initially synthesized by germyl anion reagents in poor yields, Ge_5Ph_{12} was synthesized in our laboratory in good yields via the hydrogermolysis reaction. The pentagermane did not exhibit any luminescent behavior or unusual optical properties, but rather was a colorless solid with a UV/visible absorbance maximum at 295 nm.[18,19]

The goal of this work, in synthesizing and fully characterizing longer discrete oligomeric germanium compounds, is rooted in finding compounds that mirror those of the polymeric germanium species in their physical properties. The investigation of the

physical properties of the oligomeric compounds synthesized in this work was thus a priority and the electronic and optical properties of these species are described in this chapter.

UV/VISIBLE SPECTROSCOPY

The absorbance of radiation within the UV/visible range in these oligomeric germanium systems is typically regarded as a result of the promotion of an electron from the HOMO (highest occupied molecular orbital) to the LUMO (lowest occupied molecular orbital), which is attributed to a σ to σ* electronic transition.[20] Several reports have already detailed the effects of substituents and changes in the length of the oligomeric germanium chain on the physical properties of these systems.[20] In the simple digermane $R_3GeGePh_3$ (R = H, Me, Bu^s, $C_{18}H_{37}$, Hex^n, Bu^n, and Bu^i), DFT calculations were conducted and it was observed that an increase in the inductive effects of the alkyl substituents bound to the germanium resulted in an overall destabilization of the energy of the HOMO. This is due to the increased electron density being placed into the germanium backbone. Similarly, the energy of the LUMO became destabilized, but the degree of destabilization was observed to occur to a much lesser extent. Thus, as the inductive effects increased and the HOMO was destabilized, a decrease in the HOMO to LUMO energy gap was observed and the energy of the σ to σ* electronic transition diminished. This decrease in energy resulted in a bathochromic shift in the UV absorbance maximum, which was evident in the experimental absorption data observed

for the digermanes.[20] As substituents became more inductively donating, the absorption maximum shifted to longer wavelengths.

The effect of lengthening the germanium chain also results in a bathochromic shift of the absorption maximum with a larger effect than that resulting from variation of the substituents. Upon increasing the length of the germanium-germanium backbone, the LUMO becomes stabilized via conjugation, as expected from the σ* character. Adversely, as the proportion of electron-rich R_2Ge^{II} centers to the terminal R_3Ge^{III} centers increases, the energy of the HOMO increases, or becomes destabilized. Due to the destabilization of the HOMO and the stabilization of the LUMO, the HOMO-LUMO gap decreases and the absorbance maximum red-shifts.[20]

The effect of increasing the chain length ultimately becomes limited. When correlating the absorbance maximum versus the weight average molecular weight, M_n, of polymeric germanium species such as $(R_2Ge)_n$ (R = Me, Bu, Hex, Et), a minimum energy was reached for the absorbance maximum.[21] This is likely due to attaining the maximum number of *trans*-coplanar germanium atoms in the ordered regions of the polygermane. Therefore, the addition of a single germanium atom has a greater impact on the absorbance maximum when added to a small chain of germanium atoms versus a larger chain of germanium atoms. It is the number of *trans*-coplanar germanium atoms that have a larger impact on the σ-delocalization and the HOMO-LUMO gap rather than simply the number of germanium atoms. It can be reasoned then that by choosing specific substituents and establishing a predetermined chain length, an oligogermane could be selectively tailored to contain a specific absorbance maximum.

The UV/visible spectrum of the wavelength plotted versus the extinction coefficient for the tri- and pentagermane species (**5** and **7**) synthesized through the protection/deprotection strategies is shown in **Figure 4.1**. The spectrum of **5** contains a maximum absorbance as a shoulder off the main peak (CH_2Cl_2), which corresponds to absorbances of the alkyl and aryl groups at 237 nm with an extinction coefficient of 4.90 x 10^4 $M^{-1}cm^{-1}$. The pentagermane (**7**) spectrum also contained a shoulder at 243 nm and has an extinction coefficient of 1.15 x 10^5 $M^{-1}cm^{-1}$. Upon lengthening the germanium backbone from three to five germanium atoms, the absorbance maximum therefore exhibits a slight bathochromic shift, indicating the HOMO and LUMO gap in the two compounds is only slightly diminished upon lengthening the chain of germanium atoms. The values of the absorbance maxima for **5** and **7** are similar to those reported by many digermanes, such as $PhMe_2GeGePh_3$ (244 nm), $Bu^tMe_2GeGePh_3$ (238 nm), and $Hex^n{}_3GeGePh_3$ (241 nm), indicating an overall lack of σ-delocalization in these two oligogermanes.[22]

The UV/visible spectrum of $Br(GePh_2)_4Br$ (**10)** is shown in **Figure 4.2**, and has an absorbance maximum at 278 nm (ε = 8270 $M^{-1}cm^{-1}$). While significantly red shifted compared to the oligogermane **7**, this value is slightly blue shifted relative to the reported value for Ge_4Ph_{10} at 282 nm.[23] The difference between the two values likely stems from the presence of additional phenyl groups at each of the terminal germanium atoms in Ge_4Ph_{10}, as the π*-systems of the phenyl rings can perturb the energies of the frontier orbitals, such that the HOMO-LUMO gap in Ge_4Ph_{10} is slightly diminished versus that of **10**.

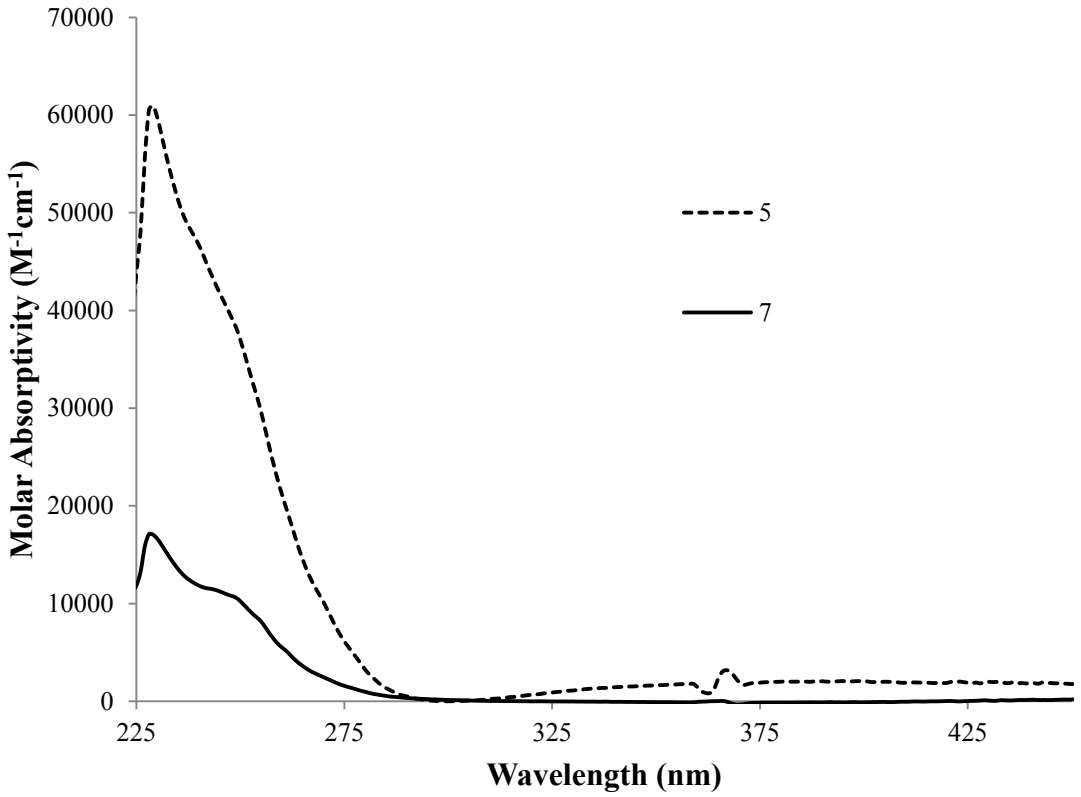

Figure 4.1. UV/Visible spectrum, wavelength versus molar absorptivity, of compounds $EtOCH_2CH_2(GeBu_2)(GePh_2)(GeBu_2)CH_2CH_2OEt$ (**5**) and $EtOCH_2CH_2(GeBu_2)_2(GePh_2)(GeBu_2)_2CH_2CH_2OEt$ **(7)**, recorded in CH_2Cl_2.

The UV/visible spectrum of $H(GePh_2)_4H$ (**11)**, is also shown in **Figure 4.2**, and contained a λ_{max} at 257 nm ($\varepsilon = 3150\ M^{-1}cm^{-1}$). This value is blue shifted compared to both **10** and Ge_4Ph_{10} as the 1s orbitals of the hydrogen atom do not sufficiently interact with the σ-system of the Ge_4 chain due to the significant difference in energy and size of the respective orbitals. The observed absorbance maximum of **11** was red shifted when compared to the trigermane $H(GePh_2)_3H$ (245 nm), as the σ-delocalization becomes enhanced by the presence of one additional germanium atom, thus decreasing the energy between the frontier orbitals.

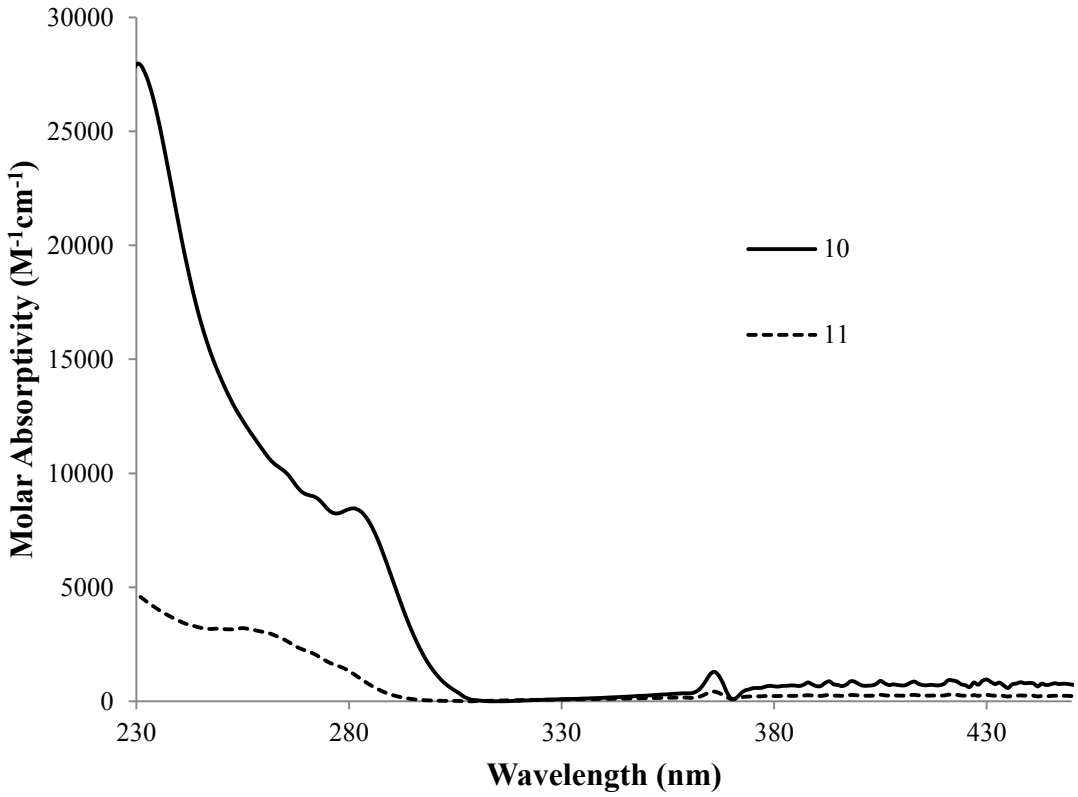

Figure 4.2. UV/Visible spectra, wavelength versus molar absorptivity, for the compounds $Br(GePh_2)_4Br$ **(10)** and $H(GePh_2)_4H$ **(11)**, recorded in CH_2Cl_2.

The absorbance of the two isopropyl terminated oligogermanes $Pr^i_3Ge(GePh_2)_4GePr^i_3$ (**12**) and $Pr^i_3Ge(GePh_2)_3GePr^i_3$ (**14**) are shown in **Figure 4.3**. The oligogermane **14** exhibited an absorbance maximum that can be observed at 300 nm (ε = 3880 $M^{-1}cm^{-1}$) in its UV/visible spectrum recorded in CH_2Cl_2, while the oligogermane **12**, had an absorbance at 310 nm (ε = 2290 $M^{-1}cm^{-1}$). The absorbance for both **14** and **12** are red shifted in comparison to the compound Ge_5Ph_{12} (λ_{max} = 295 nm).[19] The red shift observed for the absorbance maxima of **12** and **14** versus Ge_5Ph_{12} is expected since the isopropyl groups present on the terminal germanium atoms on both **12** and **14** are more inductively donating in comparison to phenyl groups. Thus, the HOMO is destabilized in

these oligogermane and the absorption is shifted to longer wavelengths. The absorbance of **12** is red-shifted from that of **14** due to the added R_2Ge^{II} center, which is responsible for destabilizing the HOMO and stabilizing the LUMO in the oligogermane. The maximum absorbance for both **12** and **14** are similar to those observed for several alkyl-substituted polymeric species $(GeR_2)_n$ (R = Et, 305 nm; R = Pr^n, 300 nm; R = Bu^n, 316 nm) that were recorded in pentane.[21] Thus the degree of σ-delocalization appears to be similar to that observed in polymeric germanium systems.

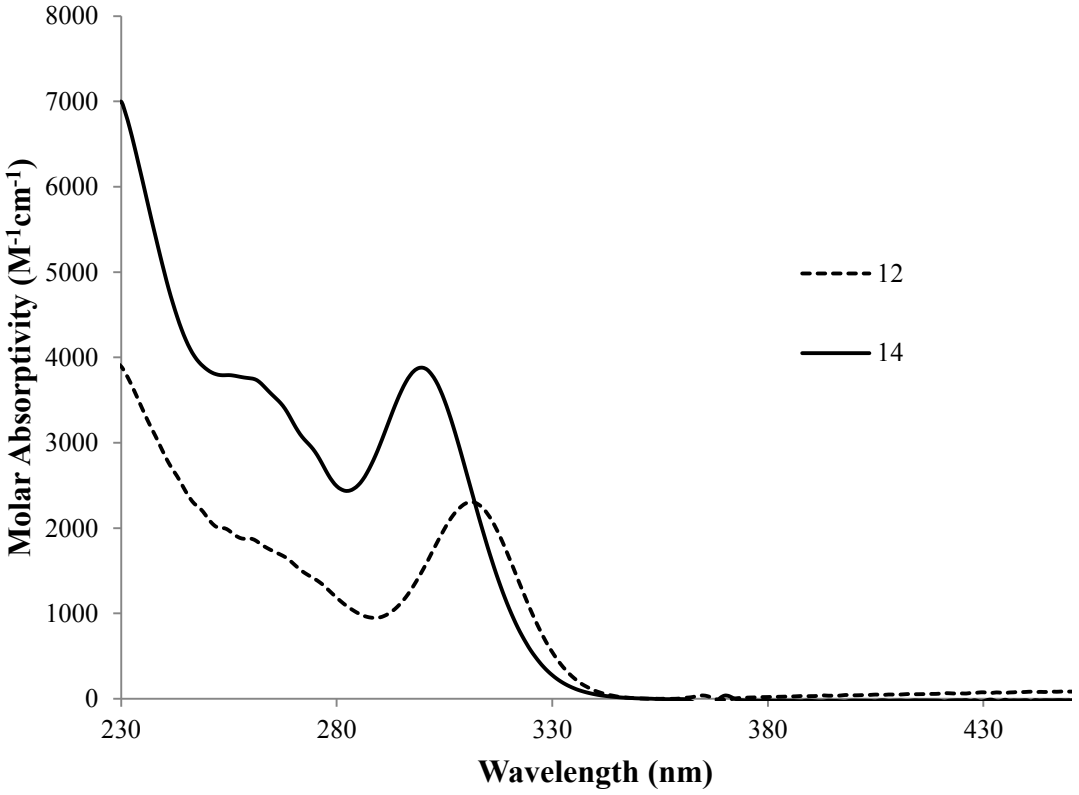

Figure 4.3. UV/Visible spectra, wavelength versus molar absorptivity, of $Pr^i_3Ge(GePh_2)_4GePr^i_3$ (**12)** and $Pr^i_3Ge(GePh_2)_3GePr^i_3$ (**14)** when recorded in CH_2Cl_2.

As the achievable length of oligomeric germanium compounds increases, it is of interest to determine if these species exhibit physical properties that are typical of polymeric germanium species. Several polymeric germanium and silicon species have been reported to be thermochromic.[1,2,21] Of the reported cases, three distinct types of thermochromism are observed in a range of systems when in solution. The first type of thermochromism is typically observed with highly unsymmetrical atactic material. An example of this type of thermochromism was found for poly(*n*-hexylmethylsilane), where the absorbance maximum steadily red shift as the temperature of the sample decreased from room temperature (λ_{max} = 306 nm) to a limiting value of approximately 330 nm.[1] This observed thermochromism was correlated to conformational changes, as the temperature was decreased, the proportion of *trans*-conformations increases and gauche conformation decreases, allowing for an increase of the σ-delocalization (shown in **Figure 4.4**). The two germanium containing polymers, $(Et_2Ge)_n$ and $(PhHexGe)_n$ did not show strong thermochromic behavior as the absorption maxima only steadily red shift from 300 nm and 330 nm to limiting values of 305 nm and 335 nm, respectively.[21] In these cases, the λ_{max} of the compound gradually moves to longer wavelengths, until a maximum wavelength is reached.

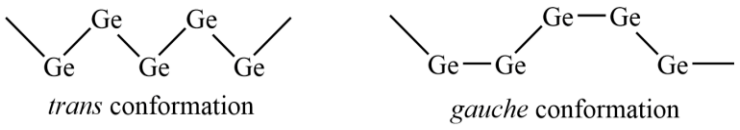

Figure 4.4. Representation of the *trans* and *gauche* conformations.[21]

In a second type of thermochromism, which typically involves unsymmetrical materials with sterically demanding substituents, compound solutions undergo a slightly

hypsochromic rather than bathochromic shift with decreasing temperatures. This type of thermochromism is rationalized as follows. The conformation of the atoms within the structure will be such that the lowest energy arrangement possible is maximized. In compounds such as poly(cyclohexylmethyl-silane), poly(methylphenylsilane), and poly(isopropylmethylsilane), it is proposed that a decrease in temperature results in a decrease in the average length of the chromophore due to disruption of the *trans* sequences along the polymer backbone often resulting in a corkscrew-like conformation.[21]

The third type of observed thermochromism involves a small bathochromic shifts as temperature decreases until a polymer-dependent temperature is reached. At that point, a new sharp peak forms significantly red-shifted from the initial peak, and the initial peak decreases in intensity. This event is observed in many symmetrically substituted polymers including dialkyl polysilanes.[1]

The variable temperature UV/visible spectra of **12** were recorded at temperatures from 95 °C to 5 °C in toluene at a concentration of 2×10^{-4} M. The temperature range was chosen to prevent water condensation within the spectrometer. Toluene was chosen as the solvent, as opposed to CH_2Cl_2, as it remains a liquid within the temperature range of the experiment. Spectra shown in **Figure 4.5** were recorded after the sample was maintained at the required temperature for 15 minutes, and the spectra were taken in 10 °C intervals. The absorbance spectrum, when observed at 5 °C, contains a λ_{max} at 309 nm. Gradually, as the temperature is increased, the absorbance maximum increased non-uniformly to a maximum value of 314 nm at 95 °C, and therefore only a slight hypsochromic shift is observed with decreasing temperature.

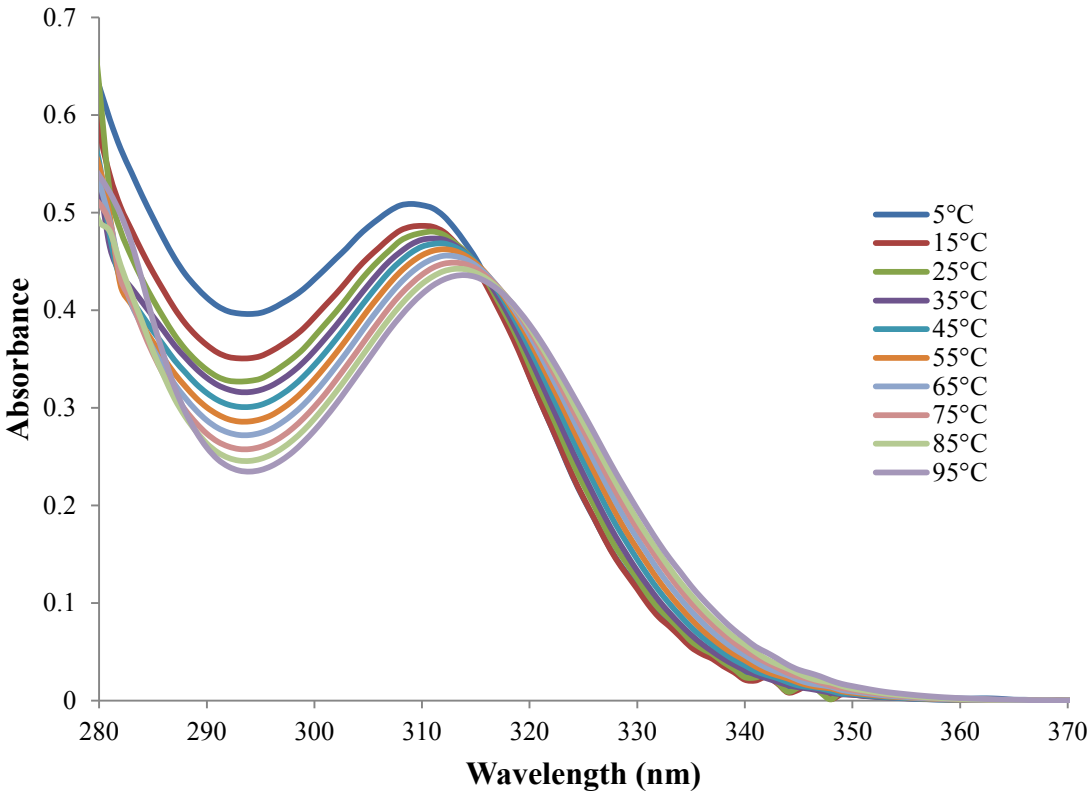

Figure 4.5. Absorbance spectra of **12** when recorded at variable temperature between 5 and 95 °C in toluene.

The trend observed for **12** more closely resembles the second type of thermochromism, which is described above. For **12**, it is proposed that at lower temperatures the sterically demanding isopropyl groups cause the terminal germanium atoms to spend a greater amount of time in a configuration similar to that of the crystal structure, where the central four germanium atoms are within a single plane with the terminal atoms canted above and below the plane. While some molecules contain enough energy to reach a completely planar conformation along the germanium backbone, this does not represent the majority of the molecules. Upon increasing the temperature the number of molecules with enough energy to force the structurally encumbering isopropyl

groups toward co-planarity with the four internal germanium atoms and extend the delocalization increases. The increased delocalization decreases the energy of the HOMO and therefore shifts the absorbance maximum to longer wavelength at higher temperatures.

ELECTROCHEMISTRY

In addition to their optical properties which can be probed in a facile manner through UV/visible spectroscopy, oligomeric germanium compounds also possess interesting electronic properties. Several studies have reported on the electrochemical properties of oligomeric germanium compounds.[4,18,20,22,24-27] Of the many reports, several trends in their electrochemical behavior become apparent. By increasing the degree of catenation, oligomeric germanium compounds become easier to oxidize. It has also been established that the introduction of more highly electron donating groups at the germanium atoms decreases the oxidation potential of the oligogermanes. Linear oligogermanes containing aryl substituents on at least one formally divalent germanium atom also exhibit n-1 successive irreversible ox waves, where n equals the number of germanium atoms.[19,24,25]

The oligogermanes **5** and **7** were studied using cyclic voltammetry in CH_2Cl_2 with 0.1 M $[Bu_4N][PF_6]$ as the supporting electrolyte, and the voltammogram for the positive potentials of the two are shown if **Figure 4.6**. As with previously reported data, both compounds contained no reversible oxidation waves and exhibited n – 1 waves, where n equals the number of catenated germanium atoms. The voltammogram for **5** contained two oxidation waves at 1286 (± 14) and 1559 (± 4) mV, where **7** exhibited four

oxidations waves at 1106 (± 7), 1304 (± 21), 1567 (± 20), and 1976 (± 21) mV. As expected, the first oxidation wave for compound **7** was less positive than that of compound **5**, indicating that the first electron removed from the HOMO of **5**, presumably from the σ-bonding HOMO, is more easily removed than that for compound **7**. The trigermane Ge_3Ph_8 exhibited two oxidation waves, the first of which was at 1696 mV.[24] This value is more positive than that of **5,** and therefore the HOMO in Ge_3Ph_8 is more stabilized in comparison to that of **5**, as expected. In comparison to **7**, the compound Ge_5Ph_{12} exhibited a first oxidation wave at 1385 mV in its cyclic voltammogram.[19] Between compounds having the same number of catenated germanium atoms, a trend exists where the perphenylated species exhibits a first oxidation wave that is more positive than **5** and **7**, indicating the perphenylated species is more difficult to oxidize. This trend is expected as alkyl groups present on **5** and **7** are more electron-donating than phenyl groups, and the added electron density destabilizes the HOMO, therefore requiring less energy for an electron to be removed.

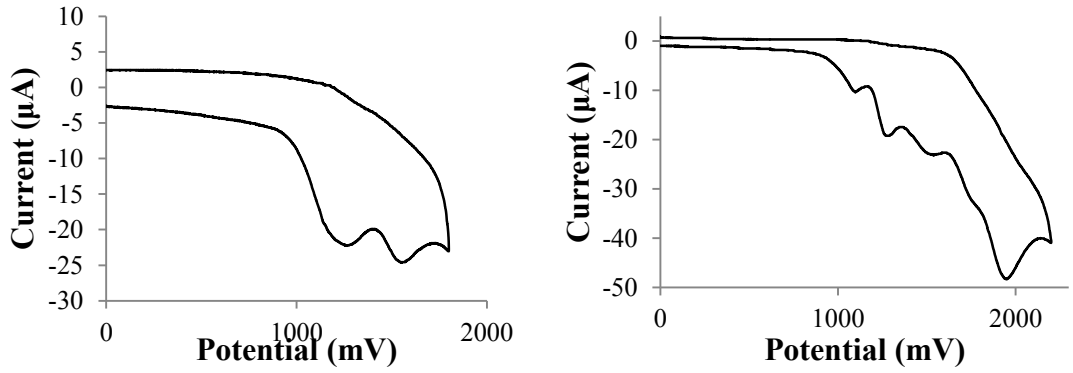

Figure 4.6. Cyclic voltammograms of the compounds **5** and **7**, recorded in CH_2Cl_2.

Differential pulse voltammetry (DPV) was the electrochemical technique of choice for many of the oligogermanes studied in this work. Unlike CV, DPV utilizes a

preset voltage which is consistently applied with a series of pulses containing steadily increasing amplitudes that are superimposed. The resultant current is then measured at the end of the pulses. In polarography, the total current is a combination of both the Faradaic current, which is the current generated through the oxidation or reduction of a chemical and charging current. The charging current is the current induced by the charging of the interface of the electrode. By applying small pulses of voltage, then measuring the current at the end of the pulse, the charging current has time to decay to zero, leaving only the Faradaic current to be measured. DPV allows the sensitivity to be 100 to 1000-fold greater than that of CV, and the peaks are better resolved. The electrochemical investigations reported herein were recorded using DPV due to the increased sensitivity and resolution.

The DPVs for compounds **10**, **11**, **12** and **14** are shown in **Figure 4.7**. The DPV for the bromine terminated tetragermane, **10**, exhibits three successive oxidation waves at 1660 (± 0), 1857 (± 5), and 2060 (± 0) mV. Two other oxidation waves are observed in the voltammogram. It has been determined the wave located at ca. 680 mV is most likely due to residual Br_2, while the peak present at ca. 960 mV is due to small impurities. The first, or least positive, oxidation wave was observed to be close to the first oxidation wave for Ge_4Ph_{10} (1644 mV), indicating the energy of HOMO for **10**, is slightly more stable than that of Ge_4Ph_{10}.

The DPV of **11** was of interest. The electrochemical data for only one species containing a germanium bound hydrogen has previously been reported.[19] Compound **11** did not follow the trend observed for other oligogermanes containing aryl groups, but rather exhibited four successive oxidation waves observed at 1433 (± 9), 1697 (± 5), 1882

(± 2), and 2093 (± 9) mV. The first oxidation wave was observed at a less positive potential than **10**, which is expected as **10** contains two electronegative bromine substituents at the terminal germanium atoms of the Ge_4 chain.

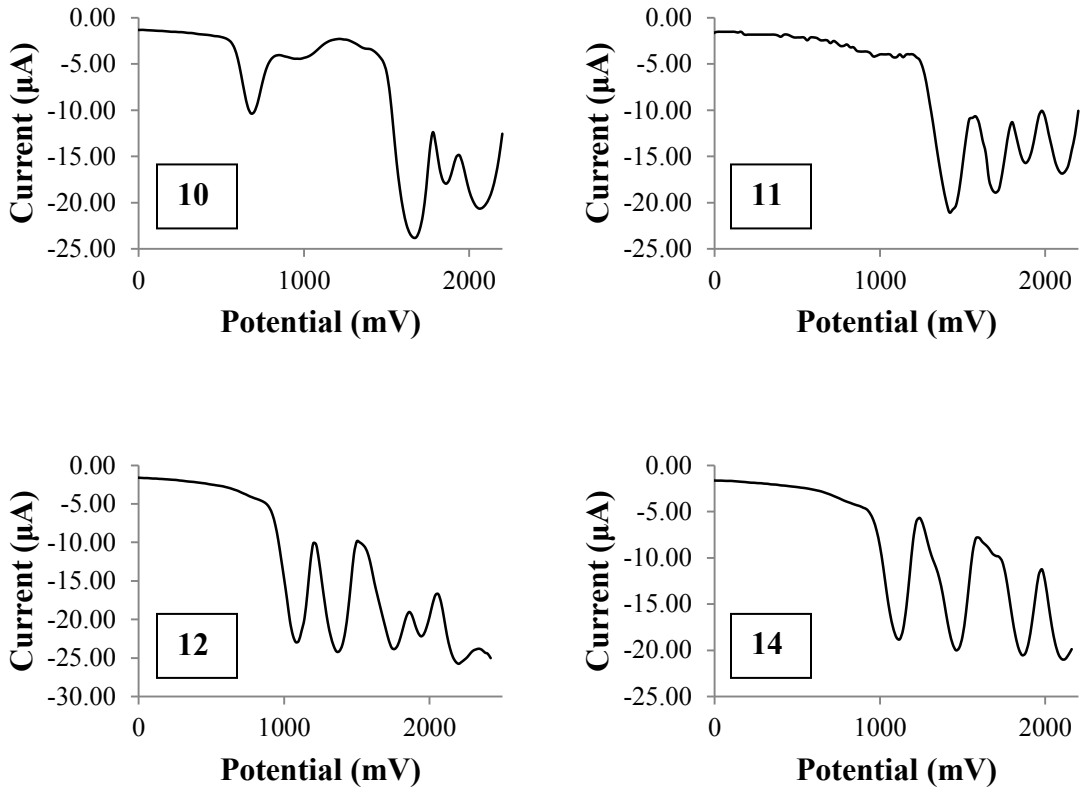

Figure 4.7. DPV voltammograms of **10**, **11**, **12**, and **14** recorded in CH_2Cl_2.

The electrochemistry of oligogermane **12** was also of much interest. Five successive, irreversible oxidation waves were observed at 1100 (±16), 1387 (± 12), 1767 (± 5), 1943 (± 5) and 2200 (± 0) mV. The first oxidation wave was at a less positive potential observed for any other linear oligogermanes. This indicates that the HOMO, which is the source of the first electron removed, is destabilized relative to those in oligogermanes having less than six catenated germanium atoms.

The compound **14** followed the expected electrochemical trends of previously reported oligogermanes. The pentagermane exhibited four irreversible oxidation waves at 1127 (± 9), 1480 (± 16), 1870 (± 8) and 2117 (± 5) mV. While still following known trends, the first oxidation wave was only slightly more positive than the first oxidation wave of **12**, indicating that the HOMO of **14** was only slightly stabilized with respect to compound **12**. Some concerns were expressed as to the validity of **14** being a pentagermane, rather than a hexagermane, as the first oxidation wave of the two compounds were within 27 mV of each other. Evaluation of the subsequent oxidation waves indicated that the two were in fact not identical compounds. The second, third, and fourth oxidation waves were different by ca. 93, 103, and 174 mV, respectively for those of **12**. Extending the sweep range to more positive potentials resulted in an oxidation wave slightly above 2500 mV, at which point the solvent begins to oxidize.

The nature of the oxidation events occurring in the CV and DPV of oligogermanes are still unknown. For oligogermanes, the oxidation is irreversible, indicating a chemical reaction is occurring after each oxidation. Attempts have been made to ascertain the reason n – 1 oxidation waves are observed for these systems. In **Scheme 4.1**, the proposed decomposition pathways for compound **12** after the first oxidation event occurs are shown. These possible decomposition pathways include homolytic cleavage of a germanium-germanium single bond to generate two germanium-based radicals, germylene extrusion with concomitant chain contraction by one germanium atom, and homolytic germanium-germanium bond cleavage with simultaneous germylene extrusion followed by recombination of the two radical species to generate a new oligogermane. Any products from the decomposition reactions are then

oxidized as the sweep continues, and all three possible decomposition pathways would then lead to a total of five oxidation events.

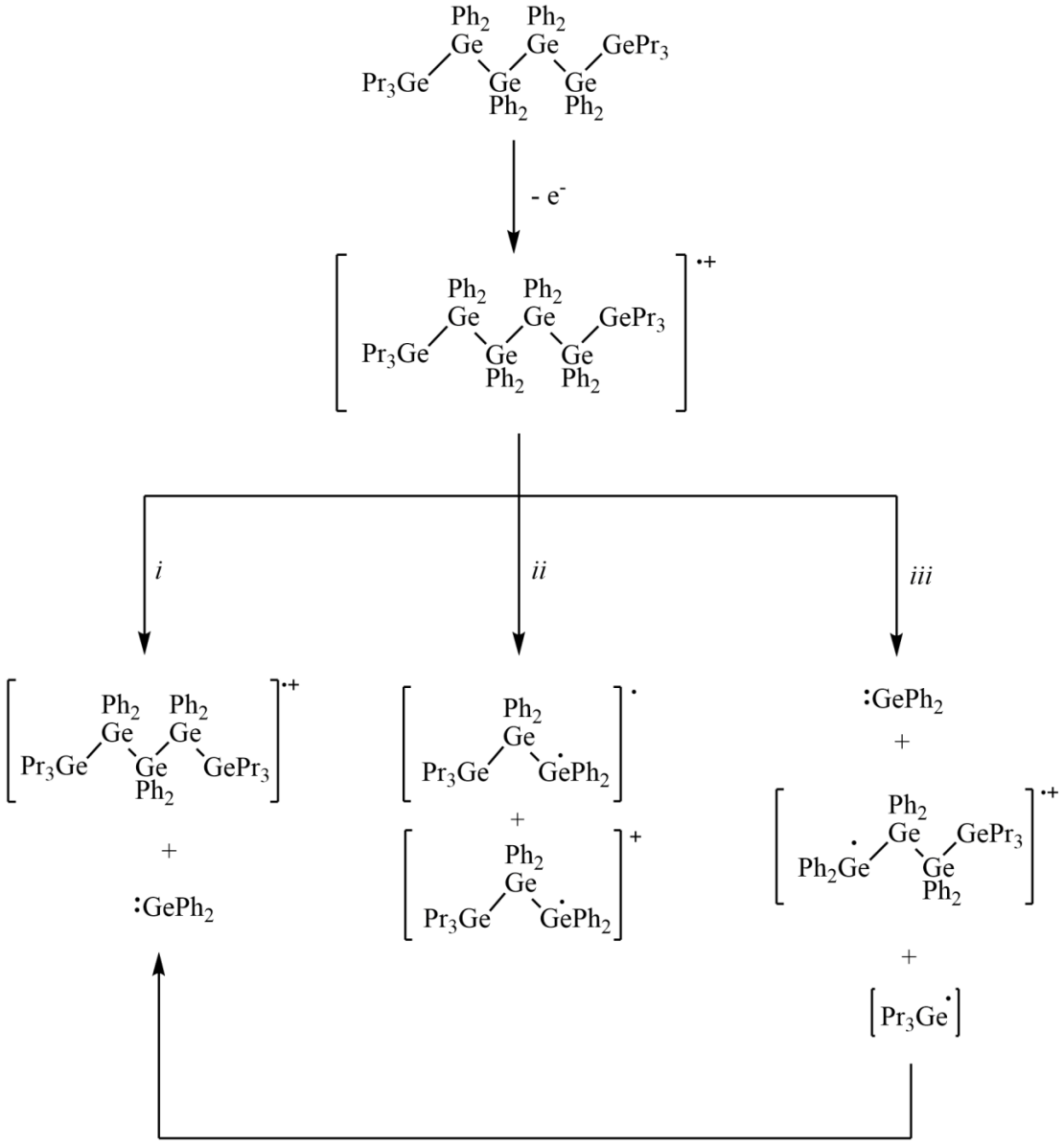

Scheme 4.1. Possible decomposition pathways for chemical reactions occurring after an oxidation event. *i*) germylene extrusion with concomitant chain contraction by one germanium atom, *ii*) homolytic cleavage of a germanium-germanium single bond to generate two germanium-based radicals, iii) homolytic germanium-germanium bond cleavage with simultaneous germylene extrusion followed by recombination of the two radical species to generate a new oligogermane.

Of the three proposed decomposition pathways, two include the extrusion of germylene. Thus bulk electrolysis experiments were conducted on **12** in the presence of the germylene trapping reagents 2,3-dimethyl-1,3-butadiene (DMB), benzil, acetic acid, and 1,2-diphenylacetylene. As found in a similar experiment using the digermane $Bu^n_3GeGePh_3$[19], no trapping products were identifiable. Therefore, no conclusive evidence has been obtained for the formation of germylene products and further investigations will be necessary to confirm the formation of these species.

LUMINESCENCE AND DICHROIC BEHAVIOR

In addition to the properties in the UV/visible spectrum and electrochemistry of **12**, the hexagermane contains new properties which have not previously been observed in other oligomeric germanium compounds, the first of which is luminescence. While several polymeric germanium species have been reported to exhibit luminescent behavior, it has yet to be observed for discrete germanium molecules.[3-5,8] In **Figure 4.8**, the absorption spectrum has been overlaid with the fluorescence emission spectrum, and both spectra were recorded in CH_2Cl_2. When excited at 312 nm, a broad emission is observed at 370 nm for **12**, and this emission is nearly identical to that of the polygermane $((Me_3SiOC_6H_4MeGe)_n$, that was observed at 369 nm when excited at 332 nm.[8] The observed fluorescence of hexagermane, **12**, is an indication that oligogermanes might in fact function as useful small-molecule models for the larger polymeric germanium systems.

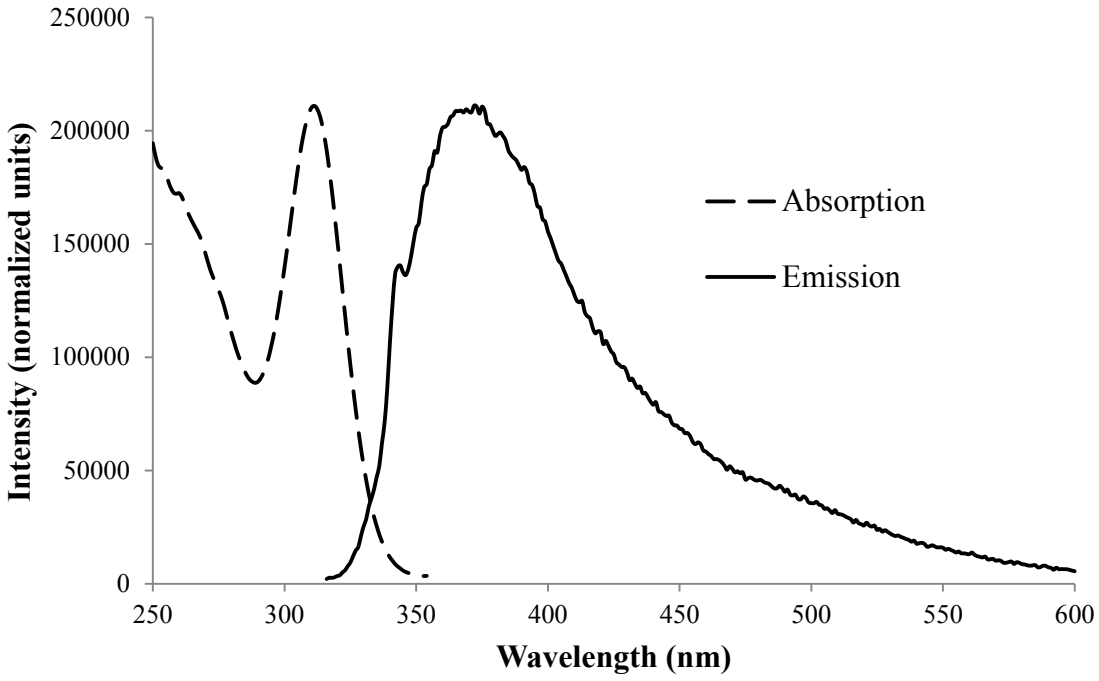

Figure 4.8. Overlaid absorbance and fluorescence emission spectrum of **12** when excited at 312 nm.

The hexagermane **12** not only exhibited fluorescence properties, but crystals of the compound also exhibited interesting optical properties. While under ambient light crystals of **12** appeared colorless, viewing the crystals through plane-polarized light revealed a colorful display. As shown in **Figure 4.9**, when crystals were observed under "left" polarized light, they appeared pale yellow in color, but under "right" polarized light, crystals of **12** appeared deep blue in color.

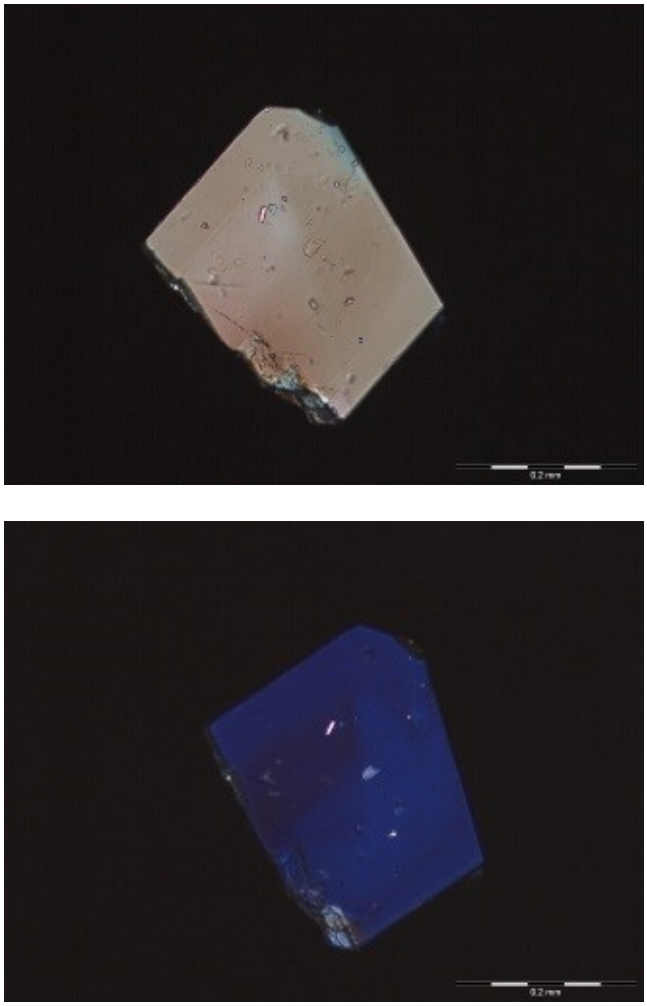

Figure 4.9. Crystals of **12** when observed under "left" (top) and "right" (bottom) polarization.

The dichroic phenomenon is due to the packing of **12** in the crystal. As shown in **Figure 3.8** and expanded on in Chapter 3, the hexagermane contains four *trans*-coplanar germanium atoms stacked in a columnar fashion as well as two terminal germanium atoms which are canted above and below the plane, also disposed in a column-like fashion. A packing diagram of **12** is shown in **Figure 4.10**. Arrangement of the Ge_6 chain imparts a long-range chirality in the solid state which leads to the observed dichroic

behavior of polarized light, causing light present in different polarized planes traveling through the compound experience a varying level of absorption.

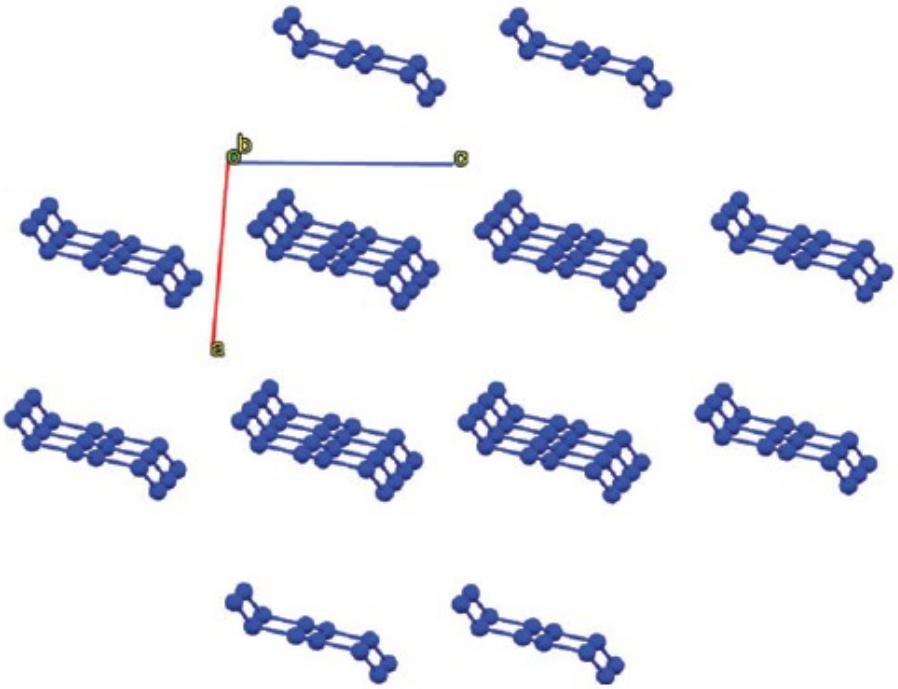

Figure 4.10. Packing diagram of **12** along **b** axis.

EXPERIMENTAL

General Considerations

Variable temperature UV/visible spectra were obtained on a Carey 5000 spectrometer in toluene; all other UV/visible spectra were recorded using a Hewlett-Packard 8453 diode array spectrometer in CH_2Cl_2. Electrochemical data (CV, DPV, BE) were obtained using a DigiIvy DY2312 potentiostat using a glassy carbon working electrode, a platinum wire counter electrode, and an Ag/AgCl reference electrode in

CH_2Cl_2 solution using 0.1 M $[Bu_4N][PF_6]$ as the supporting electrolyte. Bulk electrolysis was conducted in a two compartment cell using a reticulated vitreous carbon electrode (BASi). Crystal pictures were observed using an Olympus BX51 microscope and a U-AN360P polarizer using Olympus MicroSuite and ColorView Soft Imaging System Camera. The crystal was placed in Series A Cargille Certified Refractive Index Liquid for observations. Fluorescence spectra were obtained using a Fluorolog 3 and recorded in CH_2Cl_2.

REFERENCES

(1) Miller, R. *Chem. Rev.* **1989**, *89*, 1359.

(2) Miller, R. D.; Hofer, D.; Rabolt, J. F. *J. Am. Chem. Soc.* **1985**, *107*, 2172.

(3) Katz, S. M.; Reichl, J. A.; Berry, D. H. *J. Am. Chem. Soc.* **1998**, *120*, 9844.

(4) Okano, M.; Mochida, K. *Chem. Lett.* **1990**, 701.

(5) Mochida, K.; Hata, R. *Polyhedron* **1996**, *15*, 3027.

(6) Rabolt, J. F.; Hofer, D.; Miller, R. D. *Macromolecules* **1986**, *119*, 611.

(7) Hallmark, V. M.; Zimba, C. G.; Sooriyakumaran, R.; Miller, R. D.; Rabolt, J. F. *Macromolecules* **1990**, *23*, 2346.

(8) Huo, Y.; Berry, D. H. *Chem. Mater.* **2005**, *17*, 157.

(9) Reichl, J. A.; Popoff, C. M.; Gallagher, L. A.; Remsen, E. E.; Berry, D. H. *J. Am. Chem. Soc.* **1996**, *118*, 9430.

(10) Kobayashi, S.; Cao, S. *Chem. Lett.* **1993**, 1385

(11) Motonaga, M.; Nakashima, H.; Katz, S.; Berry, D. H.; Imase, T.; Kawauchi, S.; Watanabe, J.; Fujiki, M.; Koe, J. R. *J. Organomet. Chem.* **2003**, *685*, 44.

(12) Amadoruge, M. L.; Weinert, C. S. *Chem. Rev.* **2008**, *108*, 4253.

(13) Weinert, C. S. In *Comprehensive Organometallic Chemistry III*; Crabtree, R. H., Mingos, D. M. P., Eds.; Elsevier: London, 2006; Vol. 3, p 699.

(14) Weinert, C. S. *Dalton Transactions* **2009**, 1691.

(15) Weinert, C. S. *Comments on Inorganic Chemistry* **2011**, *32*, 55.

(16) Dräger, M. *Silicon Germanium Tin Lead Cmpds* **1983**, *7*, 299.

(17) Mochida, K.; Hodota, C.; Hata, R.; Fukuzumi, S. *Chem. Lett.* **1998**, 263.

(18) Roller, S.; Dräger, M. *J. Organomet. Chem.* **1986**, *316*, 57.

(19) Samanamu, C. R.; Amadoruge, M. L.; Schrick, A. C.; Chen, C.; Golen, J. A.; Rheingold, A. L.; Materer, N. F.; Weinert, C. S. *Organometallics* **2012**, *31*, 4374.

(20) Amadoruge, M. L.; Gardinier, J. R.; Weinert, C. S. *Organometallics* **2008**, *27*, 3753.

(21) Mochida, K.; Chiba, H. *J. Organomet. Chem.* **1994**, *473*, 45.

(22) Schrick, E. K.; Forget, T. J.; Roewe, K. D.; Schrick, A. C.; Moore, C. E.; Golen, J. A.; Rheingold, A. L.; Materer, N. F.; Weinert, C. S. *Organometallics* **2013**, *32*, 2245.

(23) Roller, S.; Simon, D.; Dräger, M. *J. Organomet. Chem.* **1986**, *301*, 27.

(24) Amadoruge, M. L.; Short, E. K.; Moore, C.; Rheingold, A. L.; Weinert, C. S. *J. Organomet. Chem.* **2010**, *695*, 1813.

(25) Samanamu, C. R.; Amadoruge, M. L.; Yoder, C. H.; Golen, J. A.; Moore, C. E.; Rheingold, A. L.; Materer, N. F.; Weinert, C. S. *Organometallics* **2011**, *30*, 1046.

(26) Samanamu, C. R.; Materer, N. F.; Weinert, C. S. *J. Organomet. Chem.* **2012**, *698*, 62.

(27) Mochida, K.; Hodota, C.; Hata, R. *Organometallics* **1993**, *12*, 586.

CHAPTER V

CONCLUSION

In 1886 Winkler discovered the element germanium located within the mineral argyrodite in Germany. Though it was only a year later when the first organometallic germanium compound Et_4Ge was reported, it wasn't until 1925 when the first compound containing a single germanium-germanium bond was synthesized. Since 1925, the synthesis of longer chains of germanium atoms has been difficult as organometallic oligomeric germanium compounds are often difficult to purify due to their high reactivity with air and moisture, and unsatisfactory methods for the formation of germanium-germanium bonds were available.

Over the years, reactions that were successful in forming germanium-germanium bonds often required harsh reaction conditions, produced low yields, or resulted in product mixtures. Although several polymeric germanium species have been successfully synthesized, these systems cannot be completely characterized with respect to their configuration. It has been postulated that multiple arrays of germanium atoms located in a *trans* co-planar fashion exist in these systems that are separated by sections of disorder by at least one germanium atom being

significantly shifted out-of-plane. Arrays of *trans*-coplanar germanium atoms account for the σ-delocalization which are characteristic of heavier Group 14 elements containing metal-metal bonds.

Since 1925, little development has been successful for the preparation of discrete oligomeric germanium compounds. The longest, completely characterized, linear oligogermane reported prior to the research reported in this work was the perphenylated pentagermane Ge_5Ph_{12} by Dräger. This compound synthesized in 1986, was only obtained in 0.2 % yield, and was a component of a mixture of other oligomeric germanium compounds containing less than five atoms. In the 27 years since the reported synthesis of the perphenylated pentagermane, no reports of fully characterized oligogermanes having longer chains have appeared. Though a few publications describe the synthesis of longer chains of germanium atoms, none have been accompanied by crystal structure data, and the compounds that have been reported are poorly characterized.

With a need for better methods of forming a single germanium-germanium bond, the hydrogermolysis reaction was introduced in 2006, where reaction of a germanium compound containing an amide group and a compound with a germanium-bound hydrogen could react in acetonitrile for two days to selectively form a single germanium-germanium bond in good to excellent yields. This advancement created a stepping stone for which longer oligomeric germanium compounds could be synthesized as discrete molecules.

In 2010, the perphenylated oligogermane Ge_5Ph_{12} was successfully synthesized as the only product using the hydrogermolysis in 83 % yield from two equivalents of Ph_3GeNMe_2 and $HPh_2GeGePh_2GePh_2H$. The hydrogermolysis allowed for a significantly increased yield of the reaction and also prevented formation of any unwanted side products. With hydrogermolysis as a tool, it was the goal to synthesize a new longer oligomeric germanium compounds having six or more consecutive germanium atoms.

The initial attempts at meeting this goal involved the sequential addition of two germanium atoms to the chain by use of a hydrogen protection/deprotection strategy. An ethoxyethyl protecting group, present on the germanium atoms to be added to the chain, allowed for further chain growth since it could be removed with diisobutylaluminum hydride, to generate a Ge – H bond in place of the $–CH_2CH_2OEt$ protecting group. While this method allowed for the synthesis of both a tri- and pentagermane with the formula $EtOCH_2CH_2(GeBu_2)_nGePh_2(GeBu_2)_nCH_2CH_2OEt$ (n = 1, 2), further chain growth appeared to be unsuccessful. The difference in the physical properties of the tri- and pentagermane were minimal as the UV/visible λ_{max} was red-shifted by only 6 nm upon lengthening of the chain of germanium atoms. Both compounds did exhibit the n – 1 oxidation waves in their cyclic voltammograms that are typically observed with oligomeric germanium compounds.

Since the protection/deprotection strategies failed to provide oligogermanes containing more than five consecutive germanium atoms, new synthetic methods were needed to synthesize these compounds. Many strategies were used to combine linear segments of germanium atoms in order to synthesize a linear hexagermane, but all failed

or inadequately provided data to confirm synthesis of a linear hexagermane. As a result, a new strategy was used in which a cyclic oligogermane was employed to quickly and efficiently prepare a long-chain oligogermane.

Using a procedure reported by Dräger, a perphenylated cyclic tetragermane $(GePh_2)_4$ was synthesized using Wurtz-type coupling. The cyclic product was ring-opened by titration with Br_2 to give a linear tetragermane $Br(GePh_2)_4Br$ with a bromine atom on each of the terminal germanium atoms. Subsequent conversion of the bromine terminated tetragermane $Br(GePh_2)_4Br$ to the hydrogen terminated tetragermane $H(GePh_2)_4H$ was achieved using the reagent $LiAlH_4$. The last step in synthesizing the hexagermane was use of the hydrogermolysis reaction with two equivalents of $Pr^i_3GeNMe_2$ and one equivalent of $H(GePh_2)_4H$. The hydrogermolysis reaction yielded the hexagermane $Pr^i_3Ge(GePh_2)_4Pr^i_3$ as a white solid.

The hexagermane $Pr^i_3Ge(GePh_2)_4Pr^i_3$ exhibits five oxidation waves in its DPV with the first oxidation wave occurring at 1080 mV. Optical properties for the hexagermane are also of interest as the λ_{max} was observed at 310 nm, a value similar to that observed for many polymeric germanium species. For the first time, luminescence was achieved with a discrete oligomeric germanium compound as $Pr^i_3Ge(GePh_2)_4Pr^i_3$ exhibited an emission peak at 370 nm when excited at 312 nm in dichloromethane. Crystals of the hexagermane also exhibited interesting dichroic properties as they changed colors from pale yellow to deep blue when viewed under different orientations of plane polarized light, despite the crystals being colorless when viewed with ambient light.

The synthesis of the smaller oligomers of the series $Pr^{i}_{3}Ge(GePh_2)_nPr^{i}_{3}$, where n = 1, 2, or 3, were attempted. While the pentagermane was successfully synthesized from $H(GePh_2)_3H$, the synthesis of the tri- and tetragermane were unsuccessful. The proposed reason for the lack of success in the synthesis of these compounds is the inherent excess electron density present on the germanium-bound hydrogen as isopropyl groups present on germanium atoms β or γ to the germanium-bound hydrogen. The effect of the isopropyl groups decrease as the alkyl group moves further away from the reactive germanium-bound hydrogen site. This reactivity is evident as the tetragermane was formed but the reaction used for its synthesis failed to go to completion, while no evidence for the preparation of the trigermane was observed even after an extended reaction time of ten days.

With the successful synthesis of the hexagermane $Pr^{i}_{3}Ge(GePh_2)_4Pr^{i}_{3}$, oligomeric germanium compounds are finally beginning to exhibit properties that mirror those typically observed in polymeric species. Not only can these discrete molecules become models for polymeric species, they might serve as new species which may themselves be useful as optical and electronic materials. Further research will be conducted to build upon the known strategies presented here, to reach new chain lengths and to synthesize new compounds, where the optical and electronic properties of these systems can be specifically tailored.

APPENDICES

Table A.1. X-ray crystallographic data for $(GePh_2)_4$, **8**.

Empirical formula	$C_{48}H_{40}Ge_4$
Formula weight (g/mol)	907.16
Temperature (K)	100(2)
Wavelength (Å)	0.71073
Crystal system	Monoclinic
Space group	P2(1)/c
a (Å)	21.0256(7)
b (Å)	10.2387(3)
c (Å)	20.4770(7)
α (°)	90
β (°)	115.583(2)
γ (°)	90
Volume ($Å^3$)	3976.0(2)
Z	4
Calculated density (g/cm^3)	1.515
Absorption coefficient (mm^{-1})	3.028
F(000)	1824

Crystal size (mm)	0.20 x 0.10 x 0.10
Crystal size and shape	colorless / block
θ range for data collection (o)	1.07 to 26.52°
Index ranges	-26<=h<=25
	-12<=k<=11
	-25<=l<=25
Reflections collected	28504
Independent reflections	8180 (R_{int} = 0.0352)
Completeness to θ	25.00° (99.7 %)
Absorption correction	Multi-scan/SADABS
Maximum and minimum transmission	0.7516 and 0.5827
Refinement method	Full-matrix least-squares on F^2
Data/restraints/parameters	8180 / 0 / 469
Goodness of fit on F^2	1.040
Final R indices (I >2σ(I))	
R_1	0.0327
wR_2	0.0689
Final R indices (all data)	
R_1	0.0500
wR_2	0.0741
Largest differences in peak and hole (e Å^{-3})	0.889 and -0.669

Table A.2. Bond lengths (Å) and angles (°) for $(GePh_2)_4$, **8**.

Ge(1)-C(1)	1.950(3)	C(13)-C(14)	1.392(4)
Ge(1)-C(7)	1.952(3)	C(14)-C(15)	1.389(4)
Ge(1)-Ge(2)	2.4534(4)	C(14)-H(14A)	0.9500
Ge(1)-Ge(4)	2.4580(4)	C(15)-C(16)	1.375(4)
Ge(2)-C(13)	1.956(3)	C(15)-H(15A)	0.9500
Ge(2)-C(19)	1.958(3)	C(16)-C(17)	1.377(4)
Ge(2)-Ge(3)	2.4730(4)	C(16)-H(16A)	0.9500
Ge(3)-C(31)	1.955(3)	C(17)-C(18)	1.392(4)
Ge(3)-C(25)	1.956(3)	C(17)-H(17A)	0.9500
Ge(3)-Ge(4)	2.4713(4)	C(18)-H(18A)	0.9500
Ge(4)-C(37)	1.952(3)	C(19)-C(24)	1.386(4)
Ge(4)-C(43)	1.958(3)	C(19)-C(20)	1.394(4)
C(1)-C(6)	1.377(4)	C(20)-C(21)	1.381(4)
C(1)-C(2)	1.392(4)	C(20)-H(20A)	0.9500
C(2)-C(3)	1.390(4)	C(21)-C(22)	1.377(4)
C(2)-H(2A)	0.9500	C(21)-H(21A)	0.9500
C(3)-C(4)	1.364(4)	C(22)-C(23)	1.380(4)
C(3)-H(3A)	0.9500	C(22)-H(22A)	0.9500
C(4)-C(5)	1.378(4)	C(23)-C(24)	1.386(4)
C(4)-H(4A)	0.9500	C(23)-H(23A)	0.9500
C(5)-C(6)	1.389(4)	C(24)-H(24A)	0.9500
C(5)-H(5A)	0.9500	C(25)-C(26)	1.381(4)
C(6)-H(6A)	0.9500	C(25)-C(30)	1.394(4)
C(7)-C(12)	1.384(4)	C(26)-C(27)	1.391(4)

C(7)-C(8)	1.388(4)	C(26)-H(26A)	0.9500
C(8)-C(9)	1.383(4)	C(27)-C(28)	1.379(4)
C(8)-H(8A)	0.9500	C(27)-H(27A)	0.9500
C(9)-C(10)	1.380(4)	C(28)-C(29)	1.384(4)
C(9)-H(9A)	0.9500	C(28)-H(28A)	0.9500
C(10)-C(11)	1.371(4)	C(29)-C(30)	1.380(4)
C(10)-H(10A)	0.9500	C(29)-H(29A)	0.9500
C(11)-C(12)	1.390(4)	C(30)-H(30A)	0.9500
C(11)-H(11A)	0.9500	C(31)-C(36)	1.384(4)
C(12)-H(12A)	0.9500	C(31)-C(32)	1.393(4)
C(13)-C(18)	1.382(4)	C(32)-C(33)	1.390(4)
C(32)-H(32A)	0.9500	C(40)-H(40A)	0.9500
C(33)-C(34)	1.376(4)	C(41)-C(42)	1.384(4)
C(33)-H(33A)	0.9500	C(41)-H(41A)	0.9500
C(34)-C(35)	1.376(4)	C(42)-H(42A)	0.9500
C(34)-H(34A)	0.9500	C(43)-C(48)	1.382(4)
C(35)-C(36)	1.381(4)	C(43)-C(44)	1.388(4)
C(35)-H(35A)	0.9500	C(44)-C(45)	1.390(4)
C(36)-H(36A)	0.9500	C(44)-H(44A)	0.9500
C(37)-C(38)	1.379(4)	C(45)-C(46)	1.367(5)
C(37)-C(42)	1.399(4)	C(45)-H(45A)	0.9500
C(38)-C(39)	1.383(4)	C(46)-C(47)	1.373(5)
C(38)-H(38A)	0.9500	C(46)-H(46A)	0.9500
C(39)-C(40)	1.377(4)	C(47)-C(48)	1.390(4)
C(39)-H(39A)	0.9500	C(47)-H(47A)	0.9500
C(40)-C(41)	1.374(4)	C(48)-H(48A)	0.9500

C(1)-Ge(1)-C(7)	107.62(11)	C(37)-Ge(4)-Ge(1)	114.81(7)
C(1)-Ge(1)-Ge(2)	113.03(8)	C(43)-Ge(4)-Ge(1)	116.78(8)
C(7)-Ge(1)-Ge(2)	113.42(8)	C(37)-Ge(4)-Ge(3)	115.64(8)
C(1)-Ge(1)-Ge(4)	116.46(8)	C(43)-Ge(4)-Ge(3)	113.75(8)
C(7)-Ge(1)-Ge(4)	115.87(8)	Ge(1)-Ge(4)-Ge(3)	90.464(13)
Ge(2)-Ge(1)-Ge(4)	89.789(13)	C(6)-C(1)-C(2)	118.3(3)
C(13)-Ge(2)-C(19)	110.33(11)	C(6)-C(1)-Ge(1)	123.3(2)
C(13)-Ge(2)-Ge(1)	114.56(8)	C(2)-C(1)-Ge(1)	118.3(2)
C(19)-Ge(2)-Ge(1)	111.43(8)	C(3)-C(2)-C(1)	120.9(3)
C(13)-Ge(2)-Ge(3)	115.85(7)	C(3)-C(2)-H(2A)	119.5
C(19)-Ge(2)-Ge(3)	112.90(8)	C(1)-C(2)-H(2A)	119.5
Ge(1)-Ge(2)-Ge(3)	90.531(13)	C(4)-C(3)-C(2)	119.6(3)
C(31)-Ge(3)-C(25)	106.36(11)	C(4)-C(3)-H(3A)	120.2
C(31)-Ge(3)-Ge(4)	114.48(8)	C(2)-C(3)-H(3A)	120.2
C(25)-Ge(3)-Ge(4)	113.20(8)	C(3)-C(4)-C(5)	120.6(3)
C(31)-Ge(3)-Ge(2)	114.71(8)	C(3)-C(4)-H(4A)	119.7
C(25)-Ge(3)-Ge(2)	118.70(8)	C(5)-C(4)-H(4A)	119.7
Ge(4)-Ge(3)-Ge(2)	89.031(13)	C(4)-C(5)-C(6)	119.7(3)
C(37)-Ge(4)-C(43)	105.45(11)	C(4)-C(5)-H(5A)	120.2
C(6)-C(5)-H(5A)	120.2	C(16)-C(17)-H(17A)	120.1
C(1)-C(6)-C(5)	120.9(3)	C(18)-C(17)-H(17A)	120.1
C(1)-C(6)-H(6A)	119.6	C(13)-C(18)-C(17)	120.9(3)
C(5)-C(6)-H(6A)	119.6	C(13)-C(18)-H(18A)	119.5
C(12)-C(7)-C(8)	118.1(2)	C(17)-C(18)-H(18A)	119.5
C(12)-C(7)-Ge(1)	121.8(2)	C(24)-C(19)-C(20)	118.3(3)

C(8)-C(7)-Ge(1)	120.1(2)	C(24)-C(19)-Ge(2)	121.6(2)
C(9)-C(8)-C(7)	121.4(3)	C(20)-C(19)-Ge(2)	120.1(2)
C(9)-C(8)-H(8A)	119.3	C(21)-C(20)-C(19)	120.9(3)
C(7)-C(8)-H(8A)	119.3	C(21)-C(20)-H(20A)	119.5
C(10)-C(9)-C(8)	119.5(3)	C(19)-C(20)-H(20A)	119.5
C(10)-C(9)-H(9A)	120.3	C(22)-C(21)-C(20)	120.2(3)
C(8)-C(9)-H(9A)	120.3	C(22)-C(21)-H(21A)	119.9
C(11)-C(10)-C(9)	120.1(3)	C(20)-C(21)-H(21A)	119.9
C(11)-C(10)-H(10A)	119.9	C(21)-C(22)-C(23)	119.6(3)
C(9)-C(10)-H(10A)	119.9	C(21)-C(22)-H(22A)	120.2
C(10)-C(11)-C(12)	120.1(3)	C(23)-C(22)-H(22A)	120.2
C(10)-C(11)-H(11A)	119.9	C(22)-C(23)-C(24)	120.3(3)
C(12)-C(11)-H(11A)	119.9	C(22)-C(23)-H(23A)	119.8
C(7)-C(12)-C(11)	120.7(3)	C(24)-C(23)-H(23A)	119.8
C(7)-C(12)-H(12A)	119.6	C(19)-C(24)-C(23)	120.6(3)
C(11)-C(12)-H(12A)	119.6	C(19)-C(24)-H(24A)	119.7
C(18)-C(13)-C(14)	118.5(2)	C(23)-C(24)-H(24A)	119.7
C(18)-C(13)-Ge(2)	121.7(2)	C(26)-C(25)-C(30)	118.0(2)
C(14)-C(13)-Ge(2)	119.9(2)	C(26)-C(25)-Ge(3)	124.1(2)
C(15)-C(14)-C(13)	120.6(3)	C(30)-C(25)-Ge(3)	117.9(2)
C(15)-C(14)-H(14A)	119.7	C(25)-C(26)-C(27)	121.1(3)
C(13)-C(14)-H(14A)	119.7	C(25)-C(26)-H(26A)	119.5
C(16)-C(15)-C(14)	120.2(3)	C(27)-C(26)-H(26A)	119.5
C(16)-C(15)-H(15A)	119.9	C(28)-C(27)-C(26)	119.7(3)
C(14)-C(15)-H(15A)	119.9	C(28)-C(27)-H(27A)	120.1
C(15)-C(16)-C(17)	120.0(3)	C(26)-C(27)-H(27A)	120.1

C(15)-C(16)-H(16A)	120.0	C(27)-C(28)-C(29)	120.4(3)
C(17)-C(16)-H(16A)	120.0	C(27)-C(28)-H(28A)	119.8
C(16)-C(17)-C(18)	119.9(3)	C(29)-C(28)-H(28A)	119.8
C(30)-C(29)-C(28)	119.1(3)	C(40)-C(39)-C(38)	120.5(3)
C(30)-C(29)-H(29A)	120.4	C(40)-C(39)-H(39A)	119.8
C(28)-C(29)-H(29A)	120.4	C(38)-C(39)-H(39A)	119.8
C(29)-C(30)-C(25)	121.7(3)	C(41)-C(40)-C(39)	119.2(3)
C(29)-C(30)-H(30A)	119.1	C(41)-C(40)-H(40A)	120.4
C(25)-C(30)-H(30A)	119.1	C(39)-C(40)-H(40A)	120.4
C(36)-C(31)-C(32)	118.0(3)	C(40)-C(41)-C(42)	120.7(3)
C(36)-C(31)-Ge(3)	121.8(2)	C(40)-C(41)-H(41A)	119.7
C(32)-C(31)-Ge(3)	120.2(2)	C(42)-C(41)-H(41A)	119.7
C(33)-C(32)-C(31)	120.5(3)	C(41)-C(42)-C(37)	120.4(3)
C(33)-C(32)-H(32A)	119.7	C(41)-C(42)-H(42A)	119.8
C(31)-C(32)-H(32A)	119.7	C(37)-C(42)-H(42A)	119.8
C(34)-C(33)-C(32)	120.3(3)	C(48)-C(43)-C(44)	118.8(3)
C(34)-C(33)-H(33A)	119.8	C(48)-C(43)-Ge(4)	122.6(2)
C(32)-C(33)-H(33A)	119.8	C(44)-C(43)-Ge(4)	118.6(2)
C(33)-C(34)-C(35)	119.7(3)	C(43)-C(44)-C(45)	120.3(3)
C(33)-C(34)-H(34A)	120.1	C(43)-C(44)-H(44A)	119.9
C(35)-C(34)-H(34A)	120.1	C(45)-C(44)-H(44A)	119.9
C(34)-C(35)-C(36)	119.9(3)	C(46)-C(45)-C(44)	120.1(3)
C(34)-C(35)-H(35A)	120.0	C(46)-C(45)-H(45A)	119.9
C(36)-C(35)-H(35A)	120.0	C(44)-C(45)-H(45A)	119.9
C(35)-C(36)-C(31)	121.5(3)	C(45)-C(46)-C(47)	120.5(3)
C(35)-C(36)-H(36A)	119.2	C(45)-C(46)-H(46A)	119.8

C(31)-C(36)-H(36A)	119.2	C(47)-C(46)-H(46A)	119.8
C(38)-C(37)-C(42)	118.1(3)	C(46)-C(47)-C(48)	119.6(3)
C(38)-C(37)-Ge(4)	119.5(2)	C(46)-C(47)-H(47A)	120.2
C(42)-C(37)-Ge(4)	122.4(2)	C(48)-C(47)-H(47A)	120.2
C(37)-C(38)-C(39)	121.0(3)	C(43)-C(48)-C(47)	120.8(3)
C(37)-C(38)-H(38A)	119.5	C(43)-C(48)-H(48A)	119.6
C(39)-C(38)-H(38A)	119.5	C(47)-C(48)-H(48A)	119.6

Table A.3. Torsion angles (°) for $(GePh_2)_4$, **8**.

C(1)-Ge(1)-Ge(2)-C(13)	3.33(12)
C(7)-Ge(1)-Ge(2)-C(13)	-119.52(12)
Ge(4)-Ge(1)-Ge(2)-C(13)	122.19(8)
C(1)-Ge(1)-Ge(2)-C(19)	129.47(12)
C(7)-Ge(1)-Ge(2)-C(19)	6.61(12)
Ge(4)-Ge(1)-Ge(2)-C(19)	-111.67(8)
C(1)-Ge(1)-Ge(2)-Ge(3)	-115.59(8)
C(7)-Ge(1)-Ge(2)-Ge(3)	121.55(9)
Ge(4)-Ge(1)-Ge(2)-Ge(3)	3.265(13)
C(13)-Ge(2)-Ge(3)-C(31)	122.31(13)
C(19)-Ge(2)-Ge(3)-C(31)	-6.28(13)
Ge(1)-Ge(2)-Ge(3)-C(31)	-119.89(9)
C(13)-Ge(2)-Ge(3)-C(25)	-4.94(13)
C(19)-Ge(2)-Ge(3)-C(25)	-133.54(12)
Ge(1)-Ge(2)-Ge(3)-C(25)	112.85(9)

C(13)-Ge(2)-Ge(3)-Ge(4)	-121.04(9)
C(19)-Ge(2)-Ge(3)-Ge(4)	110.36(9)
Ge(1)-Ge(2)-Ge(3)-Ge(4)	-3.248(13)
C(1)-Ge(1)-Ge(4)-C(37)	-6.19(13)
C(7)-Ge(1)-Ge(4)-C(37)	121.92(13)
Ge(2)-Ge(1)-Ge(4)-C(37)	-121.98(9)
C(1)-Ge(1)-Ge(4)-C(43)	-130.39(12)
C(7)-Ge(1)-Ge(4)-C(43)	-2.29(13)
Ge(2)-Ge(1)-Ge(4)-C(43)	113.82(9)
C(1)-Ge(1)-Ge(4)-Ge(3)	112.53(9)
C(7)-Ge(1)-Ge(4)-Ge(3)	-119.37(9)
Ge(2)-Ge(1)-Ge(4)-Ge(3)	-3.268(13)
C(31)-Ge(3)-Ge(4)-C(37)	-121.91(12)
C(25)-Ge(3)-Ge(4)-C(37)	0.22(12)
Ge(2)-Ge(3)-Ge(4)-C(37)	121.23(8)
C(31)-Ge(3)-Ge(4)-C(43)	0.37(12)
C(25)-Ge(3)-Ge(4)-C(43)	122.50(12)
Ge(2)-Ge(3)-Ge(4)-C(43)	-116.48(9)
C(31)-Ge(3)-Ge(4)-Ge(1)	120.10(9)
C(25)-Ge(3)-Ge(4)-Ge(1)	-117.77(8)
Ge(2)-Ge(3)-Ge(4)-Ge(1)	3.242(13)
C(7)-Ge(1)-C(1)-C(6)	-99.8(2)
Ge(2)-Ge(1)-C(1)-C(6)	134.2(2)
Ge(4)-Ge(1)-C(1)-C(6)	32.2(3)
C(7)-Ge(1)-C(1)-C(2)	78.4(2)
Ge(2)-Ge(1)-C(1)-C(2)	-47.7(2)

Ge(4)-Ge(1)-C(1)-C(2)	-149.62(18)
C(6)-C(1)-C(2)-C(3)	0.6(4)
Ge(1)-C(1)-C(2)-C(3)	-177.6(2)
C(1)-C(2)-C(3)-C(4)	0.3(4)
C(2)-C(3)-C(4)-C(5)	-0.8(5)
C(3)-C(4)-C(5)-C(6)	0.3(5)
C(2)-C(1)-C(6)-C(5)	-1.1(4)
Ge(1)-C(1)-C(6)-C(5)	177.0(2)
C(4)-C(5)-C(6)-C(1)	0.7(5)
C(1)-Ge(1)-C(7)-C(12)	0.9(3)
Ge(2)-Ge(1)-C(7)-C(12)	126.7(2)
Ge(4)-Ge(1)-C(7)-C(12)	-131.4(2)
C(1)-Ge(1)-C(7)-C(8)	-179.2(2)
Ge(2)-Ge(1)-C(7)-C(8)	-53.4(2)
Ge(4)-Ge(1)-C(7)-C(8)	48.4(2)
C(12)-C(7)-C(8)-C(9)	0.9(4)
Ge(1)-C(7)-C(8)-C(9)	-178.9(2)
C(7)-C(8)-C(9)-C(10)	0.0(4)
C(8)-C(9)-C(10)-C(11)	-0.8(4)
C(9)-C(10)-C(11)-C(12)	0.6(5)
C(8)-C(7)-C(12)-C(11)	-1.1(4)
Ge(1)-C(7)-C(12)-C(11)	178.7(2)
C(10)-C(11)-C(12)-C(7)	0.4(5)
C(19)-Ge(2)-C(13)-C(18)	10.5(2)
Ge(1)-Ge(2)-C(13)-C(18)	137.16(18)
Ge(3)-Ge(2)-C(13)-C(18)	-119.38(19)

C(19)-Ge(2)-C(13)-C(14)	-170.0(2)
Ge(1)-Ge(2)-C(13)-C(14)	-43.3(2)
Ge(3)-Ge(2)-C(13)-C(14)	60.2(2)
C(18)-C(13)-C(14)-C(15)	0.3(4)
Ge(2)-C(13)-C(14)-C(15)	-179.3(2)
C(13)-C(14)-C(15)-C(16)	-0.1(4)
C(14)-C(15)-C(16)-C(17)	-0.4(4)
C(15)-C(16)-C(17)-C(18)	0.8(4)
C(14)-C(13)-C(18)-C(17)	0.2(4)
Ge(2)-C(13)-C(18)-C(17)	179.72(19)
C(16)-C(17)-C(18)-C(13)	-0.7(4)
C(13)-Ge(2)-C(19)-C(24)	-93.0(2)
Ge(1)-Ge(2)-C(19)-C(24)	138.6(2)
Ge(3)-Ge(2)-C(19)-C(24)	38.4(2)
C(13)-Ge(2)-C(19)-C(20)	87.8(2)
Ge(1)-Ge(2)-C(19)-C(20)	-40.6(2)
Ge(3)-Ge(2)-C(19)-C(20)	-140.78(19)
C(24)-C(19)-C(20)-C(21)	0.1(4)
Ge(2)-C(19)-C(20)-C(21)	179.3(2)
C(19)-C(20)-C(21)-C(22)	-0.1(4)
C(20)-C(21)-C(22)-C(23)	0.1(4)
C(21)-C(22)-C(23)-C(24)	-0.1(4)
C(20)-C(19)-C(24)-C(23)	-0.1(4)
Ge(2)-C(19)-C(24)-C(23)	-179.3(2)
C(22)-C(23)-C(24)-C(19)	0.1(4)
C(31)-Ge(3)-C(25)-C(26)	-118.7(2)

Ge(4)-Ge(3)-C(25)-C(26)	114.7(2)
Ge(2)-Ge(3)-C(25)-C(26)	12.4(3)
C(31)-Ge(3)-C(25)-C(30)	63.5(2)
Ge(4)-Ge(3)-C(25)-C(30)	-63.1(2)
Ge(2)-Ge(3)-C(25)-C(30)	-165.39(18)
C(30)-C(25)-C(26)-C(27)	-0.1(4)
Ge(3)-C(25)-C(26)-C(27)	-177.9(2)
C(25)-C(26)-C(27)-C(28)	0.1(4)
C(26)-C(27)-C(28)-C(29)	0.1(4)
C(27)-C(28)-C(29)-C(30)	-0.2(4)
C(28)-C(29)-C(30)-C(25)	0.2(4)
C(26)-C(25)-C(30)-C(29)	0.0(4)
Ge(3)-C(25)-C(30)-C(29)	177.9(2)
C(25)-Ge(3)-C(31)-C(36)	-162.7(2)
Ge(4)-Ge(3)-C(31)-C(36)	-36.9(2)
Ge(2)-Ge(3)-C(31)-C(36)	64.0(2)
C(25)-Ge(3)-C(31)-C(32)	19.9(2)
Ge(4)-Ge(3)-C(31)-C(32)	145.69(19)
Ge(2)-Ge(3)-C(31)-C(32)	-113.4(2)
C(36)-C(31)-C(32)-C(33)	0.0(4)
Ge(3)-C(31)-C(32)-C(33)	177.5(2)
C(31)-C(32)-C(33)-C(34)	0.7(4)
C(32)-C(33)-C(34)-C(35)	-1.0(4)
C(33)-C(34)-C(35)-C(36)	0.6(4)
C(34)-C(35)-C(36)-C(31)	0.1(4)
C(32)-C(31)-C(36)-C(35)	-0.4(4)

Ge(3)-C(31)-C(36)-C(35)	-177.8(2)
C(43)-Ge(4)-C(37)-C(38)	34.3(2)
Ge(1)-Ge(4)-C(37)-C(38)	-95.7(2)
Ge(3)-Ge(4)-C(37)-C(38)	160.91(19)
C(43)-Ge(4)-C(37)-C(42)	-143.8(2)
Ge(1)-Ge(4)-C(37)-C(42)	86.2(2)
Ge(3)-Ge(4)-C(37)-C(42)	-17.2(2)
C(42)-C(37)-C(38)-C(39)	2.0(4)
Ge(4)-C(37)-C(38)-C(39)	-176.2(2)
C(37)-C(38)-C(39)-C(40)	-0.1(5)
C(38)-C(39)-C(40)-C(41)	-1.4(5)
C(39)-C(40)-C(41)-C(42)	0.9(4)
C(40)-C(41)-C(42)-C(37)	1.0(4)
C(38)-C(37)-C(42)-C(41)	-2.5(4)
Ge(4)-C(37)-C(42)-C(41)	175.6(2)
C(37)-Ge(4)-C(43)-C(48)	-102.8(2)
Ge(1)-Ge(4)-C(43)-C(48)	26.0(3)
Ge(3)-Ge(4)-C(43)-C(48)	129.4(2)
C(37)-Ge(4)-C(43)-C(44)	75.5(2)
Ge(1)-Ge(4)-C(43)-C(44)	-155.67(19)
Ge(3)-Ge(4)-C(43)-C(44)	-52.3(2)
C(48)-C(43)-C(44)-C(45)	0.2(4)
Ge(4)-C(43)-C(44)-C(45)	-178.2(2)
C(43)-C(44)-C(45)-C(46)	0.1(5)
C(44)-C(45)-C(46)-C(47)	-0.4(5)
C(45)-C(46)-C(47)-C(48)	0.5(5)

C(44)-C(43)-C(48)-C(47)	-0.1(4)
Ge(4)-C(43)-C(48)-C(47)	178.2(2)
C(46)-C(47)-C(48)-C(43)	-0.2(4)

Symmetry transformations used to generate equivalent atoms.

Table A.4. X-ray crystallographic data for $Br(GePh_2)_4Br$, **10**.

Empirical formula	$C_{48}H_{40}Br_2Ge_4$
Formula weight (g/mol)	1066.98
Temperature (K)	100(2) K
Wavelength (Å)	1.54178
Crystal system	Monoclinic
Space group	P2(1)
a (Å)	12.8805(2)
b (Å)	11.9670(2)
c (Å)	13.7534(2)
α (°)	90°
β (°)	95.2590(10)
γ (°)	90°
Volume ($Å^3$)	2111.04(6)
Z	2
Calculated density (g/cm^3)	1.679
Absorption coefficient (mm^{-1})	5.751
F(000)	1052
Crystal size (mm)	0.27 x 0.24 x 0.22

Crystal size and shape	
θ range for data collection (o)	3.23 to 68.08°
Index ranges	-15<=h<=12
	-13<=k<=14
	-16<=l<=16
Reflections collected	13170
Independent reflections	6320 (R_{int} = 0.0445)
Completeness to θ	66.50° (97.5 %)
Absorption correction	Multi-scan
Maximum and minimum transmission	0.3643 and 0.3058
Refinement method	Full-matrix least-squares on F^2
Data/restraints/parameters	6320 / 1 / 488
Goodness of fit on F^2	1.019
Final R indices (I >2σ(I))	
R_1	0.0362
wR_2	0.0890
Final R indices (all data)	
R_1	0.0376
wR_2	0.0902
Largest differences in peak and hole (e Å^{-3})	0.791 and -0.561

Table A.5. Bond lengths (Å) and angles (°) for $Br(GePh_2)_4Br$, **10**.

Br(1)-Ge(1)	2.3468(8)	C(19)-C(24)	1.391(7)
Br(2)-Ge(4)	2.3612(8)	C(19)-C(20)	1.392(7)

Ge(1)-C(7)	1.944(5)	C(20)-C(21)	1.378(7)
Ge(1)-C(1)	1.952(5)	C(21)-C(22)	1.384(8)
Ge(1)-Ge(2)	2.4470(7)	C(22)-C(23)	1.385(8)
Ge(2)-C(19)	1.957(5)	C(23)-C(24)	1.388(7)
Ge(2)-C(13)	1.959(5)	C(25)-C(30)	1.392(7)
Ge(2)-Ge(3)	2.4548(6)	C(25)-C(26)	1.398(7)
Ge(3)-C(31)	1.948(5)	C(26)-C(27)	1.392(7)
Ge(3)-C(25)	1.964(5)	C(27)-C(28)	1.381(8)
Ge(3)-Ge(4)	2.4401(7)	C(28)-C(29)	1.377(8)
Ge(4)-C(37)	1.950(5)	C(29)-C(30)	1.400(7)
Ge(4)-C(43)	1.952(5)	C(31)-C(32)	1.389(7)
C(1)-C(2)	1.389(8)	C(31)-C(36)	1.416(8)
C(1)-C(6)	1.398(8)	C(32)-C(33)	1.400(7)
C(2)-C(3)	1.388(8)	C(33)-C(34)	1.372(8)
C(3)-C(4)	1.384(9)	C(34)-C(35)	1.376(7)
C(4)-C(5)	1.379(9)	C(35)-C(36)	1.395(7)
C(5)-C(6)	1.384(8)	C(37)-C(38)	1.387(8)
C(7)-C(8)	1.397(7)	C(37)-C(42)	1.399(7)
C(7)-C(12)	1.398(7)	C(38)-C(39)	1.386(7)
C(8)-C(9)	1.400(8)	C(39)-C(40)	1.392(9)
C(9)-C(10)	1.370(8)	C(40)-C(41)	1.385(10)
C(10)-C(11)	1.401(9)	C(41)-C(42)	1.377(7)
C(11)-C(12)	1.382(7)	C(43)-C(48)	1.397(8)
C(13)-C(18)	1.387(8)	C(43)-C(44)	1.392(8)
C(13)-C(14)	1.408(7)	C(44)-C(45)	1.394(8)
C(14)-C(15)	1.392(8)	C(45)-C(46)	1.384(9)

C(15)-C(16)	1.377(9)	C(46)-C(47)	1.395(9)
C(16)-C(17)	1.395(8)	C(47)-C(48)	1.382(8)
C(17)-C(18)	1.379(8)		

C(7)-Ge(1)-C(1)	111.6(2)	C(1)-Ge(1)-Br(1)	104.68(17)
C(7)-Ge(1)-Br(1)	105.99(16)	C(7)-Ge(1)-Ge(2)	119.15(15)
C(1)-Ge(1)-Ge(2)	110.62(14)	C(12)-C(11)-C(10)	119.5(5)
Br(1)-Ge(1)-Ge(2)	103.36(3)	C(11)-C(12)-C(7)	120.9(5)
C(19)-Ge(2)-C(13)	109.4(2)	C(18)-C(13)-C(14)	118.5(5)
C(19)-Ge(2)-Ge(1)	112.86(14)	C(18)-C(13)-Ge(2)	121.4(4)
C(13)-Ge(2)-Ge(1)	100.54(14)	C(14)-C(13)-Ge(2)	119.9(4)
C(19)-Ge(2)-Ge(3)	107.96(15)	C(13)-C(14)-C(15)	120.1(5)
C(13)-Ge(2)-Ge(3)	110.49(15)	C(16)-C(15)-C(14)	120.4(5)
Ge(1)-Ge(2)-Ge(3)	115.33(3)	C(15)-C(16)-C(17)	119.8(5)
C(31)-Ge(3)-C(25)	108.3(2)	C(18)-C(17)-C(16)	119.9(6)
C(31)-Ge(3)-Ge(4)	102.61(15)	C(17)-C(18)-C(13)	121.3(5)
C(25)-Ge(3)-Ge(4)	111.30(14)	C(24)-C(19)-C(20)	118.3(4)
C(31)-Ge(3)-Ge(2)	111.85(16)	C(24)-C(19)-Ge(2)	119.1(4)
C(25)-Ge(3)-Ge(2)	111.24(15)	C(20)-C(19)-Ge(2)	122.6(4)
Ge(4)-Ge(3)-Ge(2)	111.25(3)	C(21)-C(20)-C(19)	120.8(5)
C(37)-Ge(4)-C(43)	109.6(2)	C(20)-C(21)-C(22)	120.4(5)
C(37)-Ge(4)-Br(2)	104.83(15)	C(21)-C(22)-C(23)	119.7(5)
C(43)-Ge(4)-Br(2)	102.78(17)	C(24)-C(23)-C(22)	119.6(5)
C(37)-Ge(4)-Ge(3)	118.39(16)	C(19)-C(24)-C(23)	121.1(5)
C(43)-Ge(4)-Ge(3)	115.28(14)	C(30)-C(25)-C(26)	119.7(4)
Br(2)-Ge(4)-Ge(3)	103.94(3)	C(30)-C(25)-Ge(3)	118.6(4)

C(2)-C(1)-C(6)	118.9(5)	C(26)-C(25)-Ge(3)	121.5(4)
C(2)-C(1)-Ge(1)	121.7(4)	C(27)-C(26)-C(25)	119.6(5)
C(6)-C(1)-Ge(1)	119.3(4)	C(28)-C(27)-C(26)	120.3(5)
C(1)-C(2)-C(3)	120.5(5)	C(29)-C(28)-C(27)	120.6(5)
C(2)-C(3)-C(4)	120.1(5)	C(28)-C(29)-C(30)	119.7(5)
C(5)-C(4)-C(3)	119.8(5)	C(25)-C(30)-C(29)	120.1(5)
C(4)-C(5)-C(6)	120.6(6)	C(32)-C(31)-C(36)	118.4(5)
C(5)-C(6)-C(1)	120.1(5)	C(32)-C(31)-Ge(3)	122.0(4)
C(8)-C(7)-C(12)	119.1(5)	C(36)-C(31)-Ge(3)	119.4(4)
C(8)-C(7)-Ge(1)	117.6(4)	C(31)-C(32)-C(33)	120.8(5)
C(12)-C(7)-Ge(1)	123.3(4)	C(34)-C(33)-C(32)	119.7(5)
C(7)-C(8)-C(9)	119.6(5)	C(33)-C(34)-C(35)	121.0(5)
C(10)-C(9)-C(8)	120.7(6)	C(34)-C(35)-C(36)	120.0(5)
C(9)-C(10)-C(11)	120.1(5)	C(35)-C(36)-C(31)	120.0(5)
C(38)-C(37)-C(42)	119.3(5)	C(42)-C(41)-C(40)	120.4(5)
C(38)-C(37)-Ge(4)	120.7(4)	C(41)-C(42)-C(37)	120.3(5)
C(42)-C(37)-Ge(4)	120.0(4)	C(48)-C(43)-C(44)	119.0(5)
C(37)-C(38)-C(39)	120.4(5)	C(48)-C(43)-Ge(4)	122.2(4)
C(40)-C(39)-C(38)	119.9(6)	C(44)-C(43)-Ge(4)	118.8(4)
C(39)-C(40)-C(41)	119.7(5)	C(43)-C(44)-C(45)	120.6(6)
C(46)-C(45)-C(44)	119.6(6)	C(48)-C(47)-C(46)	119.6(6)
C(45)-C(46)-C(47)	120.4(5)	C(47)-C(48)-C(43)	120.7(6)

Table A.6. X-ray crystallographic data for $Pr^{i}_{3}Ge(GePh_2)_4GePr^{i}_{3}$, **12**.

Empirical formula	$C_{66}H_{82}Ge_6$
Formula weight (g/mol)	1310.86
Temperature (K)	100(2)
Wavelength (Å)	0.71073
Crystal system	Triclinic
Space group	P-1
a (Å)	11.0685(7)
b (Å)	11.3771(6)
c (Å)	12.7949(8)
α (°)	97.447(2)
β (°)	91.495(2)
γ (°)	108.292(2)
Volume ($Å^3$)	1513.09(16)
Z	1
Calculated density (g/cm^3)	1.439
Absorption coefficient (mm^{-1})	2.980
F(000)	670
Crystal size (mm)	0.30 x 0.25 x 0.20
θ range for data collection (o)	1.91 to 28.36°
Index ranges	-14<=h<=12
	-11<=k<=15
	-17<=l<=16
Reflections collected	16375
Independent reflections	7179 (R_{int} = 0.0221)

Completeness to θ	25.00° (97.6 %)
Absorption correction	Multi-scan
Maximum and minimum transmission	0.5871 and 0.4684
Refinement method	Full-matrix least-squares on F^2
Data/restraints/parameters	7179 / 0 / 325
Goodness of fit on F^2	1.040
Final R indices ($I > 2\sigma(I)$)	
R_1	0.0197
wR_2	0.0472
Final R indices (all data)	
R_1	0.0244
wR_2	0.0487
Largest differences in peak and hole (e Å^{-3})	0.397 and -0.366

Table A.7. Bond lengths (Å) and angles (°) for $Pr^i_3Ge(GePh_2)_4GePr^i_3$, **12**.

Ge(1)-C(4)	1.9892(16)	C(1)-C(3)	1.532(2)
Ge(1)-C(7)	1.9948(16)	C(1)-C(2)	1.534(2)
Ge(1)-C(1)	1.9952(16)	C(4)-C(6)	1.528(3)
Ge(1)-Ge(2)	2.4670(2)	C(4)-C(5)	1.536(2)
Ge(2)-C(16)	1.9552(15)	C(7)-C(9)	1.531(2)
Ge(2)-C(10)	1.9697(15)	C(7)-C(8)	1.534(2)
Ge(2)-Ge(3)	2.4715(3)	C(10)-C(15)	1.396(2)
Ge(3)-C(22)	1.9666(15)	C(10)-C(11)	1.402(2)
Ge(3)-C(28)	1.9682(15)	C(11)-C(12)	1.394(2)

Ge(3)-Ge(3)#1	2.4745(3)	C(12)-C(13)	1.383(3)
C(1)-C(3)	1.532(2)	C(13)-C(14)	1.387(2)
C(1)-C(2)	1.534(2)	C(14)-C(15)	1.391(2)
C(4)-C(6)	1.528(3)	C(16)-C(21)	1.396(2)
C(4)-C(5)	1.536(2)	C(16)-C(17)	1.397(2)
C(7)-C(9)	1.531(2)	C(17)-C(18)	1.393(2)
C(7)-C(8)	1.534(2)	C(18)-C(19)	1.389(2)
C(10)-C(15)	1.396(2)	C(19)-C(20)	1.385(3)
C(10)-C(11)	1.402(2)	C(20)-C(21)	1.387(2)
C(11)-C(12)	1.394(2)	C(22)-C(27)	1.397(2)
C(12)-C(13)	1.383(3)	C(22)-C(23)	1.398(2)
Ge(1)-C(4)	1.9892(16)	C(23)-C(24)	1.394(2)
Ge(1)-C(7)	1.9948(16)	C(24)-C(25)	1.381(3)
Ge(1)-C(1)	1.9952(16)	C(25)-C(26)	1.386(2)
Ge(1)-Ge(2)	2.4670(2)	C(26)-C(27)	1.393(2)
Ge(2)-C(16)	1.9552(15)	C(28)-C(33)	1.400(2)
Ge(2)-C(10)	1.9697(15)	C(28)-C(29)	1.401(2)
Ge(2)-Ge(3)	2.4715(3)	C(29)-C(30)	1.394(2)
Ge(3)-C(22)	1.9666(15)	C(30)-C(31)	1.385(3)
Ge(3)-C(28)	1.9682(15)	C(31)-C(32)	1.375(3)
Ge(3)-Ge(3)#1	2.4745(3)	C(32)-C(33)	1.397(2)

C(4)-Ge(1)-C(7)	108.99(7)	C(22)-Ge(3)-Ge(2)	115.68(4)
C(4)-Ge(1)-C(1)	108.74(7)	C(28)-Ge(3)-Ge(2)	99.69(4)
C(7)-Ge(1)-C(1)	108.48(7)	C(22)-Ge(3)-Ge(3)#1	108.47(4)
C(4)-Ge(1)-Ge(2)	109.19(5)	C(28)-Ge(3)-Ge(3)#1	112.43(4)

C(7)-Ge(1)-Ge(2)	109.49(5)	Ge(2)-Ge(3)-Ge(3)#1	114.153(10)
C(1)-Ge(1)-Ge(2)	111.91(4)	C(3)-C(1)-C(2)	109.86(14)
C(16)-Ge(2)-C(10)	107.95(6)	C(3)-C(1)-Ge(1)	112.47(11)
C(16)-Ge(2)-Ge(1)	107.71(4)	C(2)-C(1)-Ge(1)	114.69(11)
C(10)-Ge(2)-Ge(1)	110.80(4)	C(6)-C(4)-C(5)	110.79(15)
C(16)-Ge(2)-Ge(3)	111.71(4)	C(6)-C(4)-Ge(1)	113.61(12)
C(10)-Ge(2)-Ge(3)	100.93(4)	C(5)-C(4)-Ge(1)	111.31(11)
Ge(1)-Ge(2)-Ge(3)	117.330(8)	C(9)-C(7)-C(8)	110.75(13)
C(22)-Ge(3)-C(28)	105.92(6)	C(9)-C(7)-Ge(1)	112.73(12)
C(8)-C(7)-Ge(1)	111.64(11)	C(27)-C(22)-C(23)	118.27(14)
C(15)-C(10)-C(11)	117.93(14)	C(27)-C(22)-Ge(3)	120.13(11)
C(15)-C(10)-Ge(2)	121.04(11)	C(23)-C(22)-Ge(3)	121.60(12)
C(11)-C(10)-Ge(2)	120.73(12)	C(24)-C(23)-C(22)	120.80(15)
C(12)-C(11)-C(10)	120.70(16)	C(25)-C(24)-C(23)	120.09(16)
C(13)-C(12)-C(11)	120.38(16)	C(24)-C(25)-C(26)	119.99(15)
C(12)-C(13)-C(14)	119.71(15)	C(25)-C(26)-C(27)	120.02(15)
C(13)-C(14)-C(15)	120.01(16)	C(26)-C(27)-C(22)	120.80(15)
C(14)-C(15)-C(10)	121.26(15)	C(33)-C(28)-C(29)	117.99(14)
C(21)-C(16)-C(17)	117.99(14)	C(33)-C(28)-Ge(3)	120.09(12)
C(21)-C(16)-Ge(2)	121.11(12)	C(29)-C(28)-Ge(3)	121.47(11)
C(17)-C(16)-Ge(2)	120.69(11)	C(30)-C(29)-C(28)	120.68(16)
C(18)-C(17)-C(16)	121.26(15)	C(31)-C(30)-C(29)	120.17(17)
C(19)-C(18)-C(17)	119.49(16)	C(32)-C(31)-C(30)	120.16(16)
C(20)-C(19)-C(18)	120.08(15)	C(31)-C(32)-C(33)	120.05(17)
C(19)-C(20)-C(21)	120.04(16)	C(32)-C(33)-C(28)	120.93(17)
C(20)-C(21)-C(16)	121.12(15)		

Symmetry transformations used to generate equivalent atoms: #1 -x+1,-y+1,-z+1

Table A.8. X-ray crystallographic data for $Pr^{i}_{3}Ge(GePh_2)_2GePr^{i}_{3}$, **14**.

Empirical formula	$C_{42}H_{62}Ge_4$
Formula weight (g/mol)	857.27
Temperature (K)	100 K
Wavelength (Å)	0.71073
Crystal system	Triclinic
Space group	P-1
a (Å)	9.4578(17)
b (Å)	10.709(2)
c (Å)	11.485(2)
α (°)	106.109(5)
β (°)	99.150(5)
γ (°)	108.601(6)
Volume ($Å^3$)	1019.3(3)
Z	1
Calculated density (g/cm^3)	1.397
Absorption coefficient (mm^{-1})	2.947
F(000)	442
Crystal size (mm)	0.083 x 0.021 x 0.011
θ range for data collection (o)	1.918 to 26.419°
Index ranges	-11<=h<=11
	-13<=k<=13

	-14<=l<=14
Reflections collected	15147
Independent reflections	4185 (R_{int} = 0.0899)
Completeness to θ	25.000° (100.0%)
Absorption correction	Semi-empirical from equivalents
Maximum and minimum transmission	0.7454 and 0.6371
Refinement method	Full-matrix least-squares on F^2
Data/restraints/parameters	4185 / 0 / 214
Goodness of fit on F^2	1.009
Final R indices (I >2σ(I))	
R_1	0.0487
wR_2	0.0871
Final R indices (all data)	
R_1	0.1103
wR_2	0.1012
Largest differences in peak and hole (e Å^{-3})	0.687 and -0.552

Table A.9. Bond lengths (Å) and angles (°) for $Pr^i_3Ge(GePh_2)_2GePr^i_3$, **14**.

Ge(1)-Ge(2)	2.4669(7)	C(8)-H(8C)	0.9800
Ge(1)-C(1)	1.985(5)	C(9)-H(9A)	0.9800
Ge(1)-C(2)	1.995(5)	C(9)-H(9B)	0.9800
Ge(1)-C(3)	1.993(5)	C(9)-H(9C)	0.9800
Ge(2)-Ge(2)#1	2.4723(10)	C(10)-H(10A)	0.9800
Ge(2)-C(4)	1.962(5)	C(10)-H(10B)	0.9800

Ge(2)-C(5)	1.974(5)	C(10)-H(10C)	0.9800
C(1)-H(1)	1.0000	C(11)-H(11A)	0.9800
C(1)-C(6)	1.521(7)	C(11)-H(11B)	0.9800
C(1)-C(7)	1.528(7)	C(11)-H(11C)	0.9800
C(2)-H(2)	1.0000	C(12)-H(12)	0.9500
C(2)-C(8)	1.527(6)	C(12)-C(13)	1.391(7)
C(2)-C(9)	1.535(7)	C(13)-H(13)	0.9500
C(3)-H(3)	1.0000	C(13)-C(14)	1.382(7)
C(3)-C(10)	1.530(7)	C(14)-H(14)	0.9500
C(3)-C(11)	1.531(7)	C(14)-C(15)	1.374(7)
C(4)-C(12)	1.379(7)	C(15)-H(15)	0.9500
C(4)-C(16)	1.383(7)	C(15)-C(16)	1.379(7)
C(5)-C(17)	1.391(6)	C(16)-H(16)	0.9500
C(5)-C(21)	1.388(7)	C(17)-H(17)	0.9500
C(6)-H(6A)	0.9800	C(17)-C(18)	1.384(7)
C(6)-H(6B)	0.9800	C(18)-H(18)	0.9500
C(6)-H(6C)	0.9800	C(18)-C(19)	1.367(7)
C(7)-H(7A)	0.9800	C(19)-H(19)	0.9500
C(7)-H(7B)	0.9800	C(19)-C(20)	1.379(7)
C(7)-H(7C)	0.9800	C(20)-H(20)	0.9500
C(8)-H(8A)	0.9800	C(20)-C(21)	1.394(7)
C(8)-H(8B)	0.9800	C(21)-H(21)	0.9500

C(1)-Ge(1)-Ge(2)	110.61(15)	H(8B)-C(8)-H(8C)	109.5
C(1)-Ge(1)-C(2)	107.6(2)	C(2)-C(9)-H(9A)	109.5
C(1)-Ge(1)-C(3)	109.6(2)	C(2)-C(9)-H(9B)	109.5

C(2)-Ge(1)-Ge(2)	110.49(13)	C(2)-C(9)-H(9C)	109.5
C(3)-Ge(1)-Ge(2)	110.22(15)	H(9A)-C(9)-H(9B)	109.5
C(3)-Ge(1)-C(2)	108.2(2)	H(9A)-C(9)-H(9C)	109.5
Ge(1)-Ge(2)-Ge(2)#1	116.51(3)	H(9B)-C(9)-H(9C)	109.5
C(4)-Ge(2)-Ge(1)	105.10(13)	C(3)-C(10)-H(10A)	109.5
C(4)-Ge(2)-Ge(2)#1	109.50(14)	C(3)-C(10)-H(10B)	109.5
C(4)-Ge(2)-C(5)	104.9(2)	C(3)-C(10)-H(10C)	109.5
C(5)-Ge(2)-Ge(1)	111.22(14)	H(10A)-C(10)-H(10B)	109.5
C(5)-Ge(2)-Ge(2)#1	108.89(12)	H(10A)-C(10)-H(10C)	109.5
Ge(1)-C(1)-H(1)	105.8	H(10B)-C(10)-H(10C)	109.5
C(6)-C(1)-Ge(1)	111.9(3)	C(3)-C(11)-H(11A)	109.5
C(6)-C(1)-H(1)	105.8	C(3)-C(11)-H(11B)	109.5
C(6)-C(1)-C(7)	110.6(5)	C(3)-C(11)-H(11C)	109.5
C(7)-C(1)-Ge(1)	116.1(4)	H(11A)-C(11)-H(11B)	109.5
C(7)-C(1)-H(1)	105.8	H(11A)-C(11)-H(11C)	109.5
Ge(1)-C(2)-H(2)	107.2	H(11B)-C(11)-H(11C)	109.5
C(8)-C(2)-Ge(1)	114.0(3)	C(4)-C(12)-H(12)	118.8
C(8)-C(2)-H(2)	107.2	C(4)-C(12)-C(13)	122.5(5)
C(8)-C(2)-C(9)	109.6(4)	C(13)-C(12)-H(12)	118.8
C(9)-C(2)-Ge(1)	111.4(3)	C(12)-C(13)-H(13)	120.3
C(9)-C(2)-H(2)	107.2	C(14)-C(13)-C(12)	119.3(5)
Ge(1)-C(3)-H(3)	107.2	C(2)-C(9)-H(9B)	109.5
C(10)-C(3)-Ge(1)	110.2(4)	C(2)-C(9)-H(9C)	109.5
C(10)-C(3)-H(3)	107.2	H(9A)-C(9)-H(9B)	109.5
C(10)-C(3)-C(11)	110.2(4)	H(9A)-C(9)-H(9C)	109.5
C(11)-C(3)-Ge(1)	114.5(4)	H(9B)-C(9)-H(9C)	109.5

C(11)-C(3)-H(3)	107.2	C(3)-C(10)-H(10A)	109.5
C(12)-C(4)-Ge(2)	121.9(4)	C(3)-C(10)-H(10B)	109.5
C(12)-C(4)-C(16)	116.5(5)	C(3)-C(10)-H(10C)	109.5
C(16)-C(4)-Ge(2)	121.5(4)	H(10A)-C(10)-H(10B)	109.5
C(17)-C(5)-Ge(2)	120.0(4)	H(10A)-C(10)-H(10C)	109.5
C(21)-C(5)-Ge(2)	121.7(4)	H(10B)-C(10)-H(10C)	109.5
C(21)-C(5)-C(17)	118.2(5)	C(3)-C(11)-H(11A)	109.5
C(1)-C(6)-H(6A)	109.5	C(3)-C(11)-H(11B)	109.5
C(1)-C(6)-H(6B)	109.5	C(3)-C(11)-H(11C)	109.5
C(1)-C(6)-H(6C)	109.5	H(11A)-C(11)-H(11B)	109.5
H(6A)-C(6)-H(6B)	109.5	H(11A)-C(11)-H(11C)	109.5
H(6A)-C(6)-H(6C)	109.5	H(11B)-C(11)-H(11C)	109.5
H(6B)-C(6)-H(6C)	109.5	C(4)-C(12)-H(12)	118.8
C(1)-C(7)-H(7A)	109.5	C(4)-C(12)-C(13)	122.5(5)
C(1)-C(7)-H(7B)	109.5	C(13)-C(12)-H(12)	118.8
C(1)-C(7)-H(7C)	109.5	C(12)-C(13)-H(13)	120.3
H(7A)-C(7)-H(7B)	109.5	C(14)-C(13)-C(12)	119.3(5)
H(7A)-C(7)-H(7C)	109.5	C(14)-C(13)-H(13)	120.3
H(7B)-C(7)-H(7C)	109.5	C(13)-C(14)-H(14)	120.4
C(2)-C(8)-H(8A)	109.5	C(15)-C(14)-C(13)	119.2(5)
C(2)-C(8)-H(8B)	109.5	C(15)-C(14)-H(14)	120.4
C(2)-C(8)-H(8C)	109.5	C(14)-C(15)-H(15)	119.9
H(8A)-C(8)-H(8B)	109.5	C(14)-C(15)-C(16)	120.3(5)
H(8A)-C(8)-H(8C)	109.5		

Symmetry transformations used to generate equivalent atoms: #1 -x+1,-y+1,-z+1

VITA

Kimberly Diane Roewe

Candidate for the Degree of

Doctor of Philosophy

Thesis: RATIONAL SYNTHESIS AND PROPERTIS OF NEW LONG-CHAIN LINEAR OLIGOMERIC GERMANIUM COMPOUNDS

Major Field: Chemistry

Biographical:

Education:

Completed the requirements for the Doctor of Philosophy in Inorganic Chemistry at Oklahoma State University, Stillwater, Oklahoma in May, 2014.

Completed the requirements for the Bachelor of Science in Chemistry at Southwestern Oklahoma State University, Weatherford, Oklahoma in May, 2009.

Experience:

Worked as an undergraduate research assistant at Southwestern Oklahoma State University synthesizing organometallic compounds using first row transition metals and nitrogen-containing macrocycles as CXCR4 antagonists.

Interned at Oklahoma State University in the Biochemistry department sequencing virus RNA from plants found in the Tallgrass Prairie Preserve in Osage County, Oklahoma

Professional Memberships:

American Chemical Society